NASA Contractor Report 3420

Homing Performance Comparison of Selected Airframe Configurations Using Skid-to-Turn and Bank-to-Turn Steering Policies

R. T. Reichert

CONTRACT L-75242A
MAY 1981

NASA

NASA Contractor Report 3420

Homing Performance Comparison of Selected Airframe Configurations Using Skid-to-Turn and Bank-to-Turn Steering Policies

R. T. Reichert
The Johns Hopkins University
Laurel, Maryland

Prepared for
Langley Research Center
under Contract L-75242A

NASA
National Aeronautics
and Space Administration

**Scientific and Technical
Information Branch**

1981

TABLE OF CONTENTS

TABLE OF CONTENTS (CONTINUED)

TABLE OF CONTENTS (CONTINUED)

LIST OF FIGURES

LIST OF FIGURES (CONTINUED)

LIST OF FIGURES (CONTINUED)

LIST OF FIGURES (CONTINUED)

LIST OF TABLES

1.0 SUMMARY

Tactical missile agility and range capability must be improved to satisfy increasingly severe mission requirements. Preliminary analysis has indicated that bank-to-turn control may provide the needed improvement in mission performance. However, there are several technical concerns which must be addressed before bank-to-turn can be considered a viable method for controlling high performance tactical missiles. This report assesses the miss distance performance of various bank-to-turn steering policies and airframe configurations. For comparison, a moderate-lift cruciform airframe with skid-to-turn control is also included.

Two missions for which bank-to-turn steering is appropriate have been selected as a basis for this comparison. One is a long range engagement against a maneuvering aircraft. The second is a medium range engagement against a missile.

Results indicate that bank-to-turn steering can provide acceptable performance provided sufficient bank rates can be tolerated. These required bank rates may not be excessive. It is recommended that future investigation be directed towards designing coordinated autopilots for high performance bank-to-turn missiles and determining their sensitivity to airframe parameters.

2.0 EXPANDED SUMMARY

This investigation compares the performance of a moderate lift cruciform airframe (with low aspect wings) configured with both skid-to-turn and bank-to-turn steering, and a high-lift planar airframe (with larger wings) configured with bank-to-turn steering. In order to focus the study and develop meaningful results, two missions were selected for which BTT steering may be applicable. These are a long range mission for a raid suppression system (RSS) and a medium range mission for an area defense engagement. The characteristics of these missions define the particular engagement and parameter values used.

The models used for this investigation are developed in detail in Section 7 (RSS mission) and Section 11 (area defense mission). The missile is described by its lift characteristics, which are airframe configuration dependent, weight and reference area, which are mission dependent (Section 5), and guidance and autopilot lags. Thrust is assumed to overcome axial drag (but not maneuver induced drag) for the RSS mission and is assumed to be zero for the homing portion of the area defense mission. In order to assess the effect of parameter variations, two sets of subsystem time constants were selected (Sections 8 and 11). These were chosen to be representative of a slow and fast system and thus bound the range of interest.

The control features of the four steering policies investigated are summarized in Table 2.1. The performance of the moderate-lift cruciform airframe was assessed for all four policies while the high-lift planar airframe was evaluated for BTT-90 and BTT-180. For each mission the performance results are separated into three categories:

- Comparison of steering policies
- Comparison of airframe configuration
- Subsystem parameter effects.

The BTT-90 and BTT-180 configurations were assumed to have coordinated autopilots. That is, the missile maintained zero sideslip during the maneuver. The practical method to control the roll and yaw angular rates to achieve this turn coordination has not been addressed, although the requirements are outlined in Appendix D. Future studies should address

TABLE 2.1 STEERING POLICY CONTROL FEATURES

Steering Policy	Pitch Channel	Yaw Channel	Roll Channel
STT	Develop commanded acceleration. Equal positive and negative angle of attack capability.	Develop commanded acceleration. Equal positive and negative angle of sideslip capability.	Maintain roll attitude at fixed reference position.
BTT-45	Develop commanded acceleration. Equal positive and negative angle of attack capability.	Develop commanded acceleration. Equal positive and negative angle of sideslip capability.	Roll airframe to effect a combined plane maneuver. Maximum roll attitude error of 45 degrees.
BTT-90	Develop commanded acceleration. Equal positive and negative angle of attack capability.	Coordinate with roll channel to minimize sideslip. Limited angle of sideslip capability.	Roll airframe to direct lift vector. Maximum roll attitude error of 90 degrees.
BTT-180	Develop commanded acceleration. Positive angle of attack capability only.	Coordinate with roll channel to minimize sideslip. Limited angle of sideslip capability.	Roll airframe to direct lift vector. Maximum roll attitude error of 180 degrees.

the design of a coordinated control policy for high performance BTT missiles and determine the sensitivity of these autopilots to airframe parameters.

2.1 Summary of the Raid Suppression Assessment

The relative performance measure is defined as the minimum homing time required to achieve a 25 foot (7.62 meter) miss against a maneuvering target with specified heading error magnitudes of 10, 20, 30, and 40 degrees at the start of homing. The best combination of airframe and steering policy is that which consistently shows a smaller minimum homing time requirement. In order to facilitate comparison of these configurations, the weight and body cross-sectional areas, used as reference areas for aerodynamic coefficients, were made equal. The two airframe configurations differ primarily in their lift characteristics.

Figure 2.1 contains a summary of performance results for the 10 and 30 degree initial heading error cases. The shaded region for each bar corresponds to the systems configured with the fast set of system parameters, typically overall homing system time constants of 0.5 sec, while the open region corresponds to the systems configured with the slow set of system parameters, typically overall homing system time constants of 0.9 sec. Interpretation of the results of the raid suppression assessment follows.

2.1.1 Steering Policy Comparison

The results of this study indicate that the performance of the BTT-45 and STT steering are nearly identical and that the performance of BTT-90 lies between STT and BTT-180. Performance of BTT-180 is better or worse than STT depending upon system parameter selection. Provided that the bank system is fast enough relative to the pitch system, BTT-180 performance may outperform STT. For this study a roll rate capability of 250 degrees per second was sufficient when guidance lag was 0.5 second and aero/control lag was 0.4 second. It is recommended that the maximum allowable roll rate capability be strived for when designing a bank-to-turn system.

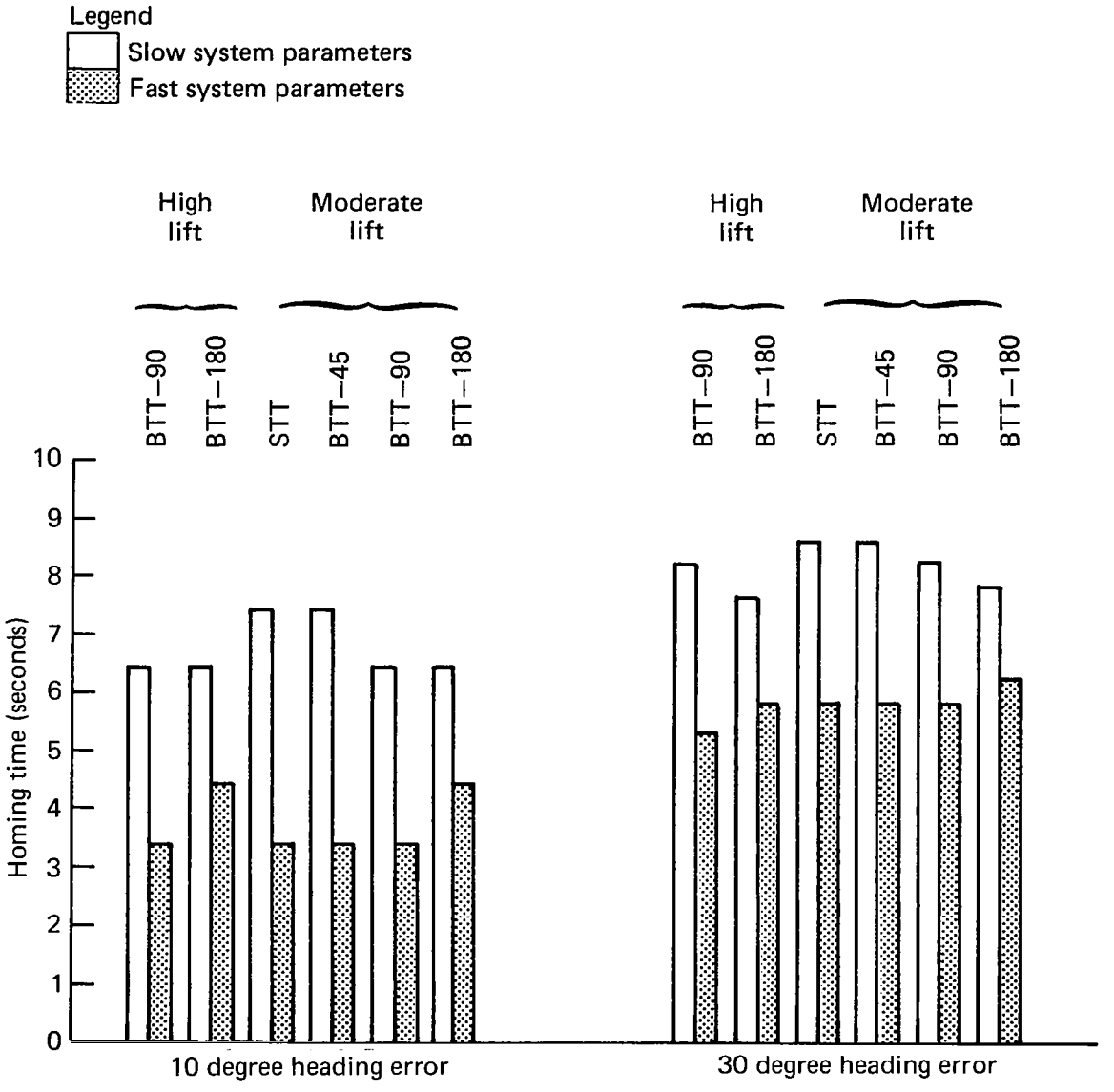

Fig. 2.1 Summary of raid suppression results.

2.1.2 Airframe Configuration Comparison

The high-lift planar airframe and moderate-lift cruciform airframe exhibit similar performance for easy engagements (small initial heading errors). However, for more difficult engagements the high-lift configuration exhibits better performance. Since the maneuverability of both configurations is equally limited by acceleration and angle-of-attack limits, the amount of maneuver-induced slowdown is smaller for the high-lift configuration, thereby resulting in better performance. For the sets of parameters investigated in this study, the performance of the high-lift planar airframe configured with its best steering policy was equal to or exceeded the performance of the moderate-lift cruciform airframe configured with its best steering policy.

2.1.3 Subsystem Parameter Effects

In each case, the smaller set of system lags resulted in the best performance. However, the relative ordering of steering policies depended upon the level of system lags as described above. In addition, it was observed that STT and BTT-45 are relatively insensitive to the distribution of overall system lag between the guidance filtering and aero/control subsystems. However, BTT-90 and BTT-180 are more sensitive to variation in the guidance filter lag than to pitch channel aero/control lag. This suggests that to get the best performance from a BTT system it is desirable to keep the guidance filter lag as small as possible.

2.2 Summary of the Area Defense Assessment

Area defense, as considered here, is a medium range engagement against a high altitude air-to-surface enemy missile. Both in-plane and cross-plane engagement geometries were considered. The measure of performance selected was the portion of the target trajectory on which the target can be successfully intercepted, where a successful intercept is defined as an intercept with less than 50 foot (15.24 meter) miss. In order to facilitate comparison of these configurations, the weights of the configurations and body cross-sectional areas, which are the reference

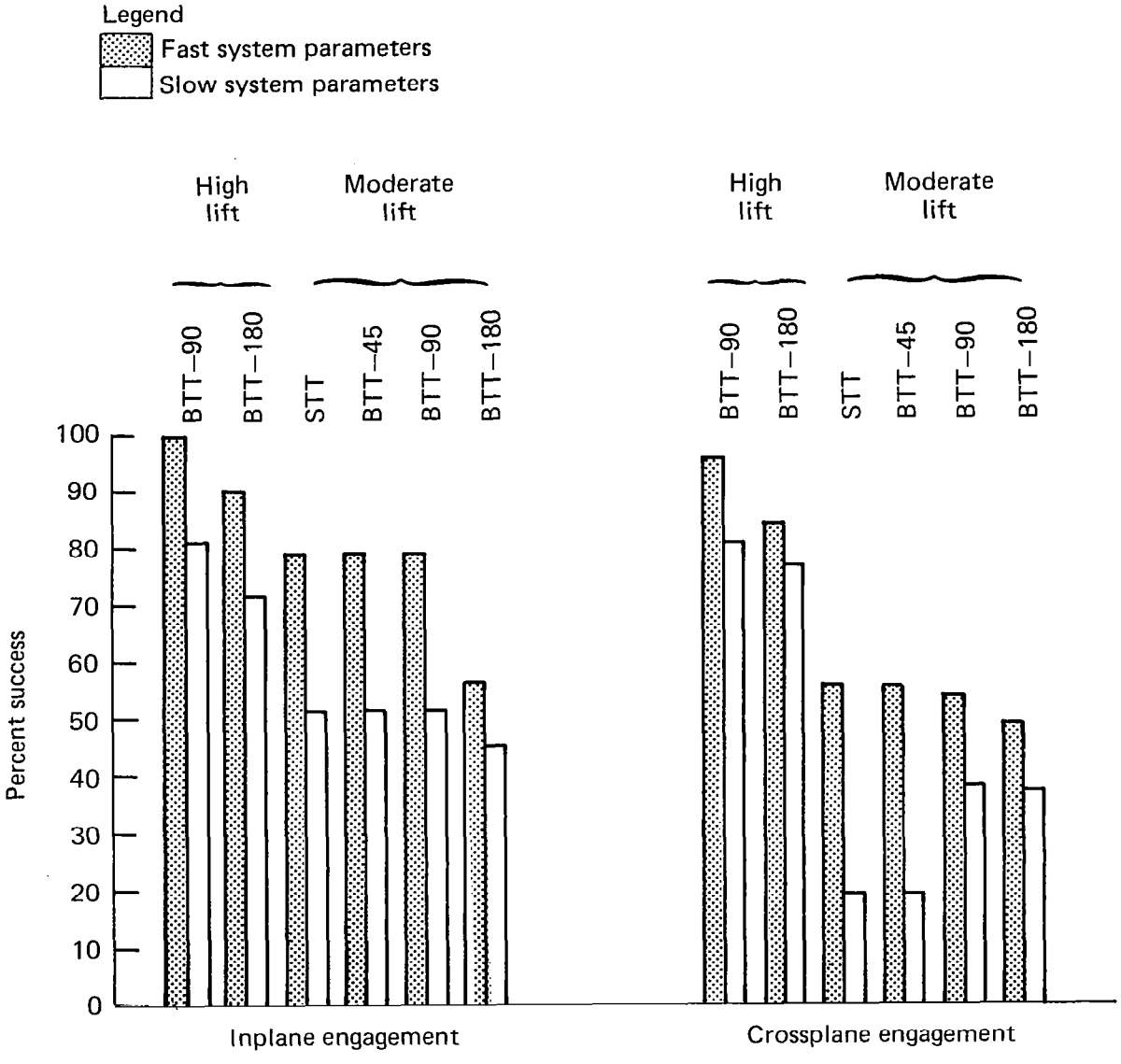

Fig. 2.2 Summary of area defense results.

areas for aerodynamic coefficients, were made equal. The two configurations differ aerodynamically primarily in their trim lift and drag characteristics (See Appendix A).

Figure 2.2 contains a summary of performance results for this area defense engagement. Unlike the measure of merit for the RSS mission, the performance measure for the area defense mission is expressed as a percent success and it corresponds to the ratio of the total length of the target trajectory over which the target is successfully intercepted to the total length of target trajectory investigated. (The portions of the target trajectory used are defined in Appendix E.) Two sets of results are shown in Figure 2.2 which compare the performance of the various configurations for the in-plane and cross-plane engagement geometries. Interpretation of these results follows.

2.2.1 Steering Policy Comparison

For the in-plane engagement geometry and a moderate-lift configuration, performance of STT, BTT-45 and BTT-90 are similar and better than BTT-180 for both sets of system parameters investigated. The BTT-180 interceptor performance is limited by the slow response time associated with the bank system, relative to the pitch system, at the conditions for this engagement.

For the cross-plane engagement, the performance of STT and BTT-45 are nearly identical. When configured with the set of system parameters corresponding to a fast system response, the performance ranking of steering policies is as follows

1. STT and BTT-45 are equivalent (55.7%)
2. BTT-90 (54.1%)
3. BTT-180 (49.3%)

For the slow set of system parameters the ranking is

1. BTT-90 (38.3%)
2. BTT-180 (37.5%)
3. STT and BTT-45 are equivalent (19.3%)

The change in performance ranking for the two sets of system parameters

investigated is associated with the larger degradation in performance exhibited by STT and BTT-45 in shifting from the in-plane to the more severe cross-plane engagement geometry.

2.2.2 Airframe Configuration Comparison

When configured with the same steering policy, the high-lift planar airframe exhibits better performance than the moderate-lift cruciform configuration. This difference is greater for the cross-plane engagement geometry. For the sets of parameters investigated in this study, the performance of the high-lift airframe configured with its best steering policy exceeded the performance of the moderate-lift cruciform airframe configured with its best steering policy.

2.2.3 Subsystem Parameter Effects

For each case, the smaller set of system lags resulted in the best performance. Increasing the maximum roll rate capability of the BTT-90 and BTT-180 configurations improves the performance of these systems by reducing the overall maneuver response time. In addition, the effective response time in the plane of the desired maneuver is affected not only by subsystem responses, but also by the amount the airframe must bank to achieve the commanded orientation. For the cross-plane engagement, the effective time constant of the response in the plane of maneuver is smaller than for the in-plane engagement since the commanded maneuver plane is closer to the initial orientation of the interceptor's maneuver plane.

3.0 INTRODUCTION

Bank-to-turn (BTT) steering offers several potential advantages which may be exploited to provide improved performance for future missile systems. For example, a planar missile airframe can be designed to have very high lifting capability in one direction without the weight and drag penalty associated with orthogonal lifting surfaces [1]. This high lift vector can then be directed using BTT control. In the case of cruciform configurations the angle-of-attack capability is often limited by roll-yaw aerodynamic stability considerations or control surface effectiveness. These constraints can be relieved by rolling or banking the airframe to an orientation which has optimum stability and control effectiveness.

In addition to its potential advantages, BTT steering introduces some technical concerns which must be carefully evaluated. For example, the methodology for designing a bank-to-turn autopilot is not well developed. Such a design must take into account the aerodynamic and kinematic coupling terms as well as allow for operation at low signal levels (i.e., small angles-of-attack) when the preferred roll orientation is poorly defined. In addition, the coupling of body motion into the guidance signals (for example, due to radome aberration errors) is another major concern for BTT systems. Recent analyses have indicated that some skid-to-turn (STT) systems can tolerate a limited amount of radome-induced instabilities without severe performance degradation [2]. In a BTT system a coupling loop is closed through roll rate as well as pitch and yaw rates [3]. It is not known whether BTT systems can tolerate coupling induced instabilities. Another concern is the interaction of BTT control with missile functions such as detection (seeker), guidance signal processing, control surface effectiveness, etc. Will BTT control increase the severity of subsystem requirements, thus making them more complicated to design and more costly?

All the above concerns must be investigated before BTT steering can be considered a viable method to control high performance tactical missiles. However, the technical concern addressed in this report is

guidance performance. BTT steering is inherently a three dimensional phenomenon since there will be acceleration components directed out of the desired plane of maneuver while the missile is banking. Does the coupling of the roll and yaw channels and the resulting out-of-plane motion negate the potential advantages of BTT steering?

The objective of this study is to assess the intercept performance of missiles using BTT and STT steering policies and its sensitivity to variations in system parameters.

In order to focus the study and develop meaningful results, two missions have been selected for which BTT steering may be applicable. These are a long range mission for a raid suppression system and a medium range mission for an area defense engagement. The characteristics of these missions define the particular engagement and parameter values used.

Appendix A by Edward T. Marley describes the airframe aerodynamic characteristics of the two configurations investigated here.

4.0 SYMBOLS

C_N	trim aerodynamic lift coefficient
C_{D_o}	aerodynamic axial drag coefficient
α	angle-of-attack
M	Mach number
q	dynamic pressure
S	reference area for aerodynamic coefficients
R_{go_i}	initial range-to-go (seeker acquisition range)
V_{mo}	initial missile velocity
V_{to}	initial target velocity
A	acceleration
Λ	effective navigation ratio
$\dot{R}$	range rate
γ_L	look angle
τ_g	guidance filter time constant
τ_a	aero/control time constant
τ_r	roll subsystem time constant
α_{lim}	angle-of-attack limit
η_{lim}	aerodynamic acceleration limit
$\dot{\phi}_{lim}$	roll rate limit
r	yaw rotation rate
ϕ	roll attitude angle
$\dot{\phi}$	roll rotation rate
η_p	acceleration in pitch plane
η_y	acceleration in yaw plane
η_{p_c}	acceleration command in pitch plane

η_{az}	acceleration component in azimuthal plane referred to a nonrolling coordinate frame
η_{az_c}	acceleration command in azimuthal plane
η_{elv}	acceleration component in elevation plane referred to a nonrolling coordinate frame
η_{elv_c}	acceleration command in elevation plane
$\dot{\sigma}_p$	pitch plane component of the line-of-sight angular rate
$\dot{\sigma}_y$	yaw plane component of the line-of-sight angular rate
$\dot{\sigma}_{az}$	azimuth plane component of the line-of-sight angular rate
$\dot{\sigma}_{elv}$	elevation plane component of the line-of-sight angular rate
$\hat{i}, \hat{j}, \hat{k}$	unit vectors of the inertial coordinate frame
$\hat{n}, \hat{r}$	unit vectors of the line-of-sight coordinate frame
T_ϕ	Euler angle transformation matrix
T_ϕ^{-1}	inverse Euler angle transformation matrix
K_1	gain in variable aero/control system time constant
K_2	gain in variable aero/control system time constant

5.0 AIRFRAME CONFIGURATION DEFINITIONS

Two airframe aerodynamic configurations were studied in this investigation. The two configurations differ primarily in their lift and drag characteristics. One has a high lift capability and might correspond to a larger-winged planar airframe. The other is a moderate-lift configuration and might correspond to an airframe having cruciform wings of low aspect ratio. Detailed descriptions of these configurations can be found in Appendix A.

The high-lift planar configuration corresponds to an airframe that has either one or two preferred maneuver directions. Negative load factors are permitted for an airframe which is symmetric about the wing plane. A configuration of this type has two preferred aerodynamic roll orientations for developing lateral maneuvers. To reverse the direction of maneuver, the missile could pitch down to a negative angle-of-attack. However, if the commanded maneuver is orthogonal to the current plane of maneuver, the missile would have to bank 90 degrees. The steering policy for this configuration is called a 90 degree bank-to-turn, or BTT-90.

Some planar configurations have only one preferred orientation. Since negative load factors are not permitted, reversing the direction of the maneuver requires banking the missile 180 degrees. For this reason, the steering policy used to control this configuration is called a 180 degree bank-to-turn, or BTT-180.

The moderate-lift cruciform configuration can represent a STT missile. A STT missile is capable of developing a lateral acceleration in any radial direction regardless of the missile spatial roll orientation. Some cruciform configurations exhibit enhanced aerodynamic stability characteristics and increased control effectiveness if the acceleration vector lies between the control panels. Since the acceleration is divided between the steering channels, this is called a combined-plane maneuver. One method to relax the angle-of-attack limit due to roll-yaw aerodynamic coupling is to bank the missile so that the desired maneuver occurs in the combined plane of the missile regardless of the spatial roll orientation. The control policy for

a missile that has two identical, orthogonal control planes and rolls to a combined-plane maneuver is called roll during turn, or RDT [4]. In this report, this steering policy is called BTT-45 since the missile would have to roll a maximum of 45 degrees to achieve a preferred orientation. Both STT and BTT-45 steering policies for the moderate-lift configuration are investigated in this report. In addition, the BTT-90 and BTT-180 steering policies are also investigated with the moderate-lift configuration. This is done for comparison with the high-lift configuration. Table 5.1 summarizes the configuration and steering policies investigated.

TABLE 5.1 SUMMARY OF AIRFRAME CONFIGURATIONS AND STEERING POLICY COMBINATIONS

CONFIGURATION	STEERING POLICIES			
High-Lift (Planar) Configuration	BTT-180	BTT-90		
Moderate-Lift (Cruciform) Configuration	BTT-180	BTT-90	BTT-45	STT

5.1 Aerodynamic Characteristics of the Raid Suppression Interceptor

A detailed description of the airframe aerodynamic characteristics is contained in Appendix A. The models used to simulate the aero/control characteristics of the various configurations considered in this study require estimates of the trim aerodynamic normal force coefficient C_N and axial drag coefficient C_{D_o}. The trim lift characteristics for the moderate and high-lift raid suppression configurations are shown in Figure 5.1. In order to facilitate comparison of the configurations, the weight and reference areas (Table 5.2) were made equal. These parameters are representative of a long range missile near the end of sustained flight. Since only the terminal homing portion of the flight is simulated in this study, the mass variation is assumed to be negligible and the engine thrust is assumed to offset axial drag.

5.2 Aerodynamic Characteristics of the Area Defense Interceptor

The trim lift characteristics for the two area defense configurations are shown in Figure 5.2. The axial drag characteristic of the moderate-

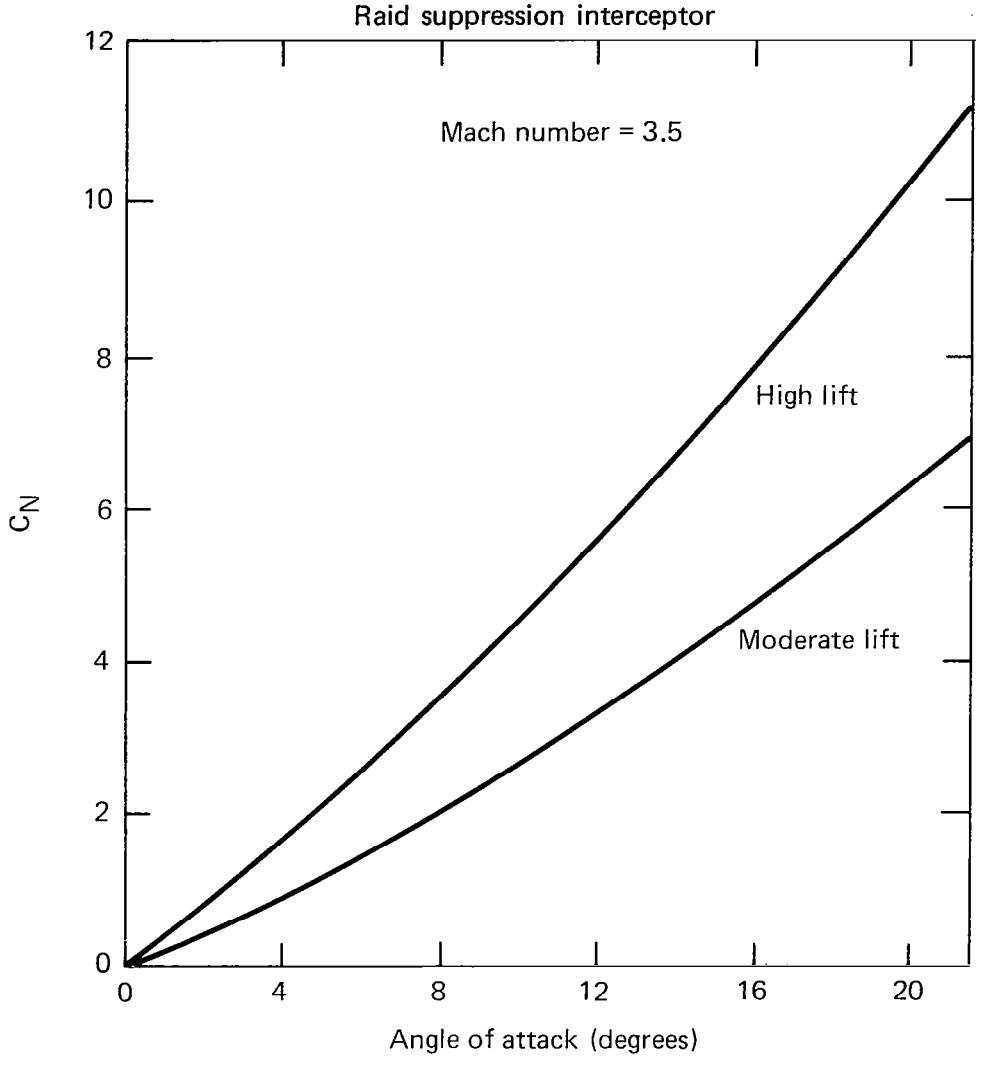

Fig. 5.1 Trim aerodynamic lift characteristics.

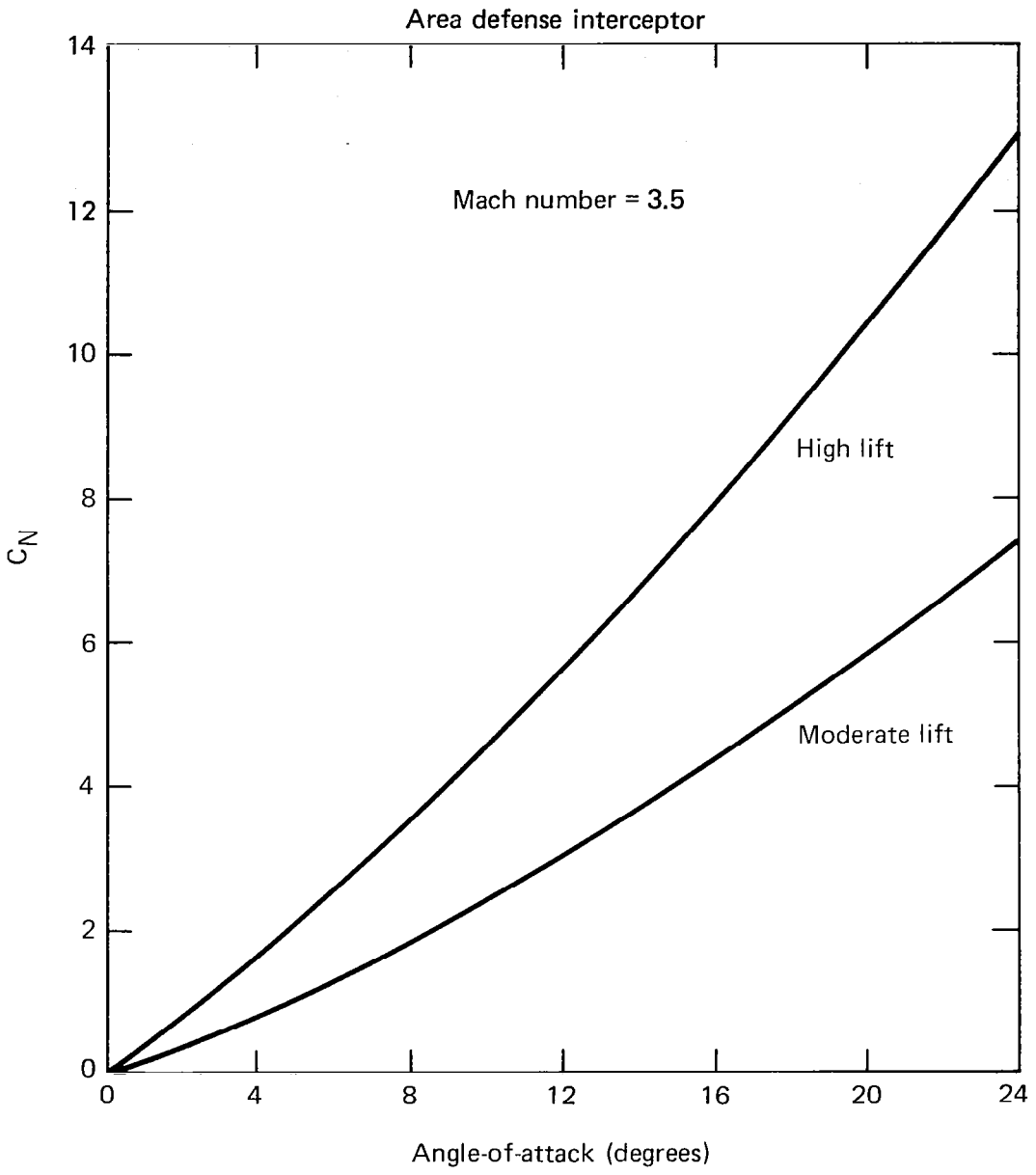

Fig. 5.2 Trim aerodynamic lift characteristics.

lift configuration is shown in Figure 5.3. It is assumed that the axial drag characteristic of the high-lift airframe configuration is 20 percent greater than for the moderate-lift configuration.

In order to facilitate comparison of the configurations, the weight and reference areas (Table 5.3) were made equal. These parameters are representative of a medium range surface-to-air interceptor near the end of flight. For the final portion of the flight simulated in this study, the mass variation is assumed to be negligible and the propulsion system is assumed to offset axial drag until terminal homing initiates. Following initiation of terminal homing, the missile is allowed to slow down with maneuver-induced and axial drag.

TABLE 5.2 SYSTEM CHARACTERISTICS FOR THE RAID SUPPRESSION INTERCEPTOR

Weight	1200 lbs	(544.3 kg)
Reference Area	1.4 ft^2	(0.13 m^2)
Acceleration Limit	30 g	
Angle of Attack Limit	25 deg	

TABLE 5.3 SYSTEM CHARACTERISTICS FOR THE AREA DEFENSE INTERCEPTOR

Weight	740 lbs	(335.7 kg)
Reference Area	1.0 ft^2	(0.093 m^2)
Acceleration Limit	30 g	
Angle of Attack Limit	25 deg	

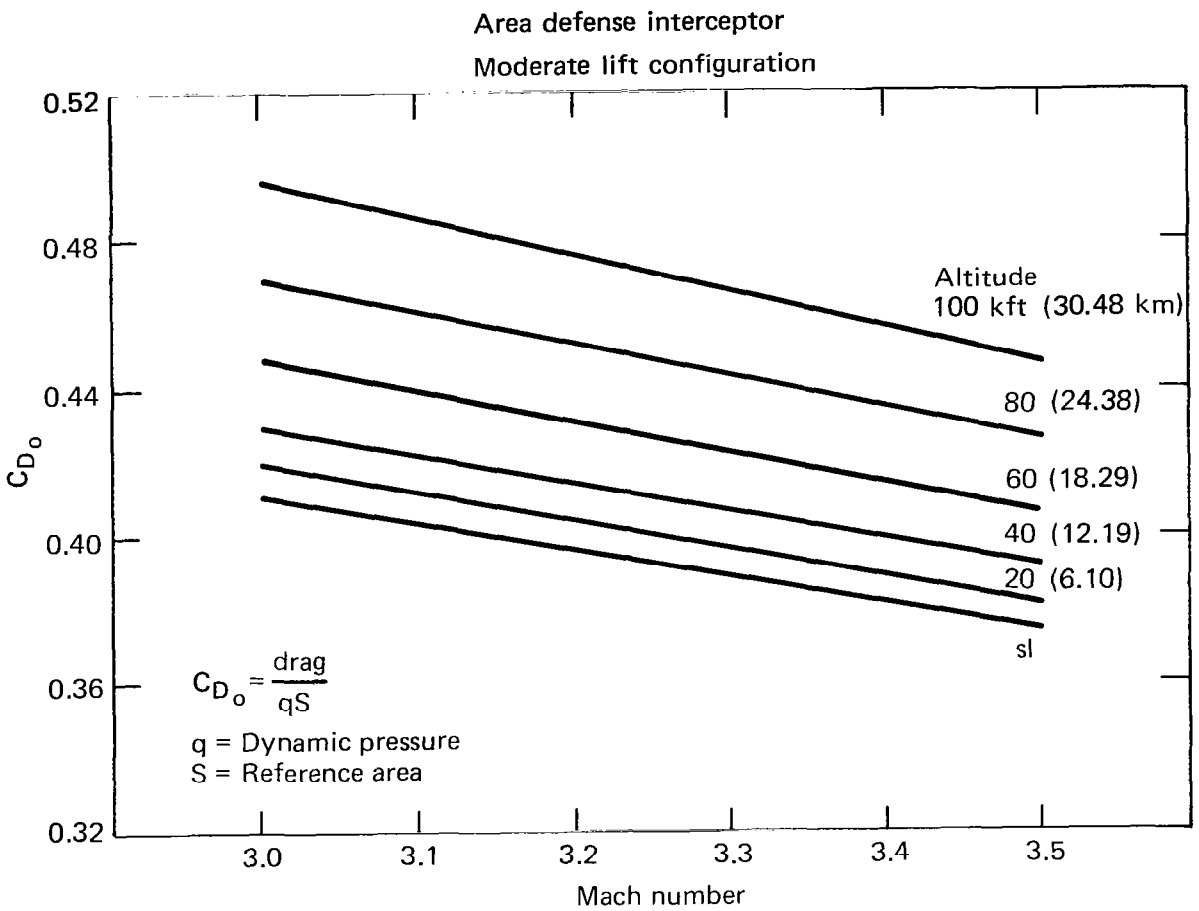

Fig. 5.3 Axial drag characteristics.

PART I

RAID SUPPRESSION ASSESSMENT

6.0 ENGAGEMENT MODEL AND PERFORMANCE CRITERION

The mission selected for the first part of the comparison study is a long range surface-to-air engagement against enemy aircraft. This raid suppression mission has wide applicability among the three services. For example, it is a mission which requires a weapon that might be used for Navy Wide Area Defense. The primary objective of this weapon is to suppress screening jammers in order to increase the effectiveness of inner and medium range fleet defenses. The Army has also considered a long range missile to help protect ground forces from air attack. Finally, the current Air Force Advanced Strategic Air-Launched Multi-Mission Missile (ASALM) is a long range weapon whose primary objective is to defeat Airborne Warning and Control (AWACS) aircraft.

Ramjet engines are attractive candidate propulsion systems because of their capability to provide long range, high speed performance. Bank-to-turn (BTT) control is applicable because of its compatibility with engine inlet configurations. In addition, many ramjet configurations are not circularly symmetric and BTT steering can be used to maintain small sideslip angles and thus control the sideslip induced roll moment. Rocket propulsion, using a trajectory different from that of a ramjet, has also been considered for long range missions. To reduce weight and drag these missiles could have a planar configuration (only one set of wings) with the lift vector directed using BTT control.

The targets described above are typically at moderate altitudes. Either a rocket or a ramjet would have a high altitude midcourse phase of its trajectory. Thus a complete system analysis would have to consider the problem of how and when to command the missile to turn down. For this configuration comparison, only the final or terminal homing portion of the flight is considered. It is assumed that the missile has turned down and that the missile and target are at the same altitude. The missile will, however, have an initial heading error, that is, the missile velocity vector will not be directed towards an intercept point.

Figure 6.1 depicts the engagement used for this part of the study.

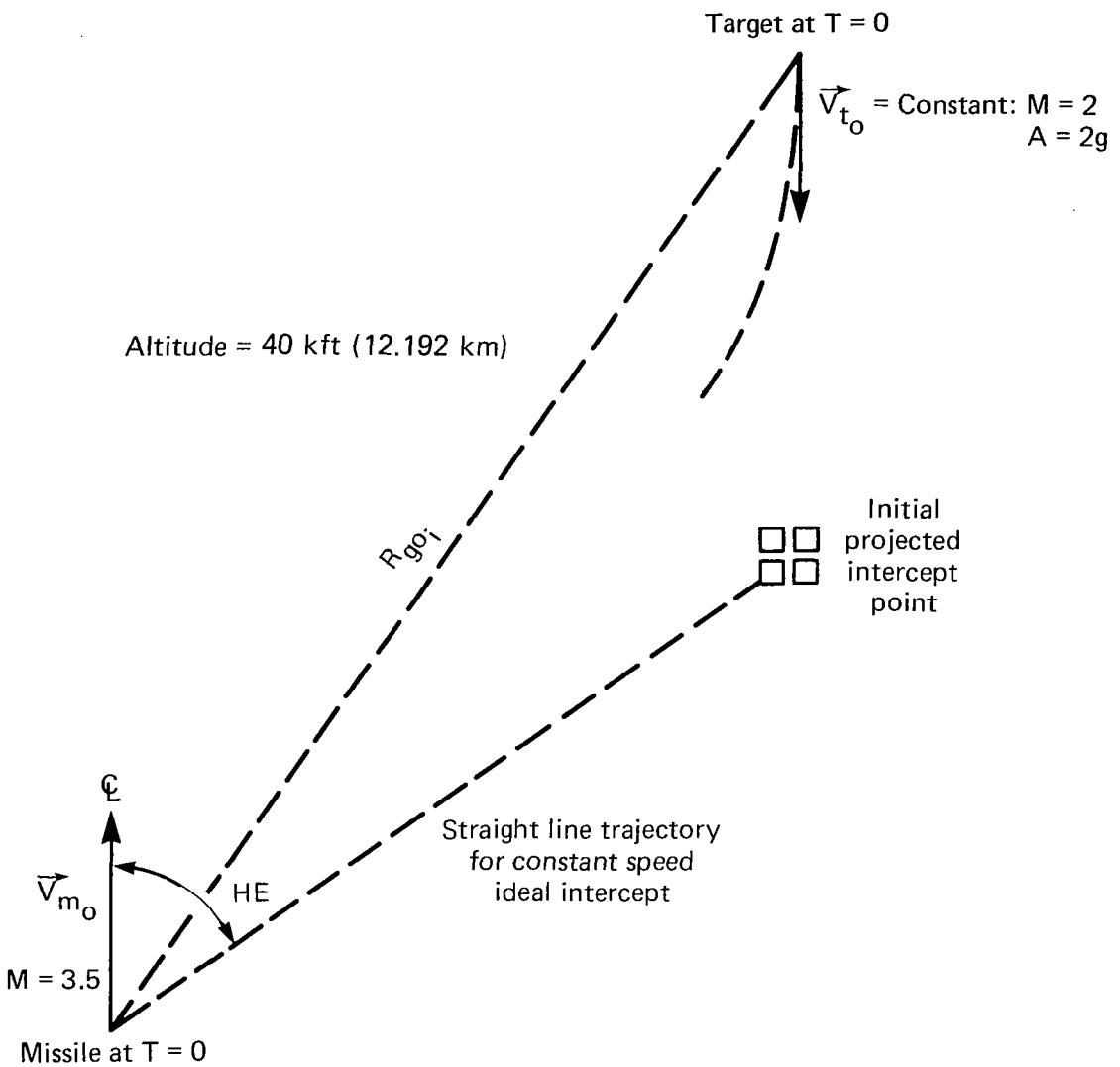

Fig. 6.1 Raid suppression engagement geometry.

The missile and target are initially at the same altitude but are headed in opposite directions. As shown in the figure, the heading error is defined to be the angle between the current velocity vector and that which would be required for a constant heading intercept, assuming both the missile and target maintain constant velocities. In addition, the Mach 2 target is executing a two gee constant altitude maneuver toward the missile. (This direction of target maneuver is more difficult for the missile to handle than if the target were pulling away from the missile).

The variable parameters of this engagement are the initial range and the heading error. The performance measure used for this phase of the study is the homing range required to null an initial heading error so that the miss distance is less than a specified level. Since terminal homing is assumed to have initiated at the beginning of the simulation, this performance measure determines the required acquisition range of an active seeker. Typically, a miss distance criterion of 25 ft. (7.62m) is used.

The performance measure is computed as follows. First, for a given heading error, the simulation is run for a number of initial ranges and the resulting miss distance is recorded. From these data a curve can be drawn illustrating miss distance versus homing range (initial range-to-go). Such a curve is illustrated in Figure 6.2. Notice that all miss distances shown in this figure are positive, rather than the positive and negative misses often shown for single plane skid-to-turn (STT) engagements. Since BTT steering is inherently three dimensional, the final miss vector can be in any orientation. Thus negative miss distances have no meaning in a BTT engagement.

The next step in computing the performance measure is to draw a horizontal line at the specified miss distance level and to record the range of the rightmost intercept of the curve with this straight line. This is the shortest range which will achieve the required performance for this configuration and this heading error.

The procedure is then repeated for a number of different initial heading errors. From these data a curve can then be drawn relating the required range to the intial heading error. Such a curve is shown in

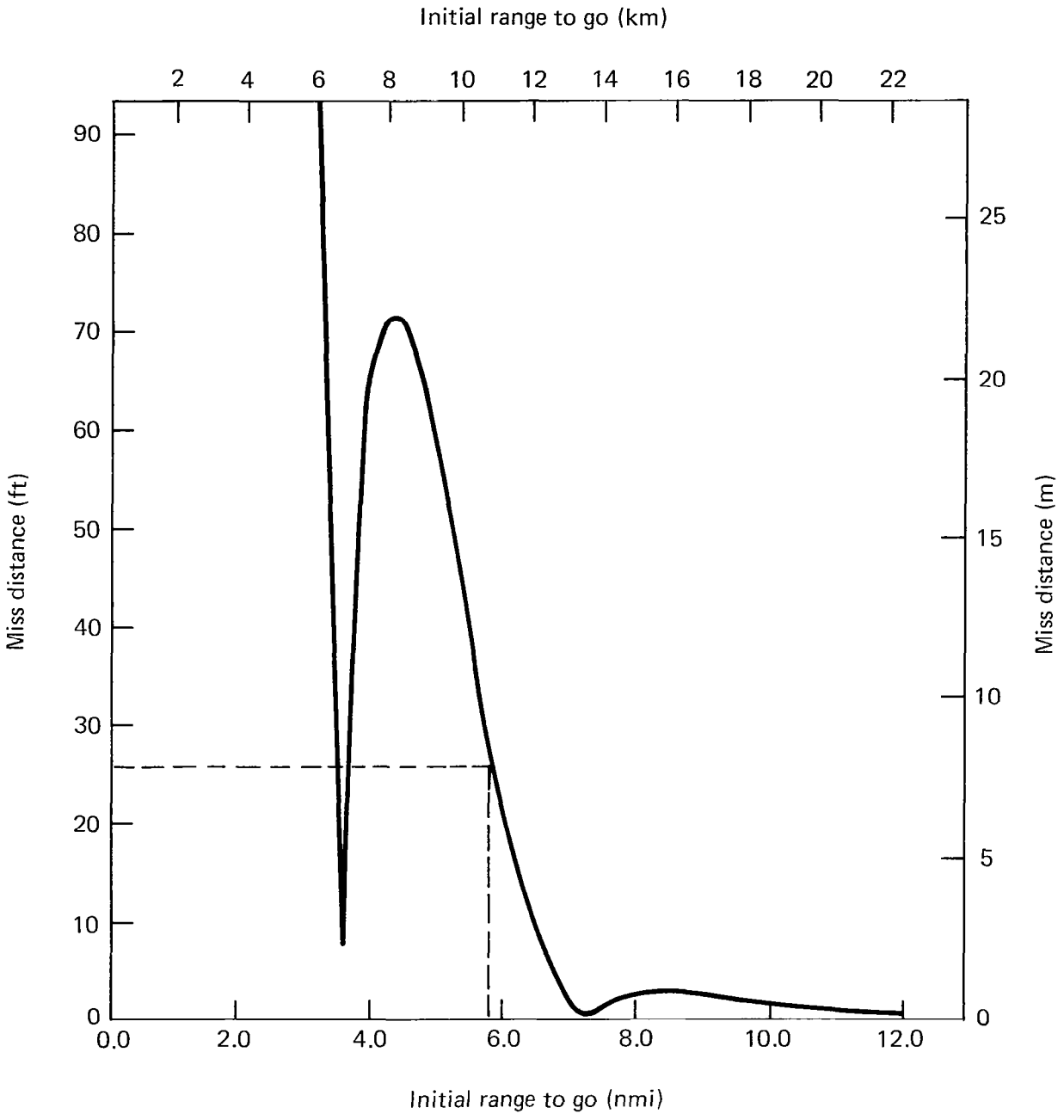

Fig. 6.2 Representative raid suppression miss distance profile.

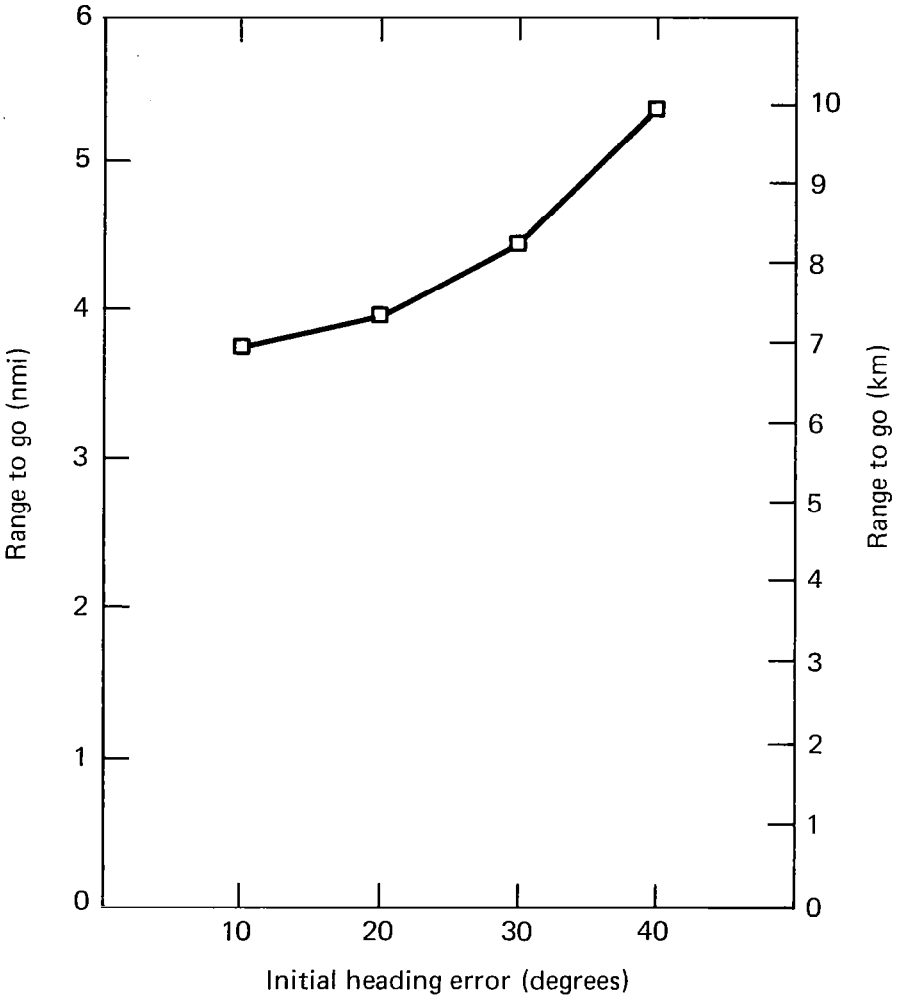

Fig. 6.3 Representative raid suppression performance criterion data.

Figure 6.3. Note that each point on this curve results from a large number of homing performance runs. The curves corresponding to the various configurations and steering policies can then be compared to reach the conclusions of this study.

The required homing range is an important parameter. It defines requirements for a seeker designer. However, interpretation of results in this study is sometimes facilitated by using the required homing time rather than range. Homing time is not proportional to homing range because of missile slow down. Where appropriate, results will be given for either or both of these measures.

7.0 MODEL DEVELOPMENT

This section documents the development of a simplified six degree-of-freedom trim aerodynamic representation of the missile homing guidance loop for the selected missile configurations. A discussion of the navigation law and fundamental elements which comprise the guidance loop is presented, followed by a detailed description of the models selected to represent the components of the aero/control and guidance subsystems.

7.1 Navigation Law

Since the advent of missile technology in the 1940's engineers have searched for the best combination of hardware and guidance algorithms to ensure adequate performance against increasingly agile threats. Before the application of modern control theory to development of closed form navigation laws in the 1960's, classical proportional navigation [5] received extensive study. Proportional navigation is a guidance algorithm in which missile lateral acceleration is made proportional to the angular rotation rate of the line-of-sight (LOS) between missile and target. The robustness and relative ease of implementation associated with proportional navigation as well as the successful deployment of missile systems employing proportion navigation continues to make this navigation law attractive. Modern guidance algorithms, which in most cases require extensive knowledge of system dynamics and error sources, have shown improved performance under nearly ideal conditions. However, as relatively large component and measurement errors are introduced, these modern algorithms exhibit poorer performance than proportional navigation under the same conditions [6].

Since it is highly probable that a Raid Suppression interceptor would encounter threats that are attempting to deny information such as range and range rate, a modern guidance algorithm may not perform as well as proportional navigation. For this reason, proportional navigation has been selected as the navigation law for this study. A discussion of the implementation of proportional navigation, within the guidance kinematic loop, is presented next.

7.2 Guidance Kinematic Loop

The proportional navigation law attempts to drive the angular rate of the LOS vector to zero by controlling missile lateral acceleration. This condition, along with the requirement that range rate is negative, is sufficient to ensure a successful intercept. The formulation of a closed loop control system, called the guidance kinematic loop, integrates the navigation law and missile dynamics into a form suitable for analysis and implementation. Figure 7.1 illustrates the fundamental components comprising the guidance loop.

The guidance loop can be separated into parts dealing with target characteristics, spatial kinematics (i.e., laws of Newtonian mechanics) and missile system dynamics. In the sense of closed loop control system analysis, the target motion may be viewed as the forcing function and the spatial kinematics as the feedback comparator which generates an actuating signal. In this case the actuating signals are a vector quantity called the LOS angular rate and a scalar quantity, range rate. The plant is the missile system hardware composed of sensing apparatus, guidance signal processing, autopilot and airframe.

The level of detail used to represent each element in the guidance loop should be consistent with the objectives of the study. For instance, analysis of high frequency system instabilities requires a representation that is accurate at those frequencies. Such a representation may require modelling the dynamics of the nonrigid system, knowledge of the full nonlinear aerodynamic characteristics and detailed modelling of the seeker track loop, guidance signal processing, autopilot and noise sources. However, for this parametric study of homing performance trends, in which the principal effects of interest occur at low frequency, it is not necessary or appropriate to develop such a complicated model. Instead, it is desirable to use a simplified representation of the more complex system that is capable of incorporating the available trim aerodynamic data and low frequency approximations to the various subsystems which comprise the guidance kinematic loop. This simplified representation may then be validated and employed to investigate relative performance for the selected missile configurations and the effects of varying the system parameters such as time

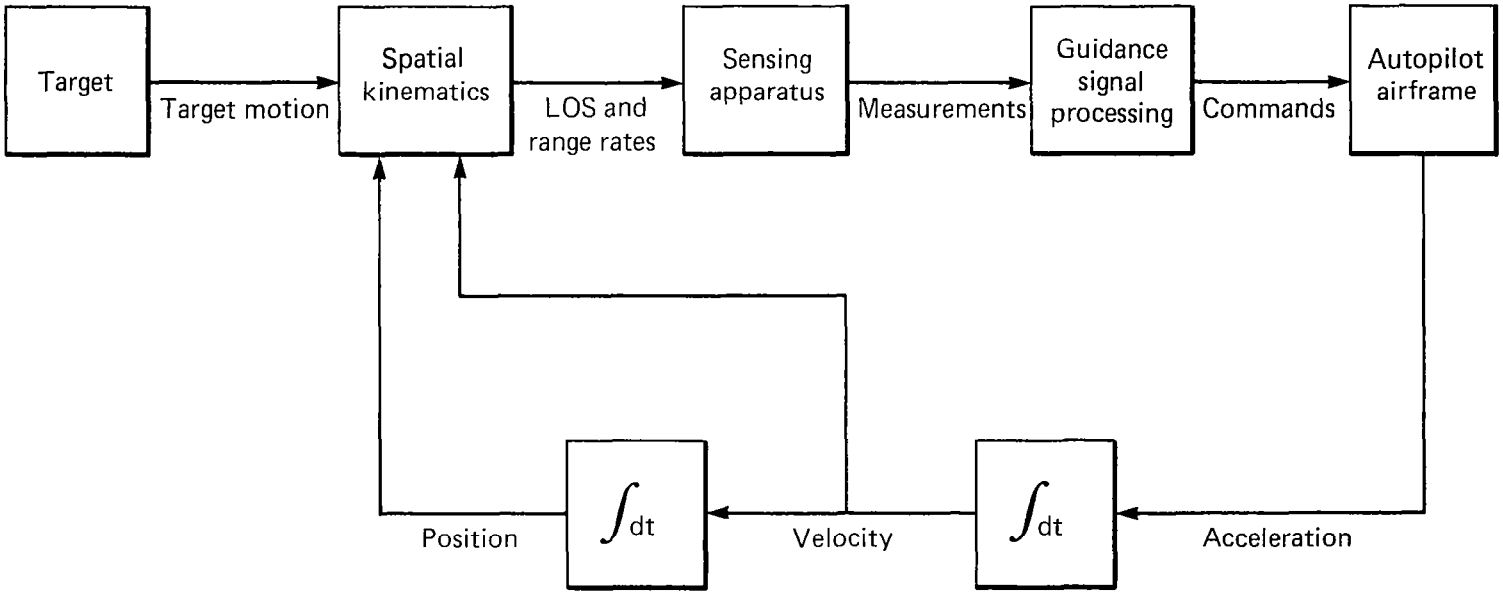

Fig. 7.1 Guidance kinematic loop.

constants and limits.

The next several sections will describe simplified representations of the elements in the guidance loop, beginning with the process by which guidance signals are formed from measurements of the relative motion between missile and target.

7.3 Forming the Guidance Signals

Consider the relative position vector, or LOS vector $\vec{R}_{mt}$, as shown in Figure 7.2. This vector may be written as the difference of the vector $\vec{R}_m$, corresponding to missile position referenced to the inertial coordinate frame, and the vector $\vec{R}_t$

$$\vec{R}_{mt} = \vec{R}_m - \vec{R}_t \quad ,$$

The time rate of change of $\vec{R}_{mt}$ may be written

$$\frac{d\vec{R}_{mt}}{dt} = \frac{d\vec{R}_m}{dt} - \frac{d\vec{R}_t}{dt} = \frac{\delta \vec{R}_{mt}}{\delta t} + (\vec{\Omega} \times \vec{R}_{mt})$$

where:

$\frac{d}{dt}$ = time derivative taken with respect to inertial coordinate frame

$\frac{\delta}{\delta t}$ = time derivative taken with respect to $\hat{r}$, $\hat{n}$ coordinate frame

$\vec{\Omega}$ = angular rotation rate of LOS vector.

Forming the vector cross product of $\vec{R}_{mt}$ with $\frac{d\vec{R}_{mt}}{dt}$ and solving for $\vec{\Omega}$ yields

$$\vec{\Omega} = \frac{\vec{R}_{mt} \times \frac{d}{dt}\vec{R}_{mt}}{\vec{R}_{mt} \cdot \vec{R}_{mt}} \quad .$$

This is the vector quantity which proportional navigation drives to zero by commanding missile lateral acceleration to be proportional to $|\vec{\Omega}|$. However, in order to form these corrective commands the missile hardware must measure the projection of the LOS angular rate vector into the missile fixed reference frame.

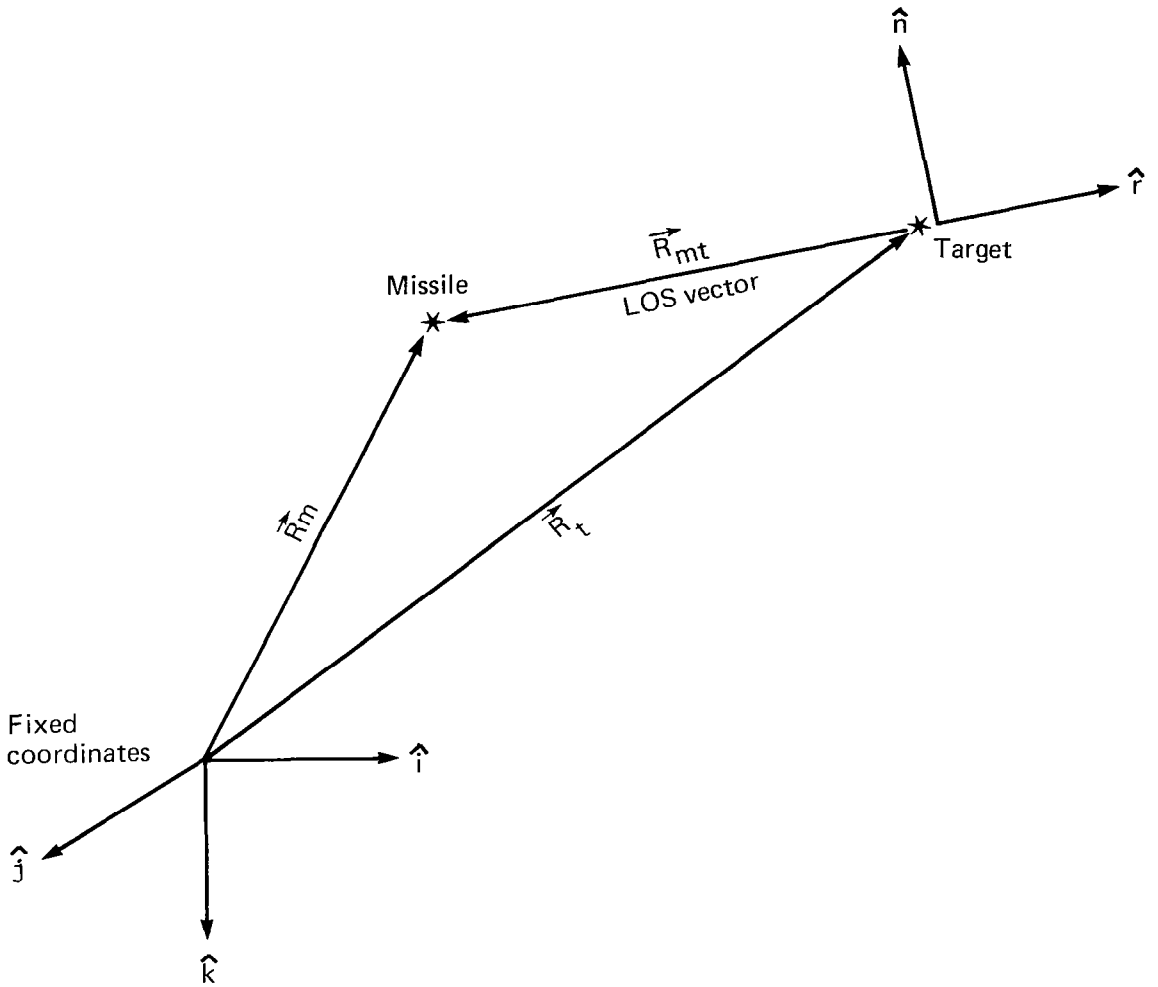

Fig. 7.2 Geometric line-of-sight.

The missile seeker is the subsystem which measures the guidance signal. Most seekers have a stabilization loop to isolate body rotations and track loop to maintain the seeker axis along the missile-target direction. The measurement of the guidance signal depends on these loops as well as the ensuing signal processing. Developing a detailed model of this measurement process requires knowledge of the dynamics of the particular seeker employed as well as information about the radome characteristics and noise sources. In order to maintain generality and to avoid obfuscation of the results in this study, it has been assumed that the components of the LOS rate vector are measured perfectly. The perfect measure is given by the projection of $\vec{\Omega}$ into missile body fixed coordinates via the direction cosine matrix transform. The next section describes how the measured LOS angular rate components are processed to form corrective steering commands.

7.4 Guidance Signal Processing

Guidance signal processing encompasses the tasks of filtering the LOS rate measurements and of forming steering commands to be used by the autopilot. Although this study assumes that the measurement of LOS rates is done perfectly (i.e., free of noise) it is necessary to include the effects of any filtering that would be included under actual conditions. It is assumed that the low frequency characteristics of the noise filtering may be adequately represented by a first order lag, whose time constant (τ_g) is to be selected as a parameter of the study.

A point of difference between skid-to-turn steering and bank-to-turn steering is the implementation of the guidance signal noise filter. In previous studies, [7], [8], it was shown that for a BTT system it is desirable to transform the measured LOS angular rate components, prior to filtering, from the body fixed reference frame to one which translates with the missile but does not roll. The filtering operation, as performed in a nonrolling reference frame, effectively removes the coupling of the noise filter dynamics from the response of the roll control subsystem. This is expected to improve performance and stability characteristics. Since the STT vehicle does not roll, it is not necessary to implement a

coordinate frame transformation on the measured LOS rates.

After filtering, the guidance signal processor formulates steering commands. Since the control variable is missile lateral acceleration, an appropriate transformation from angular rotation rate (deg/sec) of the LOS components to acceleration (g) is performed. In the case of true proportional navigation this transformation is accomplished by scaling each filtered measurement with the factor

$$\frac{\Lambda \dot{R}}{562.33\ (\cos\gamma_L)} \quad \text{g/deg/sec}$$

where Λ = effective navigation ratio

$\dot{R}$ = range rate (m/sec)

γ_L = look angle (angle from missile centerline to LOS vector).

In practice it has been observed that a navigation ratio value of 4 provides acceptable performance against most threats. For this study, the value of $\Lambda = 4$ was selected.

The total commanded lateral acceleration which will drive the angular rotation rate of the LOS to zero is given by the vector sum of the two orthogonal components. In the case of a vehicle which uses two orthogonal (Cartesian) steering channels such as STT or BTT-45, the output from the scaling operation may be directly used to command the pitch and yaw autopilots. However, in either the BTT-90 or BTT-180 configuration these Cartesian components are not compatible with the polar control format of the bank-to-turn autopilot. Therefore, a Cartesian-to-polar coordinate conversion is required. The magnitude of the resultant vector will form the pitch autopilot acceleration command and the polar orientation of the resultant vector will specify the desired roll attitude. A discussion of roll command formation will be deferred until the next section.

The Cartesian-to-polar coordinate conversion introduces a singularity into the BTT steering commands. If the magnitudes of the commanded acceleration components become sufficiently small the polar orientation angle will be undefined. To avoid this possibility, some form of dead zone is selected based upon the expected level of noise in the system. For this study, which does not include noise effects, the width of the dead zone was set such that any acceleration above 0.05 g would allow the roll autopilot to call for rotation of the airframe. Values of acceleration below this level would result in no rolling motion. A more detailed discussion of this dead zone policy is presented in Appendix B.

7.5 Steering Policies and Autopilot Representations

The previous sections have described the portion of the guidance loop that deals with measurement of the relative motion between missile and target, formation of guidance signals from these measurements and development of the components of commanded acceleration required to drive the angular rotation rate of the LOS vector to zero. It was noted that both STT and BTT-45 are compatible with the orthogonal components of the commanded acceleration vector since both steering policies have equal maneuverability in either the pitch or yaw control channels. However, for the BTT-90 and BTT-180 configurations which could have limitations placed on yaw maneuverability due to sideslip constraints, the Cartesian steering commands must be transformed to polar steering commands corresponding to pitch acceleration and desired roll attitude. This section describes the details of combining either the Cartesian or polar steering commands with an appropriate representation of the autopilot characteristics associated with the four steering policies being investigated.

Autopilots are one of the most complicated missile subsystems. Considerable effort is spent designing a system which exhibits fast response and stability throughout the flight envelope. Detailed knowledge of the full nonlinear aerodynamic characteristics is required to develop these control systems. The resulting stable combination of autopilot hardware and airframe is very complicated and difficult to model accurately. However, a low frequency representation of the autopilot is adequate for

parametric studies of homing performance. For this study, a first order lag is used to model the low frequency control characteristics and trim aerodynamic data are used to model the general lift and drag characteristics. This simplified representatation is particularly useful in evaluating the range of system parameters that yield acceptable performance since it is not necessary to completely redesign the autopilot each time a new set of parameters is investigated.

The simplified autopilot models developed for this study are intended to simulate the response of the missile that would follow as a result of exercising the control function for the given steering policy. As such, these simple models do not indicate how the actual autopilot would be implemented. Table 2.1 contains a list of the control features associated with the four steering policies being investigated. The functions of the three control channels are shown along with any restrictions. The operation of the pitch, yaw and roll channels are essentially independent for both STT and BTT-45. Thus it is possible to develop a separate model for each channel. However, in the case of BTT-90 or BTT-180, the yaw and roll channels are coupled to form a coordinated autopilot representation. The next four subsections will describe the details of these control models for each steering policy.

7.5.1 STT

Skid-to-turn is a Cartesian steering policy which utilizes both the pitch and yaw steering channels to develop the required lateral acceleration and the roll channel to stabilize the airframe roll attitude. Figure 7.3 illustrates the simplified representation of the guidance and control subsystems for the STT configuration.

Inputs to the guidance noise filters are the measured components of the LOS angular rate $(\dot{\sigma}_p, \dot{\sigma}_y)$. Following the first order filters is the scaling factor for proportional navigation. The scaled signals (n_{pc}, n_{yc}) represent the commanded acceleration for the pitch and yaw channels, respectively. In order to prevent the possibility of commanding acceleration levels which could cause structural damage to the airframe or create excessively large angles-of-attack it is necessary to limit the input to

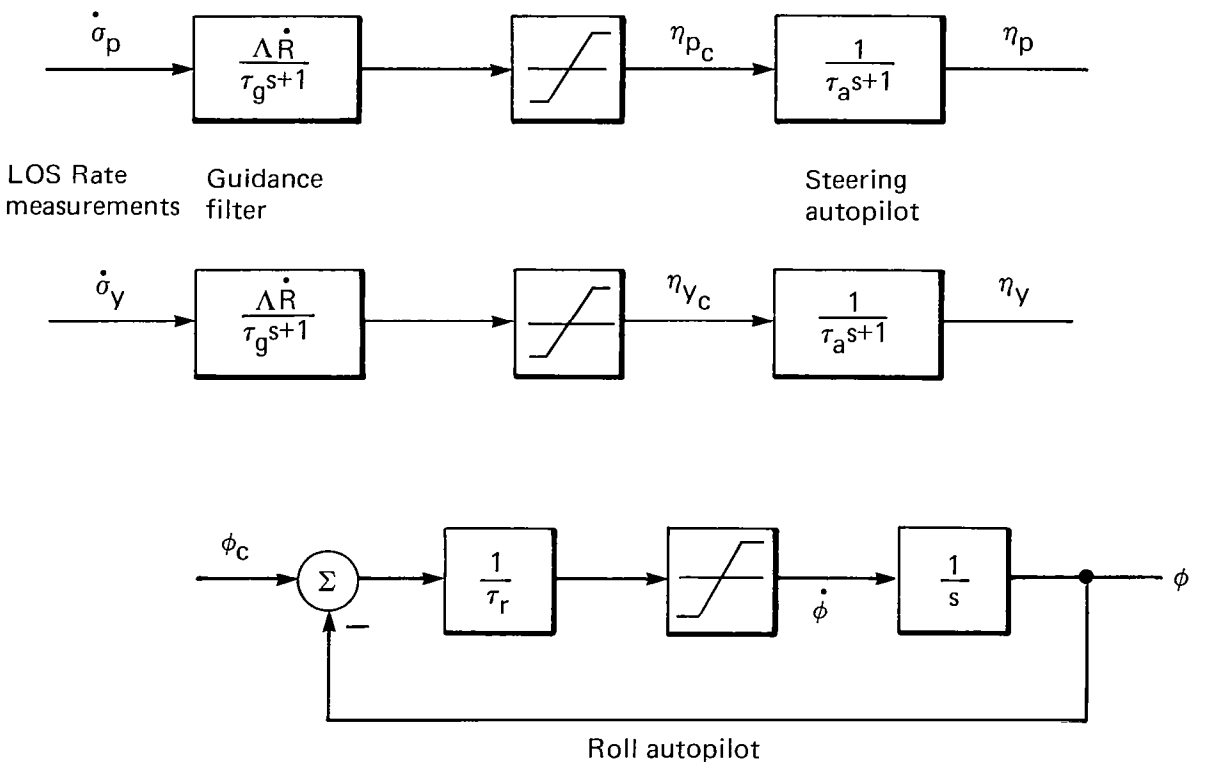

Fig. 7.3 STT functional block diagram.

the autopilot. The level of the limiter is set by the smaller value of structural limit or maximum angle-of-attack. Identical first order lags (τ_a) provide the low frequency approximation to the characteristics of autopilot and airframe (aero/control) response. The output of each lag is achieved acceleration in the respective control channel. In addition to the pitch and yaw steering channels, there is a first order control loop approximation to the roll autopilot, which includes rate limiting. The purpose of the rate limit is to avoid rotating the airframe at a rate which would exceed subsystem capabilities such as maximum seeker slew rates. The actual significance of the roll rate limit is more readily observed for the bank-to-turn configurations.

7.5.2 BTT-45

The BTT-45 steering policy is a Cartesian steering policy augmented by roll control. The purpose of rolling, as described earlier, is to effect a combined plane maneuver, which is characterized by equal acceleration components in the pitch and yaw channels. A detailed description of this steering policy can be found in Reference [4].

Figure 7.4 illustrates the guidance and control subsystem representation. The measured LOS rate components are transformed from the body fixed reference frame to a nonrolling frame where they are processed by the first order noise filters (τ_g) and scaled to form acceleration commands. After filtering and scaling, the signals are transformed back to the body fixed reference frame. The acceleration commands are limited and applied to the aero/control model. The aero/control model for the BTT configurations is different from that of the STT model. In Reference [9] it was shown that modelling the lags associated with the autopilot and airframe in a nonrolling reference frame provides a better representation of the physical process by which acceleration is developed on the missile body during a rolling maneuver. After transforming the acceleration commands to the nonrolling frame, these signals are low pass filtered by the first order aero/control lags (τ_a) in each channel and transformed back to the missile body reference frame where they represent the achieved pitch and yaw channel accelerations.

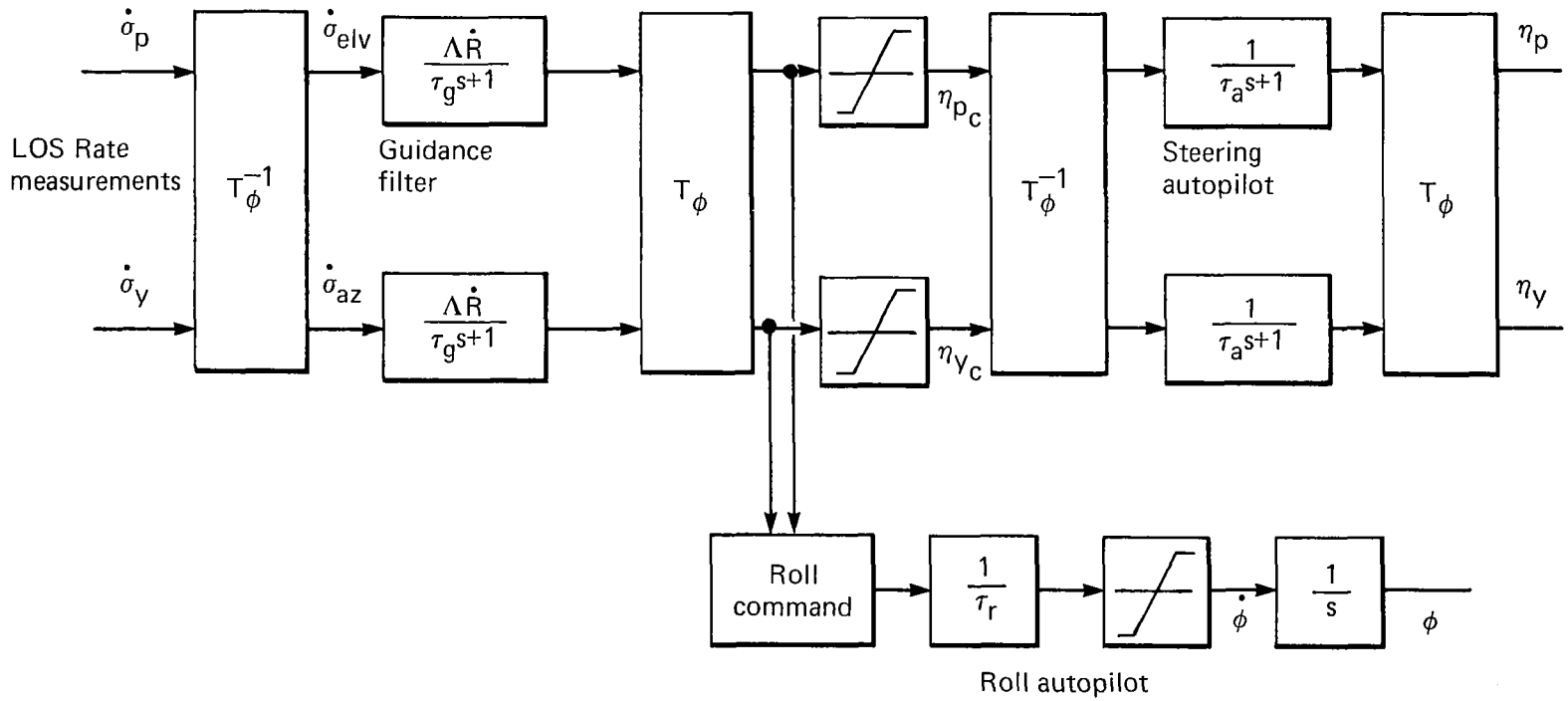

Fig. 7.4 BTT-45 functional block diagram.

Unlike the constant roll command for a STT configuration, the roll command for a BTT-45 policy changes according to the following functional relationship dependent upon commanded pitch and yaw accelerations,

$$\Delta\phi_c = \text{mod}_{90} \left[\arctan \frac{n_{yc}}{n_{pc}} + 90°\right] - 45°$$

where mod_{90} represents the modulo function with a modulus of 90 degrees. This command assures that the acceleration is equally distributed between the pitch and yaw channels and that a maximum roll excursion of 45 degrees will be required to reach the combined plane. The roll autopilot is modelled by a first order control path with rate limiting.

7.5.3 BTT-180

The BTT-180 policy would be used for a configuration which is intended to operate with positive load factors only and restricted sideslip, thus confining the lift vector to the positive half of the pitch plane (e.g., a chin-inlet ramjet-propelled missile). Maneuvers, called coordinated turns, are carried out by banking the missile airframe about the velocity vector. This requires design of a coordinated autopilot. Although the methodology for designing a coordinated autopilot is not well developed, the basic kinematic requirements which must be satisfied for a coordinated turn to occur are understood. Reference [7] has shown that this kinematic requirement may be approximated in terms of the missile body rotation rates as follows,

$$r = \dot{\phi} \tan\alpha$$

where r = yaw rotation rate

$\dot{\phi}$ = roll rate

α = total angle-of-attack.

This expression suggests that the yaw and roll control systems must be coupled in order to develop the proper response. A simple model, which is believed to reflect the characteristics of a coordinated autopilot, has been developed and is documented in Reference [8].

Figure 7.5 illustrates the guidance and control subsystem models for the BTT-180 steering policy. The inputs to the model are the measured components of LOS angular rotation rate which are filtered and scaled in

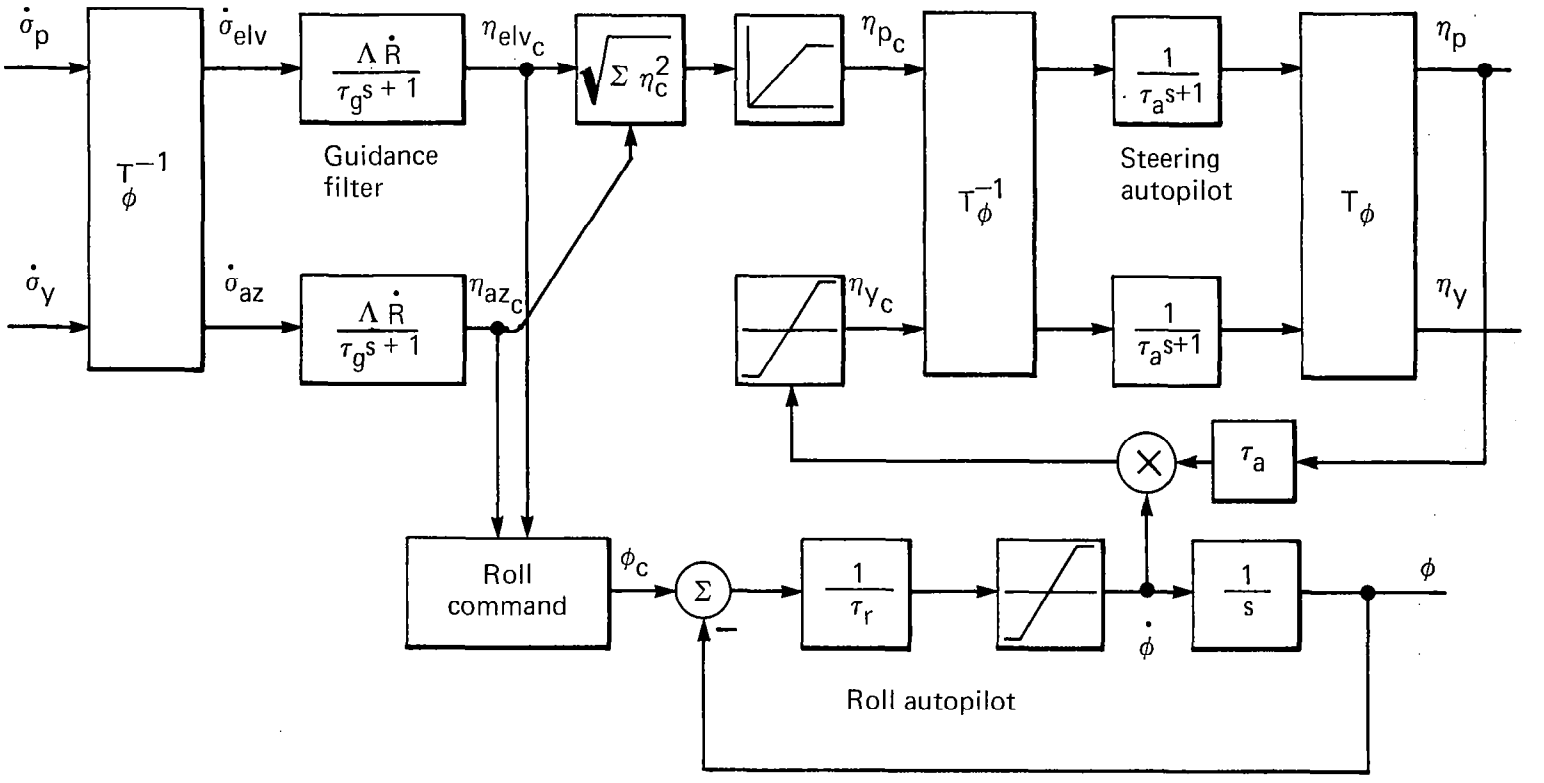

Fig. 7.5 BTT-180 (6 DOF) functional block diagram.

a nonrolling frame by the guidance signal processing section. The commanded acceleration components, in the nonrolling reference frame, are directly converted to polar steering commands. Since the magnitude of the acceleration command vector is invariant to the reference frame and since the roll control subsystem can be properly configured, it is not necessary to include a transformation from nonrolling to body reference frame here.

The magnitude of the acceleration command is limited and applied to the pitch channel of the aero/control model. Turn coordination is accomplished by forming the yaw acceleration command as a product of roll rate, yaw channel aero/control time constant (τ_a), and achieved pitch acceleration. The steering lags are represented in a nonrolling coordinate frame. The roll subsystem is modelled by a first order control loop with rate limiting. The roll system command is given by

$$\phi_c = \arctan \frac{\eta_{az_c}}{\eta_{elv_c}} .$$

A further simplification of this model is possible when it is assumed that the autopilot is capable of maintaining perfect coordination. Perfect coordination implies that sideslip is identically zero or equivalently yaw acceleration is zero. By modelling the pitch and yaw system as two separate channels, as shown in Figure 7.6, and by commanding the pitch channel with the magnitude of the acceleration command while the yaw command is zero it is possible to represent the characteristics of a perfectly coordinated autopilot. This simpler version is referred to as the 5 degree-of-freedom (5 DOF) coordination model and is used for the majority of the performance comparisons in this study. Simulation studies (see Appendix C) have shown that the 5 DOF model agrees very well with the 6 DOF model previously described. In addition, the computational costs of the 5 DOF model are less than those for the 6 DOF model.

7.5.4 BTT-90

The BTT-90 steering policy is similar to the BTT-180 steering policy. However, the constraint on negative load factors has been removed. In this

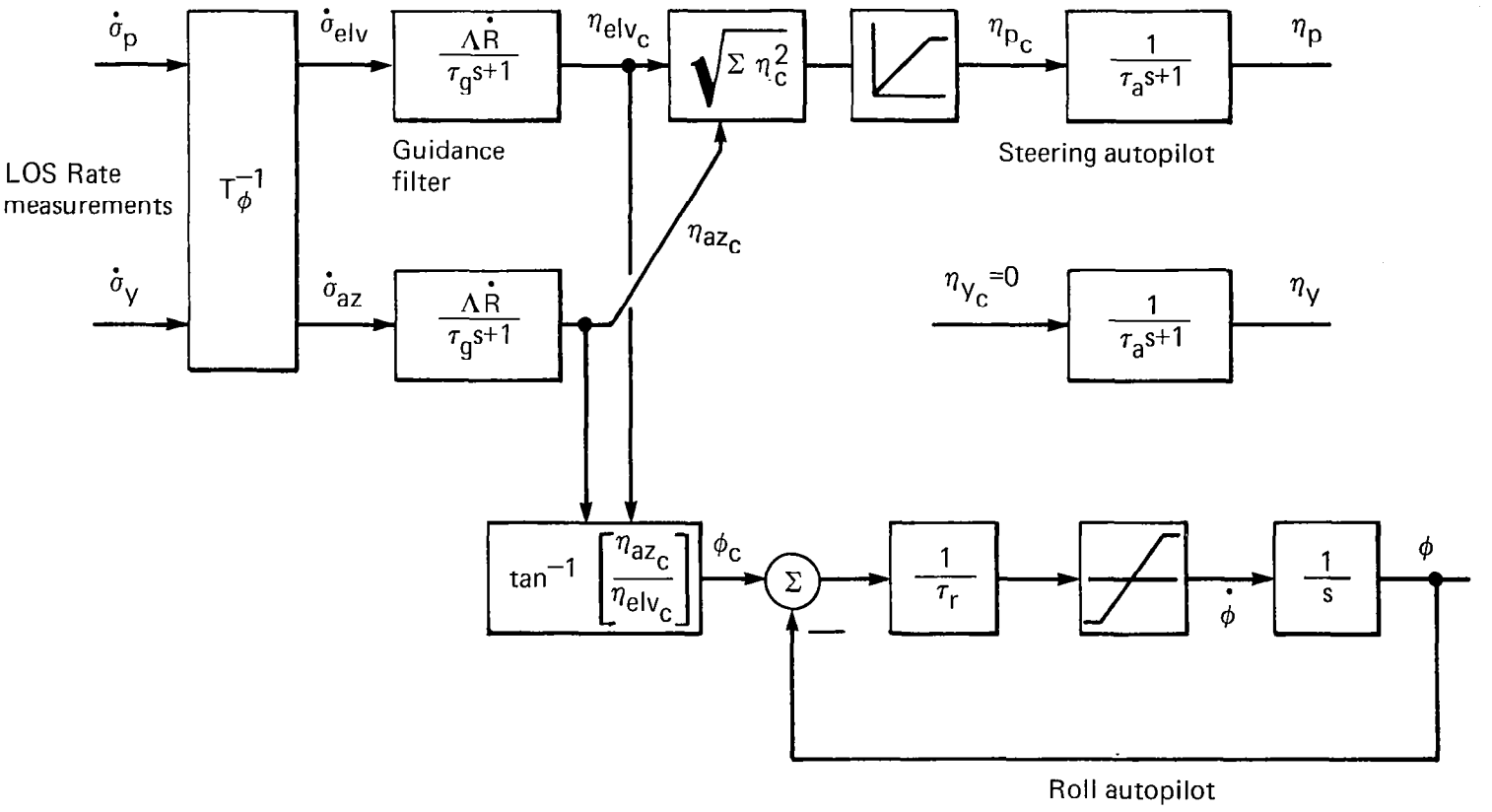

Fig. 7.6 BTT-180 (5 DOF) functional block diagram.

case, the maximum roll attitude error is 90 degrees. For example, if the missile were pulling a positive load factor and an abrupt change in command to a negative load factor were called for, this steering policy would maintain the present roll attitude and reverse the angle-of-attack in the pitch plane, whereas a BTT-180 configuration would be forced to roll the airframe 180 degrees. This type of steering policy might be used with any planar winged configuration having symmetry about the plane of the wings.

Figure 7.7 illustrates the guidance and control representation for the BTT-90 steering policy. This simplified representation assumes perfect turn coordination, thus the 5 DOF coordination model is used. The measured LOS rates are filtered and scaled to form commanded acceleration components. These commands are transformed to polar steering commands. The pitch command, given by the magnitude of commanded acceleration, is limited and scaled by the appropriate sign factor. The sign factor is determined by the amount of roll attitude error. If the roll attitude error is greater than 90 degrees the scale factor is -1 and if the error is less than 90 degrees the scale factor is +1. The roll command is given by

$$\phi_c = \arctan \frac{n_{az_c}}{n_{elv_c}}$$

and the roll attitude error is given by

$$\Delta\phi_c = \phi_c - \phi \quad .$$

The roll control subsystem is modelled as a first order control loop with rate limiting and a logic section called MRE (minimum roll excursion logic). The function of the MRE logic is to determine when the roll attitude error is larger than 90 degrees. When this occurs, the sign factor in the pitch channel is set to -1 and the roll control signal is appropriately modified to point the negative half of the pitch plane in the desired maneuver direction.

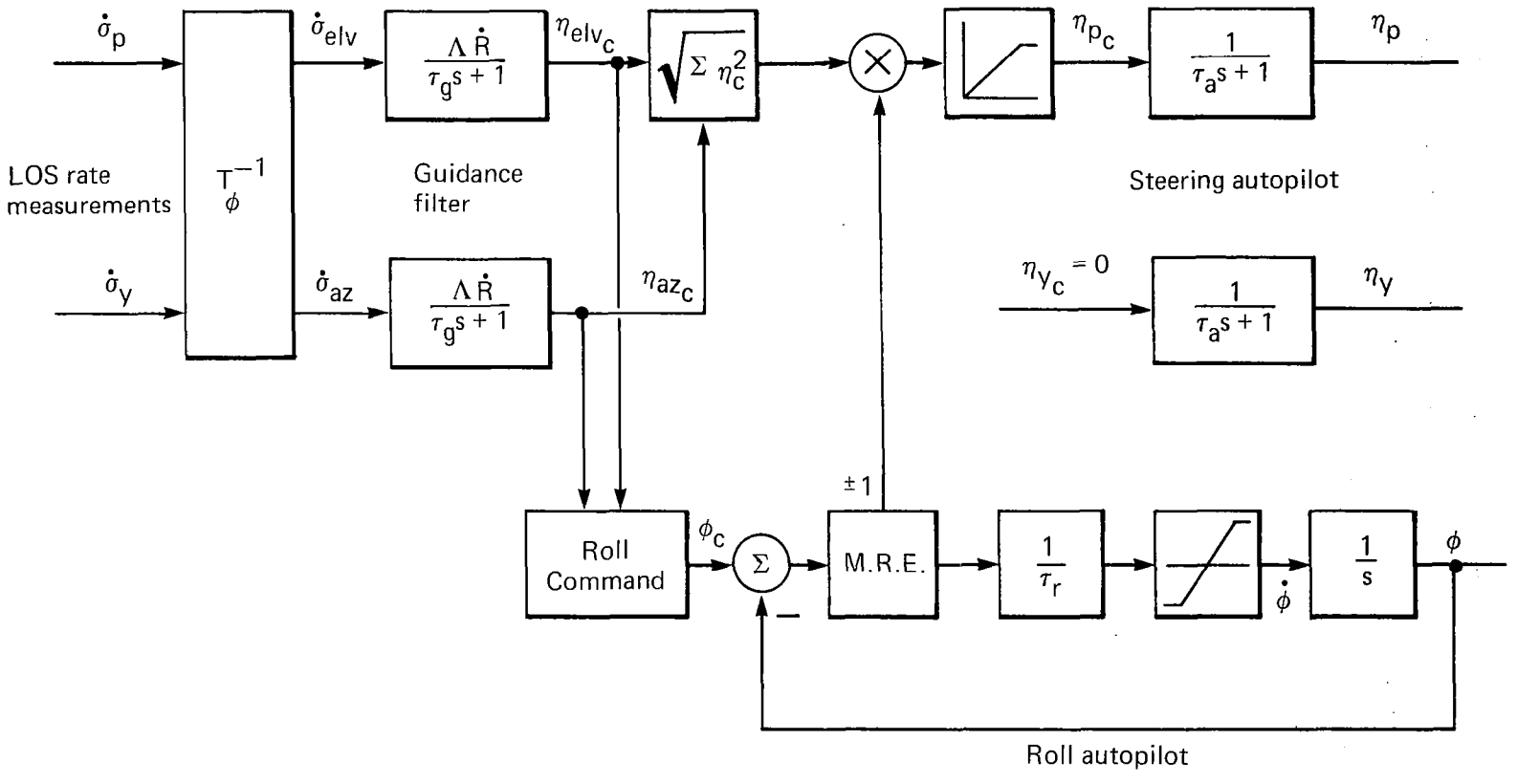

Fig. 7.7 BTT-90 functional block diagram.

It should be noted that it is possible for the BTT-90 configuration to roll more than 90 degrees for a given maneuver. This condition occurs whenever the roll command (ϕ_c) changes slowly enough for the roll system to follow it with less than 90 degrees of roll attitude error. Under this condition the BTT-90 configuration responds the same as does the BTT-180 configuration. If, for a given engagement scenario, the roll attitude error never exceeds 90 degrees, the performance of BTT-90 and BTT-180 would be identical.

This concludes the description of the representation of the aero/control models for the steering policies investigated in this study. The next section discusses the implementation of these models within a computer simulation using trim aerodynamics and 6 degrees-of-freedom.

7.6 Implementation and Validation

A composite implementation of the simplified models and aerodynamic data in computer simulation form is required to evaluate the performance of the various configurations. A 6 degree-of-freedom computer simulation of a terminal homing interceptor which includes trim aerodynamic data and simplified representations of the various control subsystems has been developed in support of other programs. The basic framework of this model has been incorporated as the simulation tool for this study. Appropriate modifications to the aerodynamic data and subsystem models have been introduced to produce an analysis tool suitable for this study.

Validation of this trim aerodynamic simulation has been performed previously for a skid-to-turn steering policy. The rates and accelerations computed using this simulation compare very well with a more detailed model of the same system (higher order pitch, yaw and roll autopilots). Relative performance trends are also similar, thus verifying conclusions drawn from from the trim aerodynamic simulation. After modifying the more sophisticated system model to accept open loop commands to the roll autopilot it was possible to compare responses of the autopilot models for a rolling maneuver, thereby verifying the bank-to-turn versions. The methodology employed was to simultaneously apply a 5 g acceleration command to the pitch channel

(with zero g to the yaw channel) and a 90 degree roll command to the roll autopilot. The response of the pitch, yaw and roll systems was observed. Figures 7.8 (a-g) contain the following comparisons

7.8a pitch acceleration

7.8b pitch body rotation rate

7.8c total angle-of-attack

7.8d yaw acceleration

7.8e yaw body rotation rate

7.8f sideslip angle

7.8g roll attitude.

In Figures 7.8a-c the response of the simplified model (dashed line) is shown to be a very good low order approximation to the more detailed version (solid line). The small magnitude of achieved body rotation rate is typical of the response obtained from a trim aerodynamic simulation since the dynamics associated with the moment equations are not modelled.

The yaw acceleration, yaw rotation rate and sideslip angle (Figures 7.8d-f) all become negative at about 0.7 second for the complex model; the responses of the simpler model do not. The overshoots in the complex model result from the overshoot in the roll response (Figure 7.8g). Since the simpler model has a first order roll model it will never overshoot its command. If a higher order roll model were included as a part of this simpler model, these responses could be tracked more faithfully.

These results are considered adequate. Therefore the simpler model is used as the simulation tool for the performance comparisons. As indicated above, this greatly simplifies the comparison of performance as system parameters are varied and reduces the computational cost.

The next section discusses the results of the performance comparison for the moderate-lift (cruciform) and high-lift (planar) airframe configurations employing the various steering policies previously described.

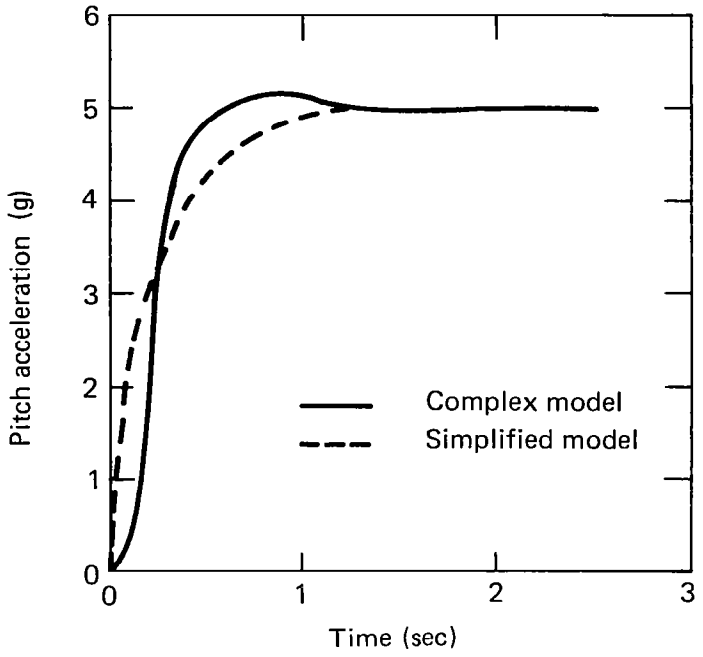

Fig. 7.8a Autopilot comparison of pitch acceleration response.

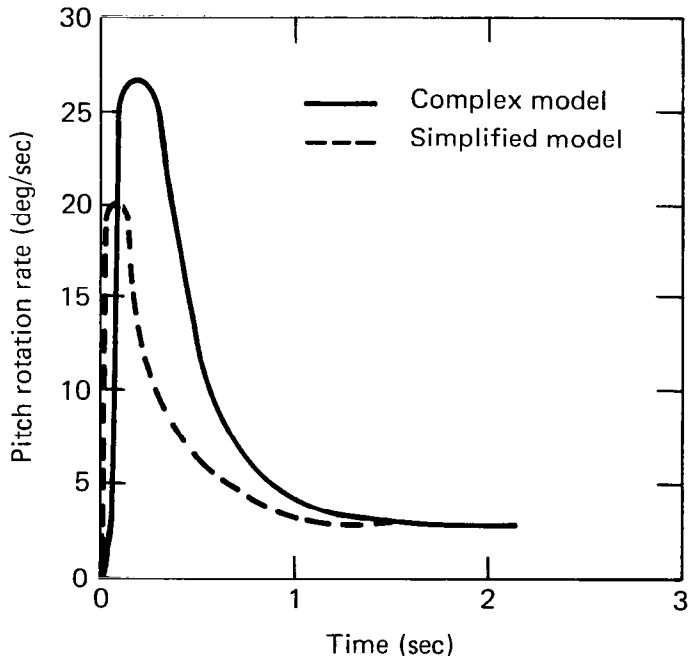

Fig. 7.8b Autopilot comparison of pitch body rotation rate.

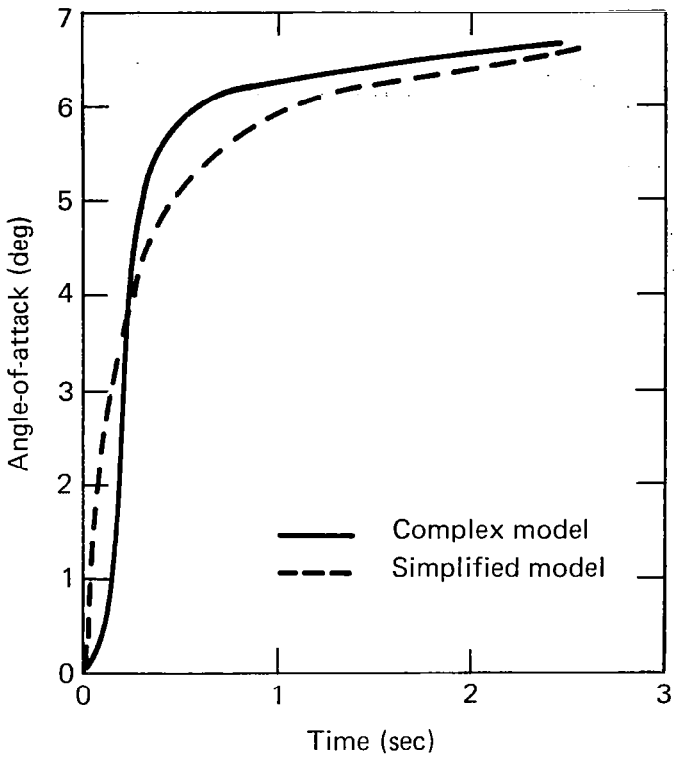

Fig. 7.8c Autopilot comparison of angle-of attack response.

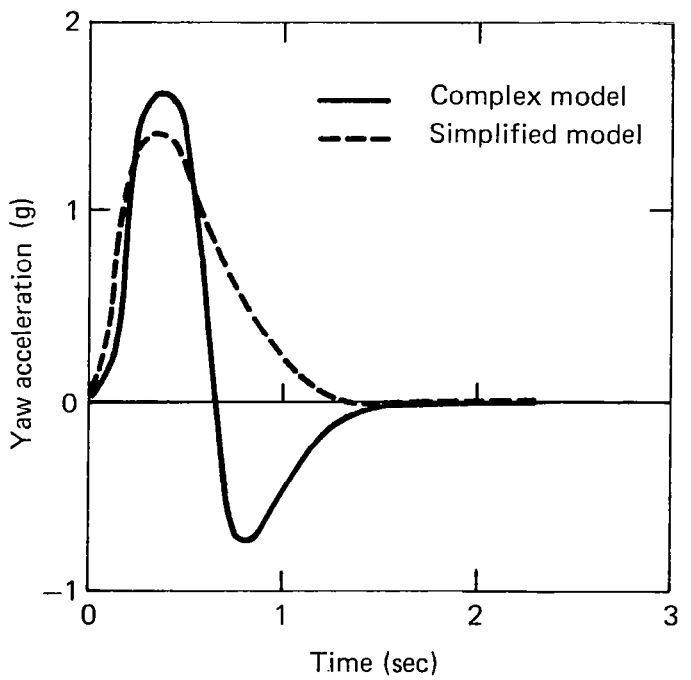

Fig. 7.8d Autopilot comparison of yaw acceleration response.

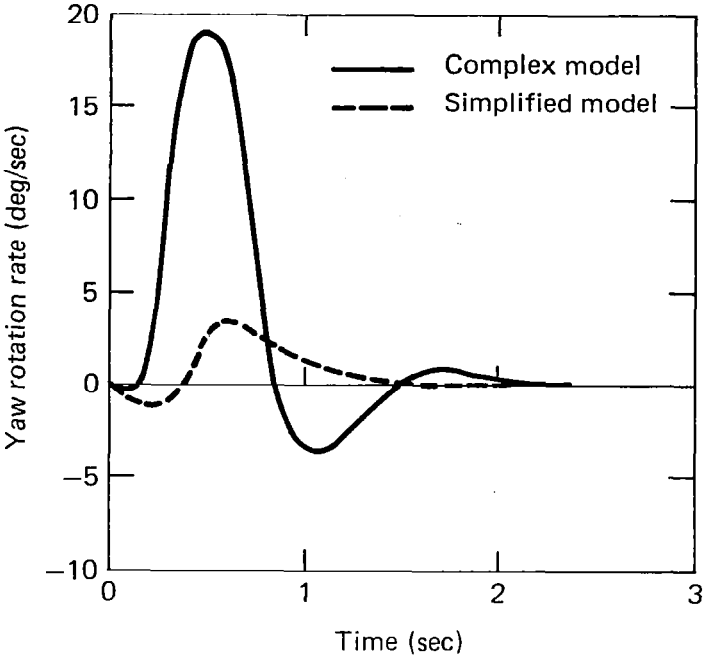

Fig. 7.8e Autopilot comparison of yaw body rotation rate.

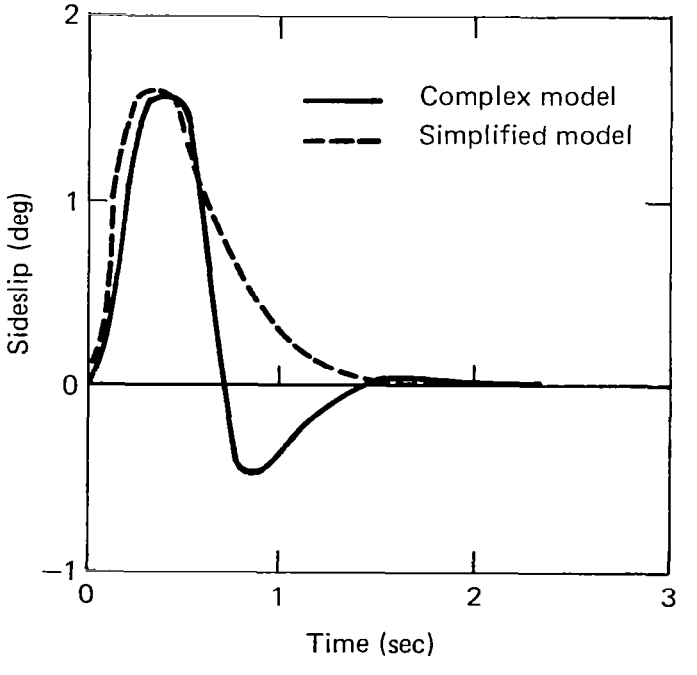

Fig. 7.8f Autopilot comparison of side slip angle response.

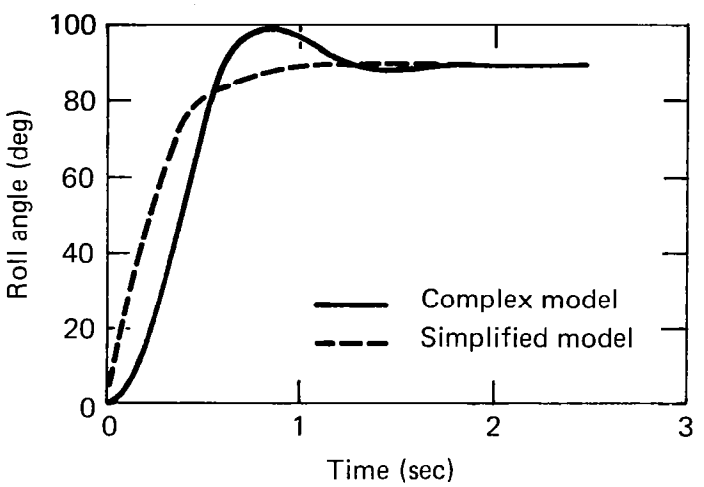

Fig. 7.8g Autopilot comparison of roll angle response.

8.0 RESULTS OF THE RAID SUPPRESSION PERFORMANCE COMPARISON

The objective of this study, as stated in the introduction, is to compare the performance of the high-lift planar airframe with the moderate-lift cruciform airframe and to assess the differences between steering policies and the effects of system parameter variations. A raid suppression engagement, described in Section 6, has been selected as a representative mission for the basis of comparison. The relative performance measure is defined as the minimum homing range (or time) required to achieve a 25 foot (7.62 meter) miss against a maneuvering Mach 2 target with specified heading error magnitudes of 10, 20, 30, and 40 degrees at the start of homing. The best airframe and steering policy combination is that which consistently shows a smaller minimum range (time) requirement.

The results of this performance assessment may be broken down into three categories as follows:

1. Comparison of steering policies for a given airframe.
2. Comparison of airframes for a given steering policy.
3. Effects of system parameter variations.

Sections 5 and 7 of this report have described the representations of the selected airframes and steering policies, and the system parameter values are chosen to be representative of the characteristics associated with a raid suppression interceptor. Two sets of values are selected corresponding to both a slow and a fast system response. Table 8.1 contains a list of these system parameters and their values.

TABLE 8.1 SYSTEM PARAMETERS

PARAMETER	SYMBOL	FAST SYSTEM	SLOW SYSTEM
aero/control lag	τ_a	0.2 sec	0.4 sec
guidance filter lag	τ_g	0.3 sec	0.5 sec
roll system lag	τ_r	0.2 sec	0.2 sec
acceleration limit	η_{lim}	30 g	30 g
angle-of-attack limit	α_{lim}	25 deg	25 deg
roll rate limit	$\dot{\phi}_{lim}$	250 deg/sec	250 deg/sec

The performance of each configuration is assessed using both sets of parameters, thereby allowing for investigation of the effect system parameters have upon the comparison.

Insight into the interpretation of the results that follow may be gained by considering the response of the various configurations for a typical engagement and by formulating concepts about how the system characteristics impact the response of each system. For the raid suppression engagement simulated here, it is initially assumed that the missile system has developed enough angle-of-attack to support itself against gravity and that all other subsystems are set to zero initial conditions. At homing initiation the target is offset to the side with some azimuthal heading error. As a consequence of the initial geometry, a large component of LOS angular rate is generated and measured by the missile tracking system. The resulting acceleration is commanded in the horizontal plane containing missile and target.

For the STT system, the result is an initial increase in yaw channel acceleration command with the response time set by the time constant τ_g. The acceleration command is limited and the achieved acceleration response time is set by the time constant τ_a. Due to the lags in the system, the response to initial conditions causes the missile to overshoot the ideal intercept trajectory. In response to the trajectory overshoot the yaw channel acceleration command reverses direction, thus correcting the missile heading. Additional errors in trajectory throughout the engagement are possible due to target acceleration and delays in missile system response. These errors may result in several additional overshoots before intercept occurs.

The fundamental system characteristics that influence STT performance are

1. Guidance filter lag
2. Aero/control lag
3. Acceleration and angle-of-attack limits
4. Trim lift characteristics.

Large values of τ_a and τ_g, resulting in a sluggish response, are expected to degrade performance. Since the lags are in series (see Figure 7.3) the sensitivity of performance to distribution of these lags is expected to be small, provided that command limiting is not prevalent. Increased lifting capability improves performance by increasing missile turning rate and by reducing maneuver-induced drag.

For the BTT-45 configuration, the response to initial conditions is characterized by a 45-degree roll maneuver followed by an increase in achieved acceleration in both steering channels. The overall initial response time is influenced by a combination of τ_g, τ_a, τ_r, and $\dot{\phi}_{lim}$. The out-of-plane motion induced by the control rolling motion is slight since very little angle-of-attack is developed before rolling. When a trajectory overshoot occurs in this engagement, the commanded acceleration changes angular orientation by 180 degrees. Since the missile and target remain coplanar, the components of the commanded acceleration remain equal during this reversal and the roll attitude command stays at 45 degrees. Thus, the missile does not roll. Since the missile does not roll in response to this overshoot or any following trajectory overshoots the system response time is solely dependent upon τ_a and τ_g, just as in the STT case. Under these conditions, the performance and sensitivity to system characteristics of BTT-45 and STT are expected to be similar.

For BTT-90 and BTT-180 the initial transient responses are equal. This initial maneuver is characterized by a 90-degree roll accompanied by an increase in pitch acceleration. The system response time is again influenced by τ_g, τ_a, τ_r and $\dot{\phi}_{lim}$. The induced out-of-plane motion is slightly larger for these systems since the duration of the roll maneuver is longer than for BTT-45 configuration. When a trajectory overshoot occurs the commanded acceleration must reverse direction. For BTT-180 the command reversal is carried out by rolling the missile airframe by 180 degrees about the velocity vector. For BTT-90, this may or may not be the case.

If for BTT-90, the roll attitude command reverses direction very rapidly, which may happen when τ_g is small and a trajectory overshoot occurs,

the roll subsystem may be incapable of tracking this command and the roll error quickly exceeds 90 degrees. As a result, the acceleration reversal is carried out by reversing the direction of the pitch acceleration and maintaining the same roll attitude. This type of response is essentially the same as for an STT system, and under these conditions performance and sensitivity to system characteristics is expected to be comparable for BTT-90 and STT. However, when τ_g is large the roll command changes more slowly and it may be possible for the roll system to track the command with less than 90 degrees of error. Under this condition the performance of BTT-90 and BTT-180 are expected to be comparable. For any given raid suppression engagement it is possible for both types of response to occur. When this happens the performance of BTT-90 will be somewhere between STT and BTT-180.

The system characteristics which influence BTT-90 and BTT-180 performance are as follows:

1. Guidance filter lag
2. Aero/control lag
3. Roll system lag
4. Roll rate limit
5. Acceleration and angle-of-attack limits
6. Trim lift characteristics.

The effects of the subsystem parameters on homing performance are more complexly interrelated for a BTT system than for a STT system. When the roll system lag is small, which is the case in this study, the roll rate limit takes precedence. A maximum roll rate limit consistent with the requirement of keeping the turn coordinated is desirable. In addition, small values of guidance filter lag and aero/control lag are desirable. Increased lifting capability is expected to improve performance by reducing maneuver drag and by increasing missile turning rate.

The next three sections will discuss the results of this study as broken down into the three categories described previously.

8.1 Comparison of Steering Policies

The performance of the STT, BTT-45, BTT-90 and BTT-180 steering policies has been assessed using the cruciform airframe characteristics. Figure 8.1 contains a graph of the comparison of performance measures for the four policies configured with the set of parameters using fast response time. The required range to go increases as initial heading error is increased for each configuration. For this set of parameters, the performance of STT, BTT-45 and BTT-90 are nearly identical, whereas the BTT-180 configuration exhibits slightly poorer performance. As described previously, it was expected that STT and BTT-45 would exhibit similar performance for this type of in-plane engagement. In addition, it was expected that BTT-90 would perform similar to STT provided that the guidance filter lag was small, as it is in this case.

A BTT-180 interceptor has some out-of-plane component of acceleration as it banks to reverse the direction of acceleration. The resulting out-of-plane excursion must be corrected by the homing guidance loop. If the bank system is fast relative to the pitch system, the out-of-plane motion is small and the acceleration direction can be reversed faster than an STT missile (see Appendix D). This is not true for the fast system parameters investigated here, resulting in the slightly poorer performance observed for the BTT-180 system.

Figure 8.2 illustrates the comparison of steering policies configured with the set of parameters using slow response time. The required range-to-go is larger than for the fast set of parameters shown in Figure 8.1. For a given steering policy the required range-to-go is nearly constant with heading error. This seemingly anomalous behavior is a result of the effect which slow down has upon the range-to-go performance criterion.

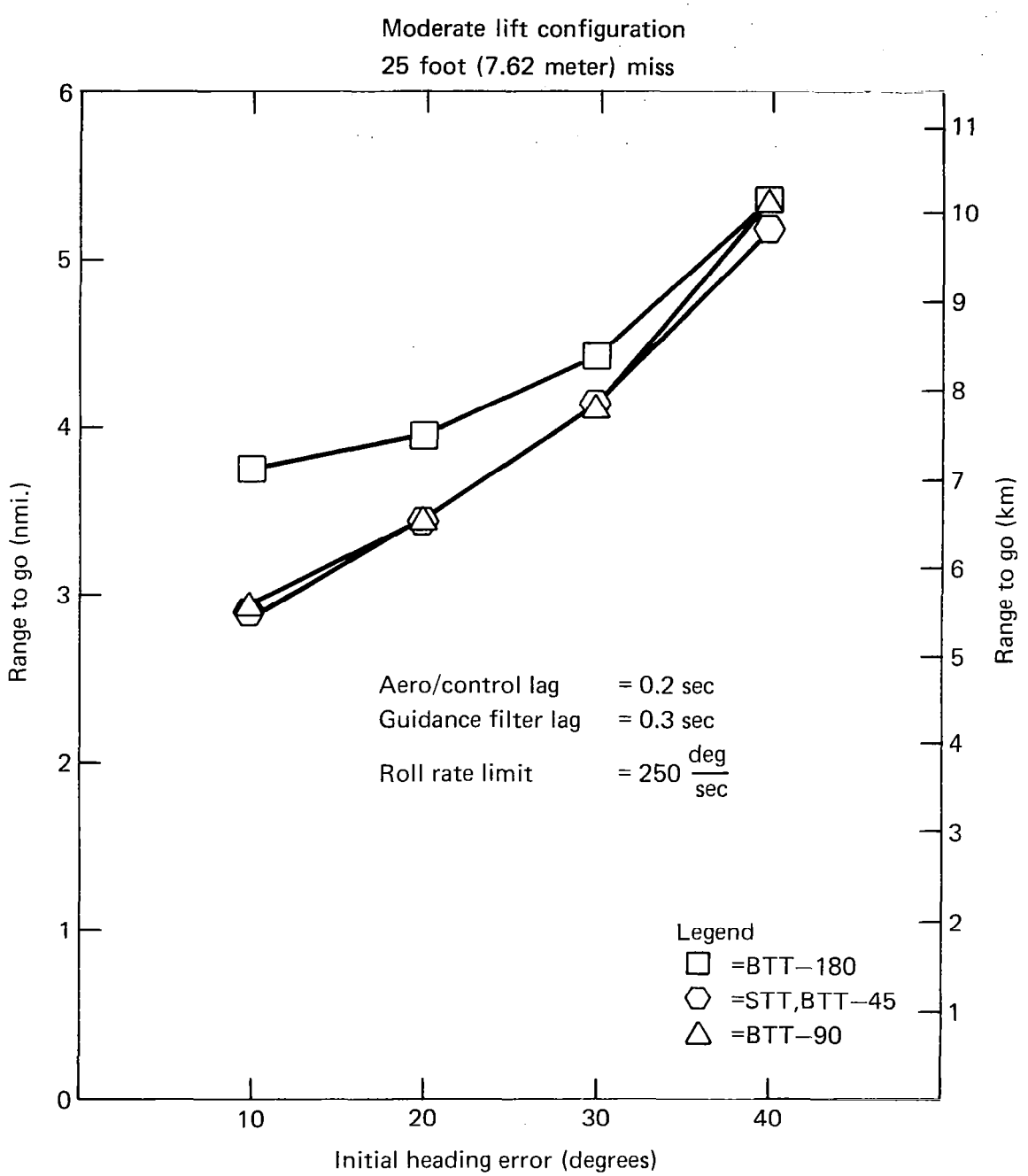

Fig. 8.1 Steering policy performance measure comparison.

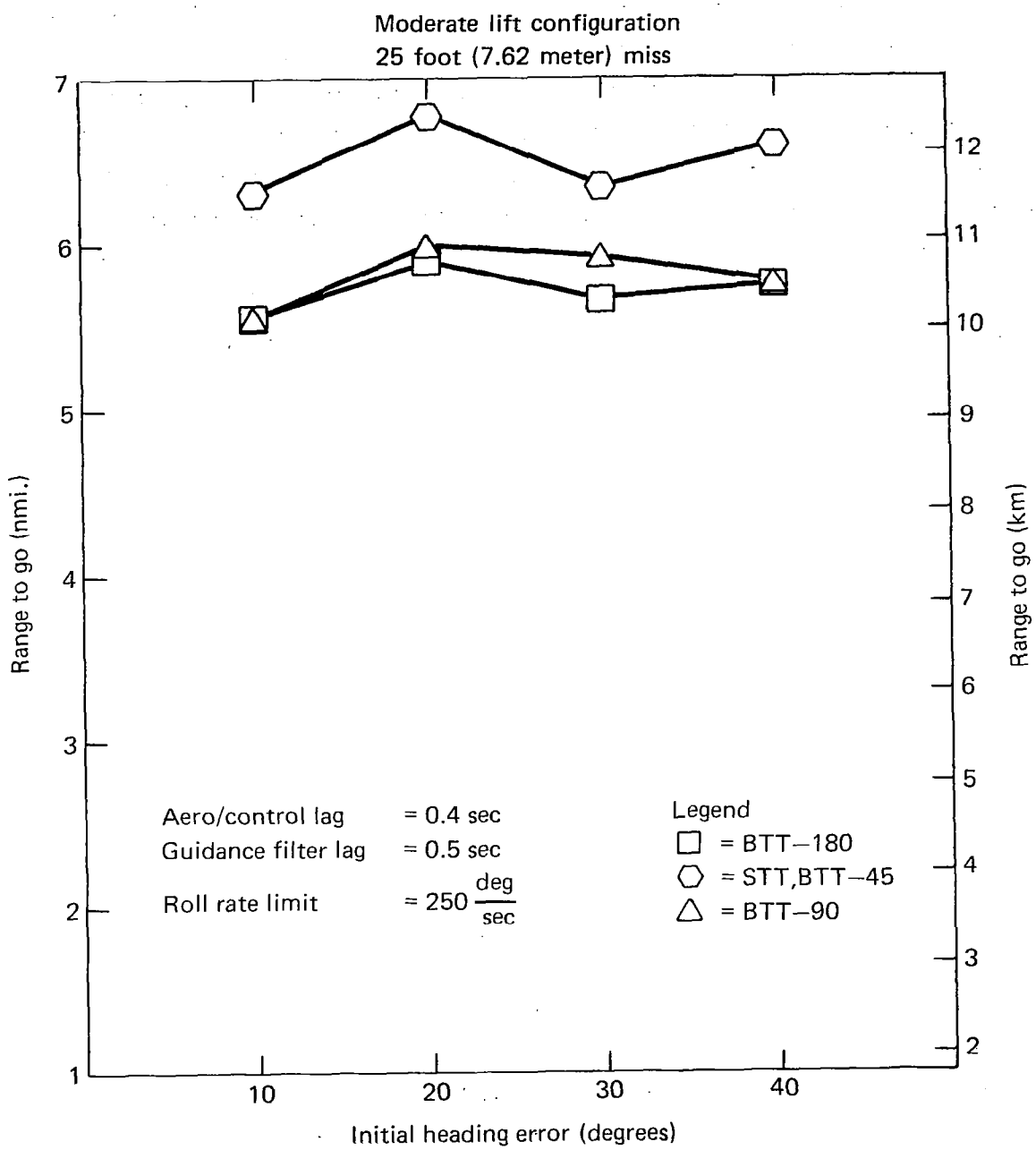

Fig. 8.2 Steering policy performance measure comparison.

As the initial heading error is increased, the missile is required to pull large angles-of-attack for longer periods of time. The actual homing time is significantly increased, thereby giving the sluggish interceptor more time to respond to trajectory overshoots and target motion. Although the range requirement is about the same for a 40-degree heading error and a 10-degree heading error, the required homing time may differ by several seconds as shown in Figure 8.3. This graph illustrates the homing time required to achieve 25-foot (7.62-meter) miss for each configuration. As the initial heading error is increased the amount of homing time required also increases as expected. These results show that BTT-180 outperforms both BTT-90 and STT, with BTT-90 performance lying between BTT-180 and STT.

Although the roll system is the same for both the slow and fast sets of parameters, it is relatively faster for the slow parameters. Thus it is possible to reverse the acceleration direction faster by banking about the velocity vector than by pitching back, as is done for the STT missile. This relatively smaller maneuver response time for BTT-180 accounts for the better performance.

Figure 8.4 and 8.5 show the performance curves when the miss criterion is 50 feet (15.24 meters) rather than 25 feet (7.62 meters) as in Figures 8.1 and 8.2. As can be seen, the relative comparison and observations made above do not change for the larger miss criterion.

8.2 Comparison of Airframe Configurations

The airframe configurations modelled in this study differ primarily in lift characteristics. Since both configurations are modelled with the same angle-of-attack limit and acceleration limit, the principal factor which accounts for differences in relative performance is the amount of maneuver-induced drag or slow down. As noted earlier the interpretation of results from a measurement of the range-to-go performance criterion may be confounded by the effects of maneuver-induced slow down; the homing time performance criterion helps to resolve the confusion. Since maneuver-

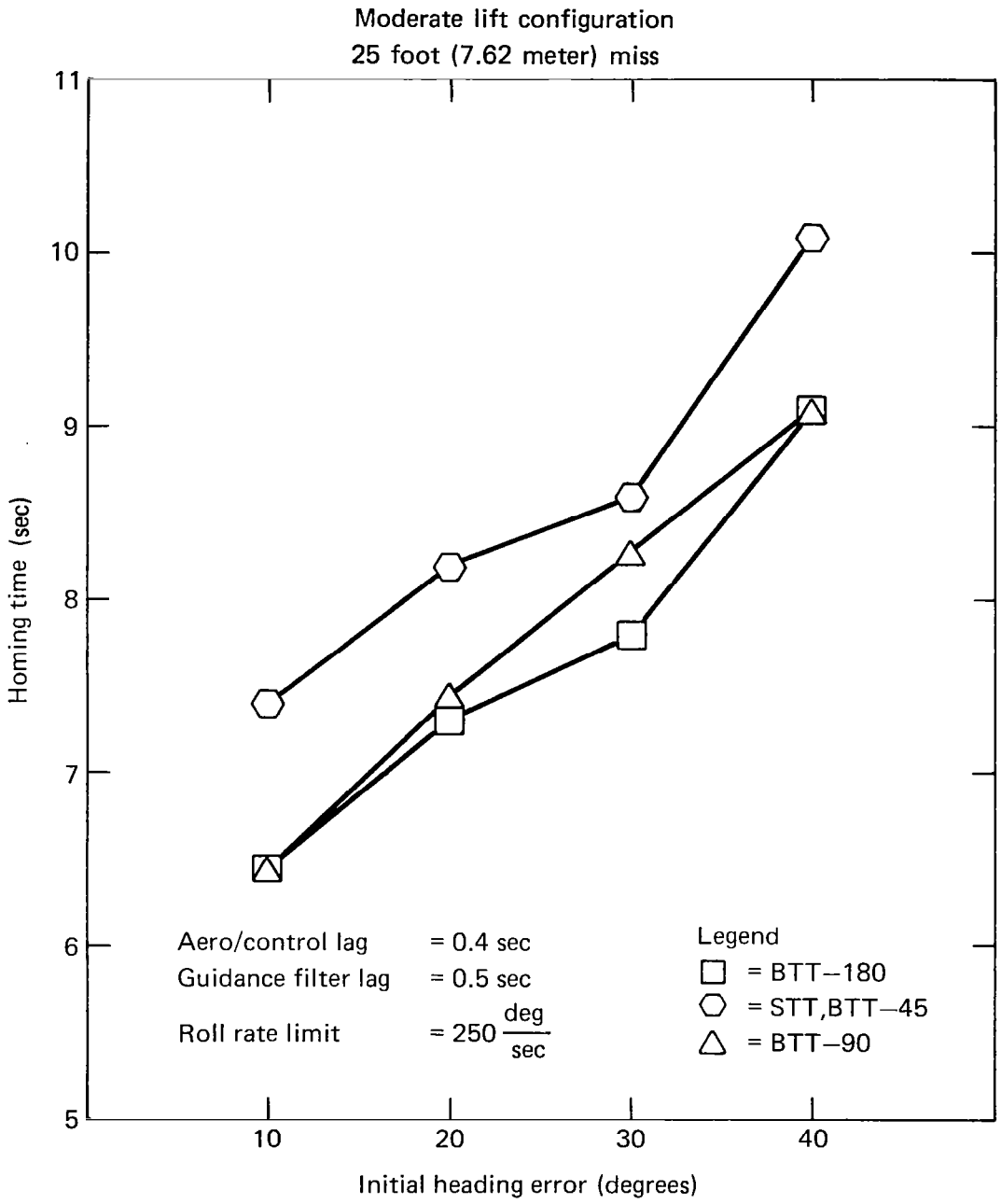

Fig. 8.3 Steering policy homing time comparison.

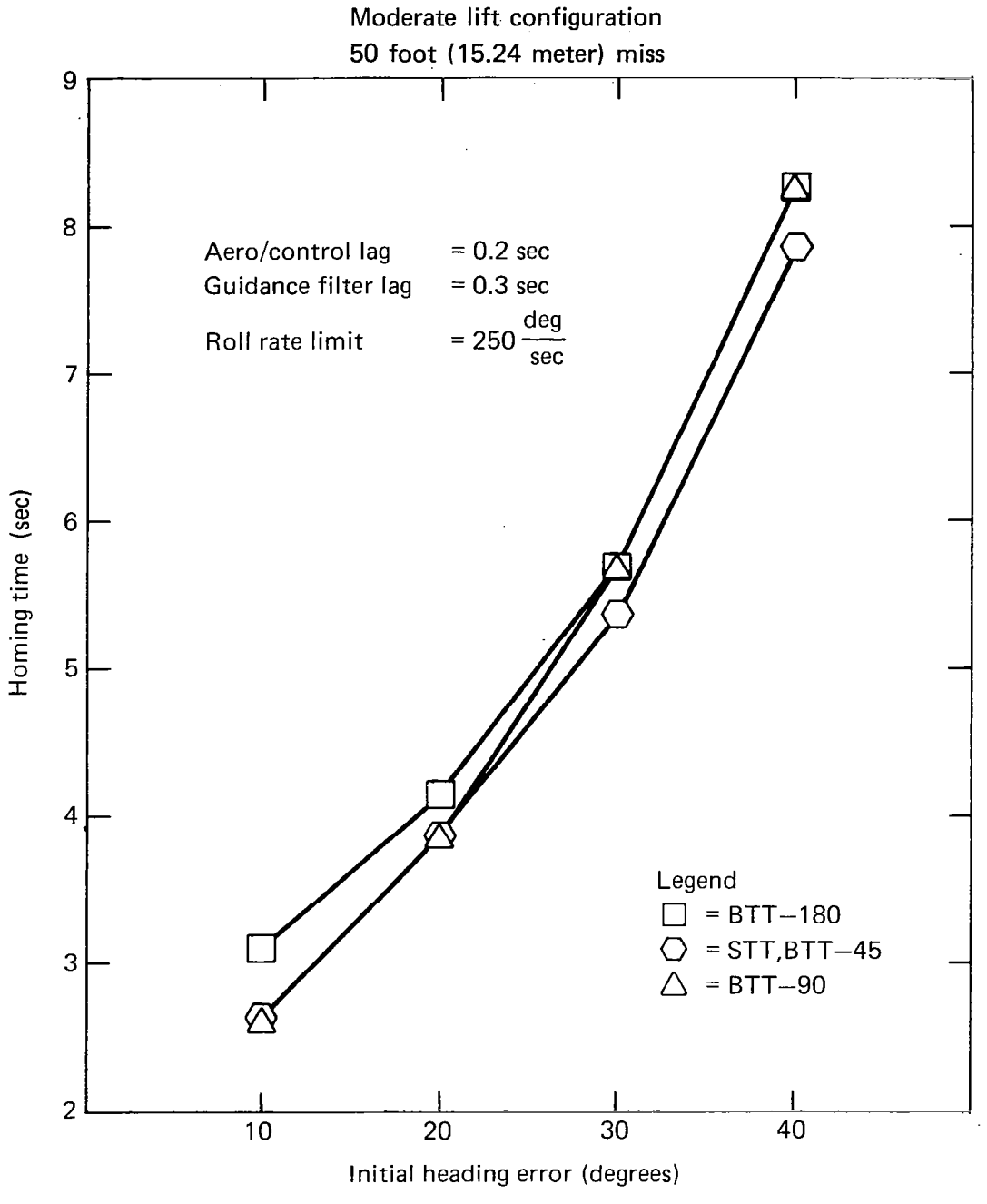

Fig. 8.4 Steering policy homing time comparison.

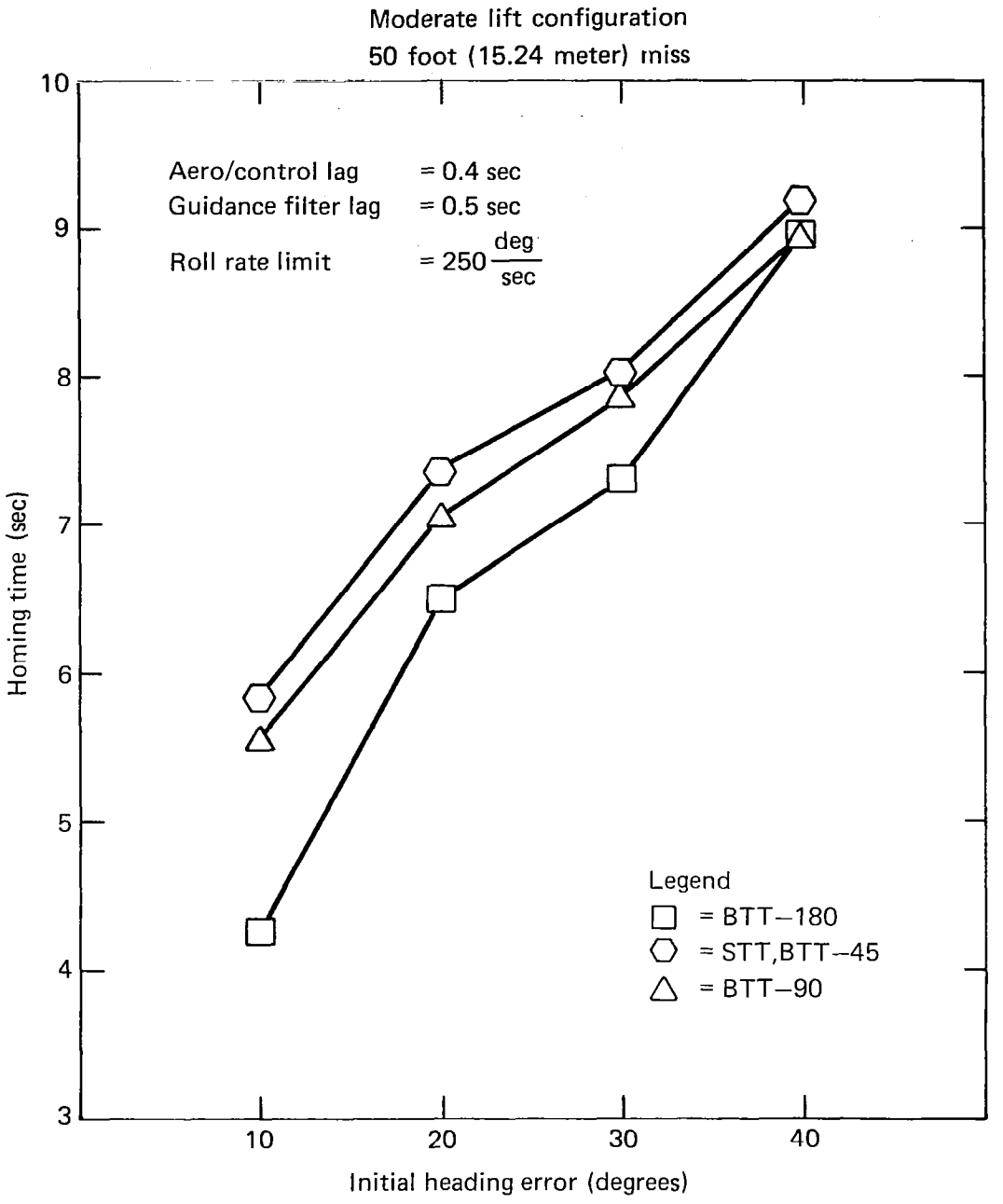

Fig. 8.5 Steering policy homing time comparison.

induced drag is the major factor of difference here, comparative results and conclusions are made using the homing time performance criterion.

The performance of the moderate-lift cruciform airframe and the high-lift planar airframe are compared for both the BTT-90 and BTT-180 steering policies. Figure 8.6 contains the comparison of configurations using the BTT-90 steering policy with fast system parameters. For the relatively easier engagements (small initial heading error) performance is comparable; however, as the engagement begins to stress the capability of both systems (larger initial heading error) the high-lift planar airframe configuration exhibits better performance than the moderate-lift cruciform configuration. As maneuver induced drag causes the missile to slow down, maneuverability is curtailed by the imposed 25 degree angle-of-attack limit. Since the planar configuration has higher lift capability, the 25 degrees of angle-of-attack translate into more gees and better performance. Figures 8.7-8.9 illustrate similar results for BTT-90 with slow parameters, BTT-180 with fast parameters and BTT-180 with slow parameters, respectively.

8.3 Effect of System Parameters on the Performance Comparison

Some of the effects which system parameter variations may have upon performance of the various configurations have been demonstrated in the previous two sections. The intent of this section is to identify the fundamental system parameter effects which influence the performance of each configuration and not to define the set of values of each parameter which yields optimum performance.

8.3.1 STT and BTT-45

The slower response caused by increases in aero/control and guidance lags degrades performance. For less strenuous engagements (small initial heading error) the degradation in performance is nearly linearly related to the increase in the sum of the parameter values. For the most strenuous engagements, which involve considerable maneuver limiting, this is not true.

The sensitivity to distribution of the guidance and aero/control lags is also illustrated in Figure 8.10. An alternate set of system lag values

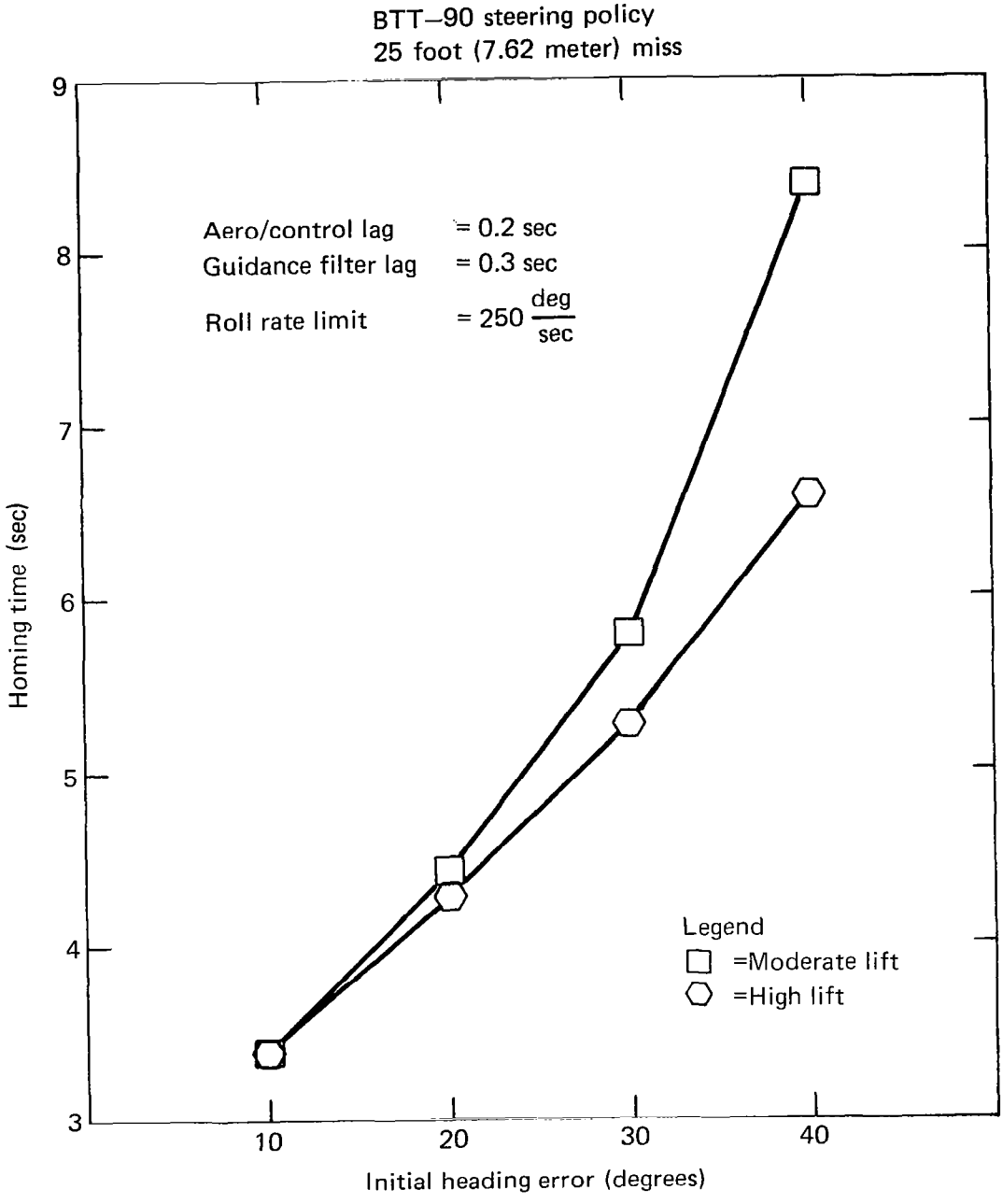

Fig. 8.6 Airframe configuration homing time comparison.

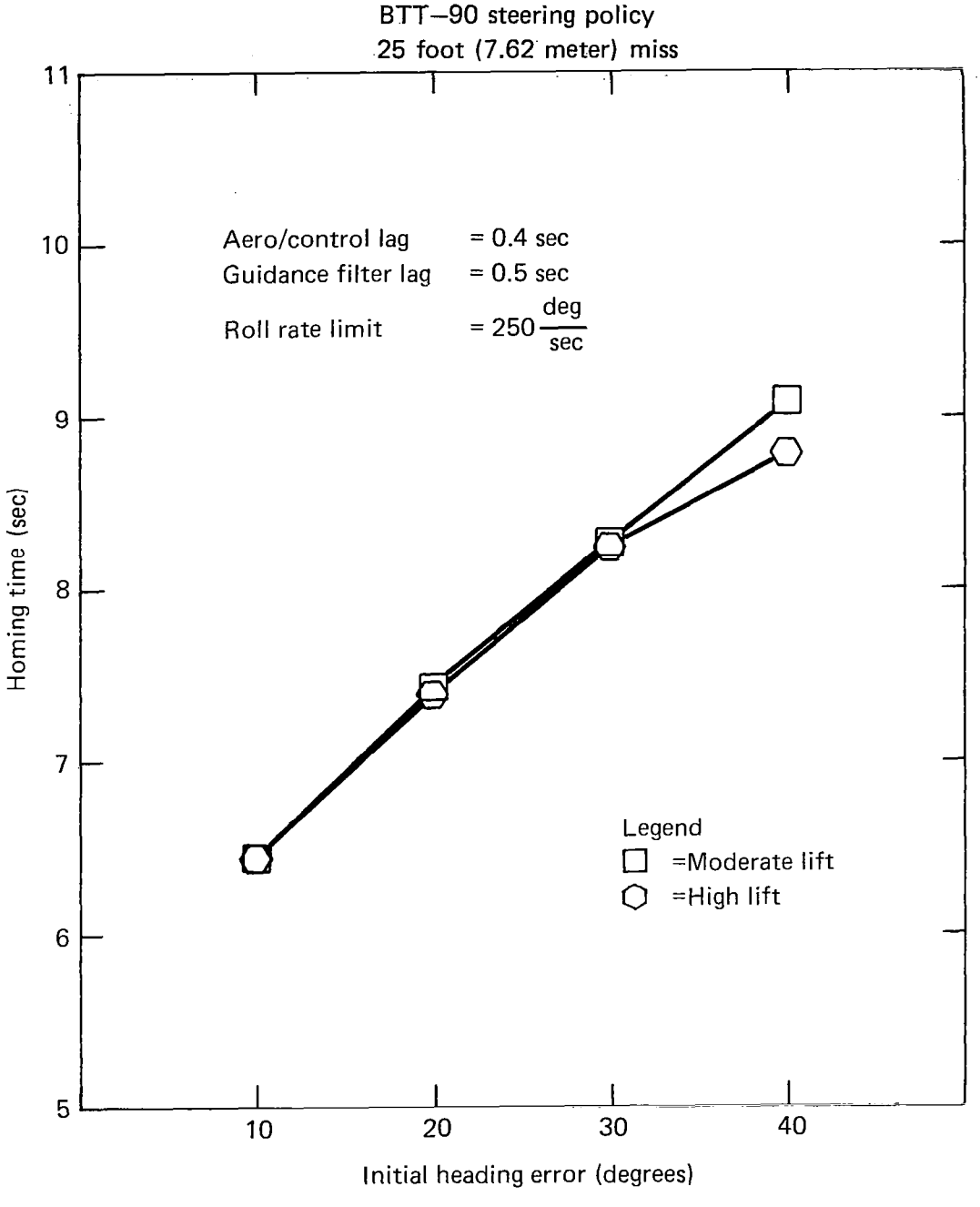

Fig. 8.7 Airframe configuration homing time comparison.

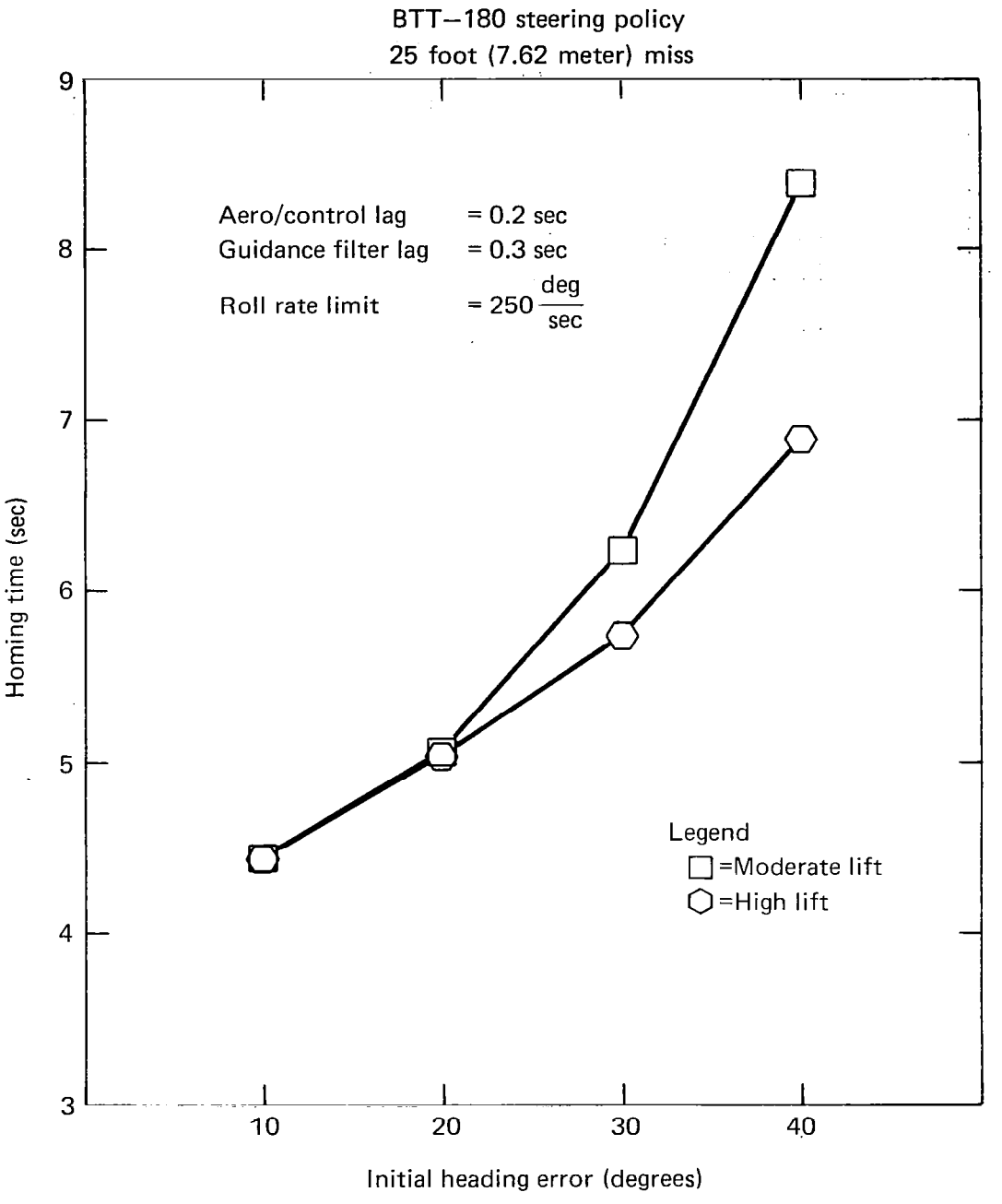

Fig. 8.8 Airframe configuration homing time comparison.

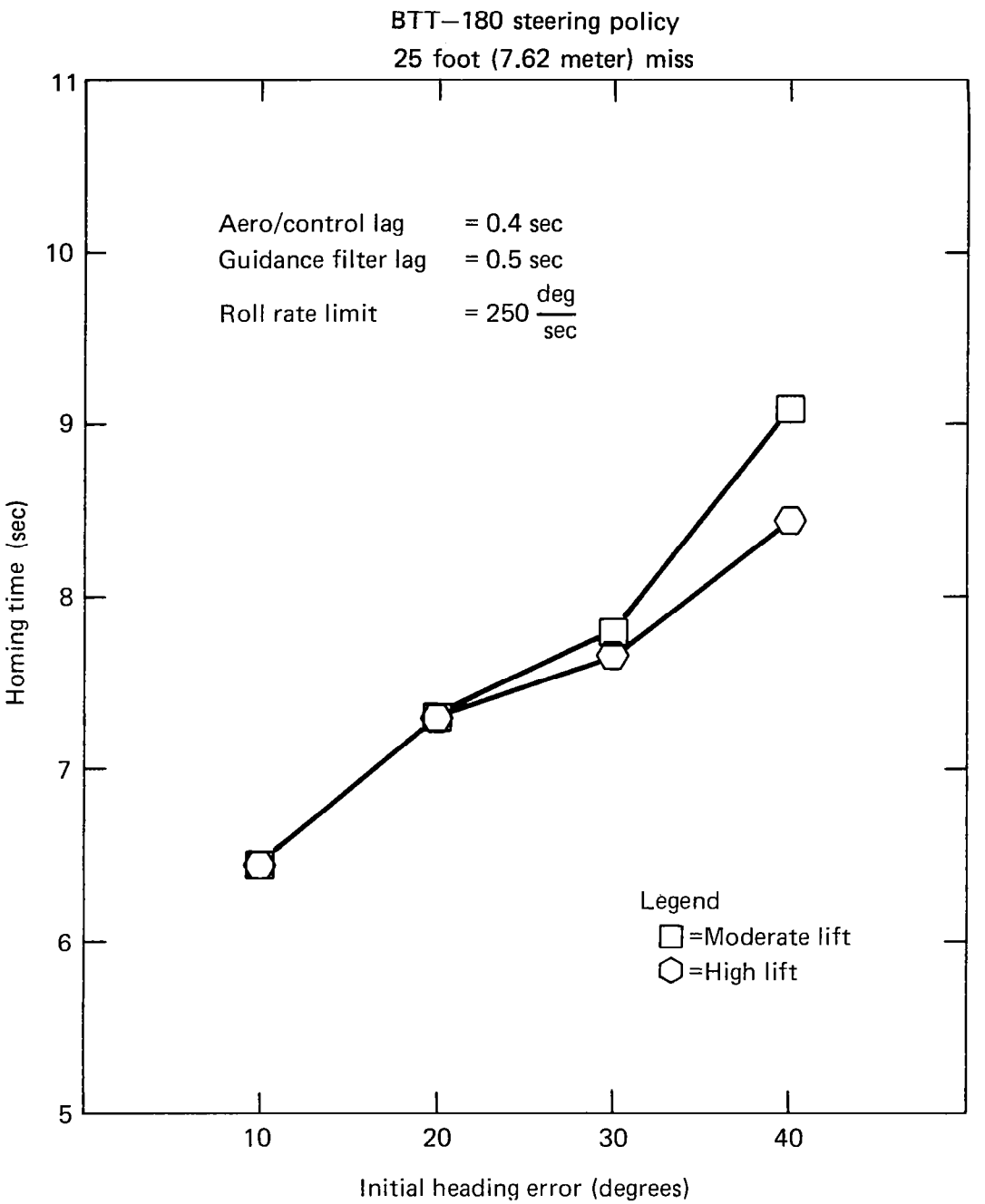

Fig. 8.9 Airframe configuration homing time comparison.

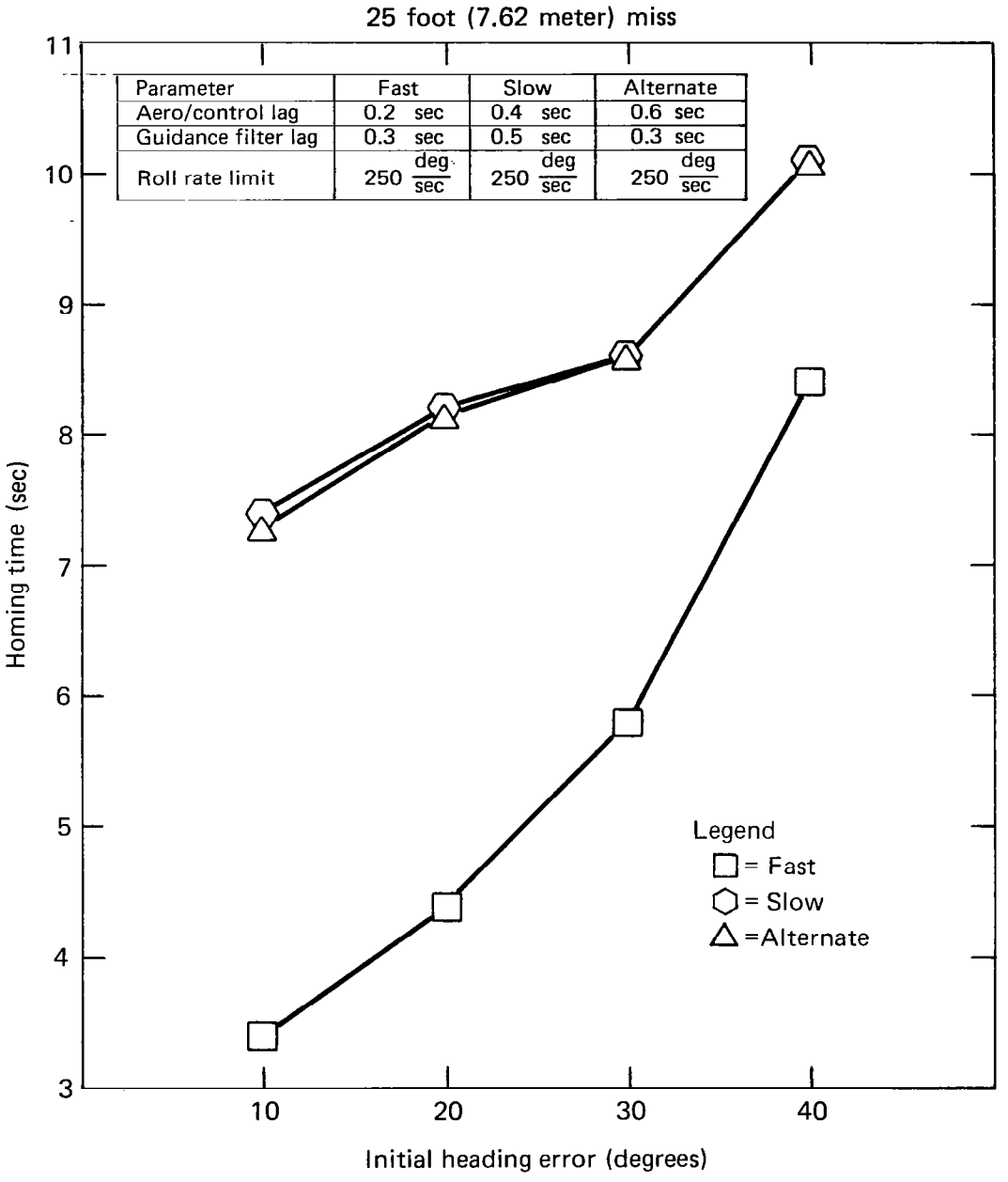

Fig. 8.10 Parameter effects for STT and BTT–45 steering.

were selected for investigation, with the guidance filter lag set at 0.3 sec (same as fast system value) and the aero/control lag set at 0.6 sec, such that the sum of both values was equal to the sum of the slow system values (Table 8.1). These data indicate that keeping the sum of the time constants equal and redistributing the lag does not affect STT and BTT-45 performance significantly. For these steering policies the guidance and aero/control lags are in series, separated only by a command limit; the distribution of lags does not greatly affect performance since command limiting is not prevalent.

8.3.2 BTT-180

The BTT-180 steering policy executes coordinated turns to maneuver. The contribution of each subsystem to the maneuver response time is quite complex and difficult to isolate. The results of this study have shown that when the response time of the bank system is fast relative to the pitch system, performance may be better than for an STT system configured with identical aero/control and guidance lags. In this study a 250 degree/second roll rate capability was sufficient for BTT-180 performance to exceed STT performance when the aero/control lag was 0.4 seconds and the guidance filter lag was 0.5 seconds.

The sensitivity of BTT-180 performance to distribution of the aero/control and guidance lags is illustrated in Figure 8.11. Unlike STT and BTT-45, BTT-180 is quite sensitive to this distribution. This figure illustrates that the sensitivity to increases in guidance filter lag is much greater than the sensitivity to increases in the pitch channel aero/control lag. While the sum of the time constants remains the same, BTT-180 exhibits up to 2 seconds less homing time requirement than STT or BTT-45.

The system response to a commanded maneuver is influenced by a combination of pitch channel aero/control lag and bank system response time. When the pitch channel aero/control lag is small, commanded acceleration magnitude is reached very rapidly and the response time of the bank subsystem may often be the limiting factor since the achieved angular orientation is controlled by this subsystem. However, when the aero/control lag

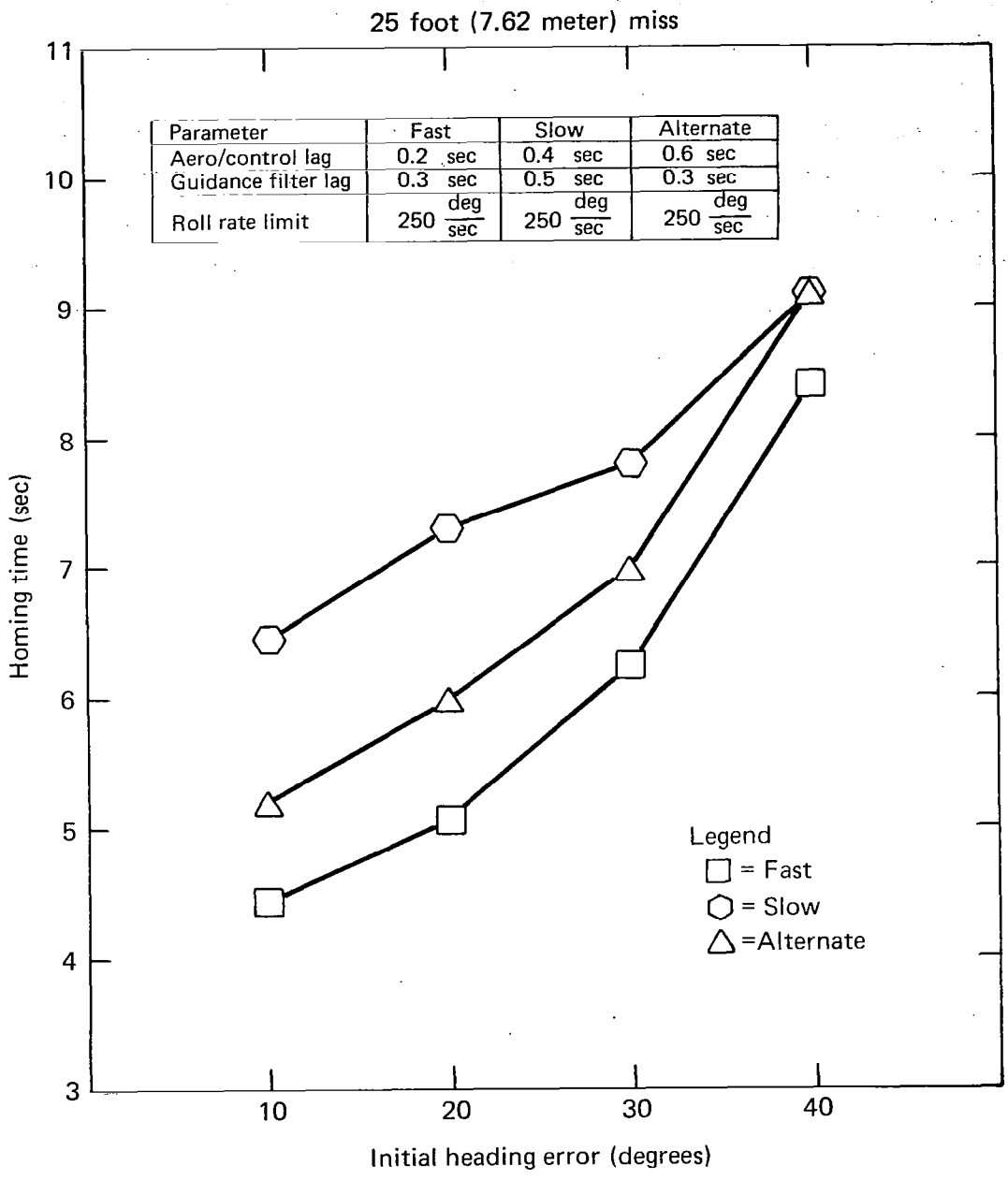

Fig. 8.11 Parameter effects for BTT–180 steering.

is large (as is the case with the slow and alternate parameter sets) the time required to achieve the commanded acceleration magnitude is longer. Thus, whenever a commanded acceleration reversal occurs the achieved acceleration in the pitch channel decreases magnitude very slowly while the bank system directs this residual acceleration into the desired orientation very rapidly. The result is an overall response time that is much faster than could be expected for an STT autopilot configured with the same aero/control lag. Further increases in the pitch channel aero/control lag do not significantly affect performance provided that the bank system response time remains unchanged. Thus, BTT-180 performance is more sensitive to changes in guidance filter lag than the aero/control lag.

8.3.3 BTT-90

The response characteristics of this configuration may vary greatly as the parameters and engagement change. Whenever trajectory overshoots result in a command to reverse the maneuver, the BTT-90 steering policy has two possible responses. If the roll attitude command changes very rapidly, which may occur if the guidance filter lag is very small or if the commanded acceleration grows very rapidly, the roll subsystem may not be able to track the command with less than 90 degrees of error. Under this condition the system responds like an STT policy; therefore, performance and sensitivity to small parameter variations is similar to STT. However, if the guidance lag is large or if the commanded reversal is not very abrupt, the roll attitude may change slowly enough for the roll subsystem to track with less than 90 degrees of error. Under this condition, performance and parameter sensitivity is similar to BTT-180.

9.0 CONCLUSIONS - RAID SUPPRESSION ASSESSMENT

Comparative performance assessments of a high-lift planar airframe configured with bank-to-turn steering and a moderate-lift cruciform airframe configured with both skid-to-turn and bank-to-turn steering have been made. A long range surface-to-air engagement against a maneuvering enemy aircraft, called a raid suppression mission, was selected as the basis for comparison in this study. The measure of performance selected was the range-to-go (i.e., seeker acquisition range) required to achieve 25 foot (7.62 meter) miss for a specified initial heading error. Simplified six degree-of-freedom trim aerodynamic terminal homing models of each configuration were developed and implemented on a digital computer to assess the performance. In order to facilitate comparison of these configurations, the weight and reference areas for aerodynamic coefficients were made equal. The two configurations differ primarily in their lift characteristics.

The control features of the steering policies investigated in this study are summarized in Table 2.1. The performance of the moderate-lift airframe was assessed for all four policies while the high-lift airframe was evaluated for BTT-90 and BTT-180. The results of this study are separated into three categories as follows:

- Comparison of steering policies
- Comparison of airframe configurations
- Subsystem parameter effects.

9.1 Steering Policy Comparison

The results of this study indicate that the performance of the BTT-45 and STT steering policies are nearly identical and that the performance of BTT-90 lies between STT and BTT-180. Performance of BTT-180 is better or worse than STT depending upon system parameter selection. Provided that the bank system is fast enough relative to the pitch system, BTT-180 may outperform STT. For this study a roll rate capability of 250 degrees per second was sufficient when guidance lag was 0.5 seconds and aero/control lag was 0.4 seconds. It is recommended that the maximum allowable roll rate capability be strived for when designing a bank-to-turn system.

9.2 Airframe Configuration Comparison

The high-lift planar airframe and moderate-lift cruciform airframe exhibit similar performance for easy engagements (small initial heading errors). However, for more difficult engagements the high-lift configuration exhibits better performance. Since the maneuverability of each configuration is equally limited by acceleration and angle-of-attack limits, the amount of maneuver-induced slow down is smaller for the high-lift configuration, thereby resulting in better performance. For the sets of parameters investigated in this study, the performance of the high-lift planar airframe configured with its best steering policy was equal to or exceeded the performance of the moderate-lift cruciform airframe configured with its best steering policy.

9.3 Subsystem Parameter Effects

In each case, the smaller set of system lags resulted in the best performance. However, the relative ordering of steering policies depended upon the level of system lags as described above. In addition it was observed that STT and BTT-45 are relatively insensitive to the distribution of overall system lag between the guidance filtering and aero/control subsystems. However, BTT-90 and BTT-180 are more sensitive to variation in the guidance filter lag than to pitch channel aero/control lag. This suggests that it is desirable to keep the guidance filter lag as small as possible for bank-to-turn systems.

PART II

AREA DEFENSE ASSESSMENT

10.0 ENGAGEMENT GEOMETRY AND PERFORMANCE CRITERION

Selection of threat maneuver characteristics used to assess homing performance is typically related to the projected mission for a given system. The systems under investigation in this study are a high-lift planar airframe and a moderate-lift cruciform airframe utilizing skid-to-turn and various bank-to-turn steering policies. The first part of this study dealt with a long range mission called a raid suppression system. The mission selected for the second part is a medium range or area defense surface-to-air engagement against an enemy missile. Applications among the services include defense of the Naval surface fleet against anti-ship missiles (ASM) and defense of ground bases for the Air Force and Army.

10.1 Area Defense Engagement Geometry

Figure 10.1 illustrates the threat geometry used in this study. Anticipated threat characteristics suggest level approach at a target velocity corresponding to MACH 3 at 80 kft (24.38 km) altitude with a 3 g turn-down maneuver for descent at a constant flight path angle. The enemy's objective is located at the origin of this graph. The target begins a turn-down maneuver at a location 155 kft (47.24 km) downrange from the objective. This turn-down maneuver is modelled by an acceleration profile illustrated in Figure 10.2. A ramp function from 0 to 3 g in 1 second initiates the maneuver. Acceleration is maintained at 3 g until the flight-path angle is 1 degree less than the final descent angle. A ramp function from 3 g to 0 in 1 second terminates the turn-down maneuver. The enemy missile continues to descend with constant velocity and flight-path angle.

The surface-to-air interceptor is typically launched under the control of a ground facility. During the early phase of flight, the range separating interceptor and target is usually too large to permit acquisition by the interceptor-borne guidance equipment. As a result the ground control facility performs the navigational function, called mid-course guidance, for the interceptor. When the interceptor-to-target range becomes small enough to permit acquisition, the interceptor initiates terminal homing. A complete system analysis would have to consider the

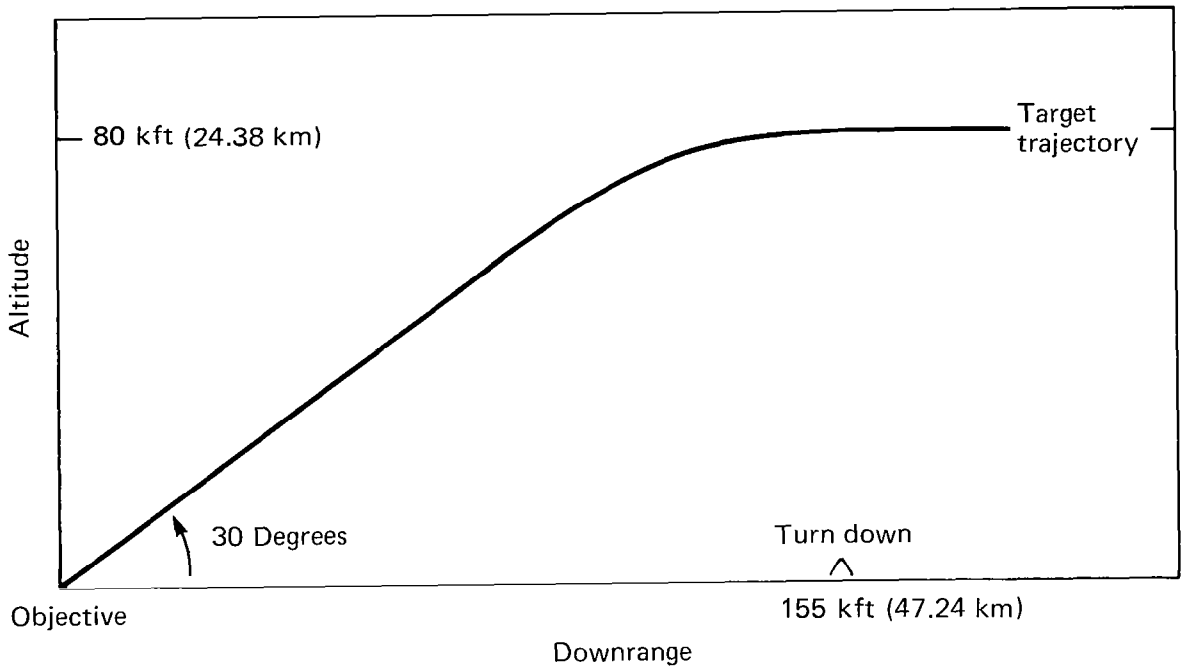

Fig. 10.1 Area defense threat geometry.

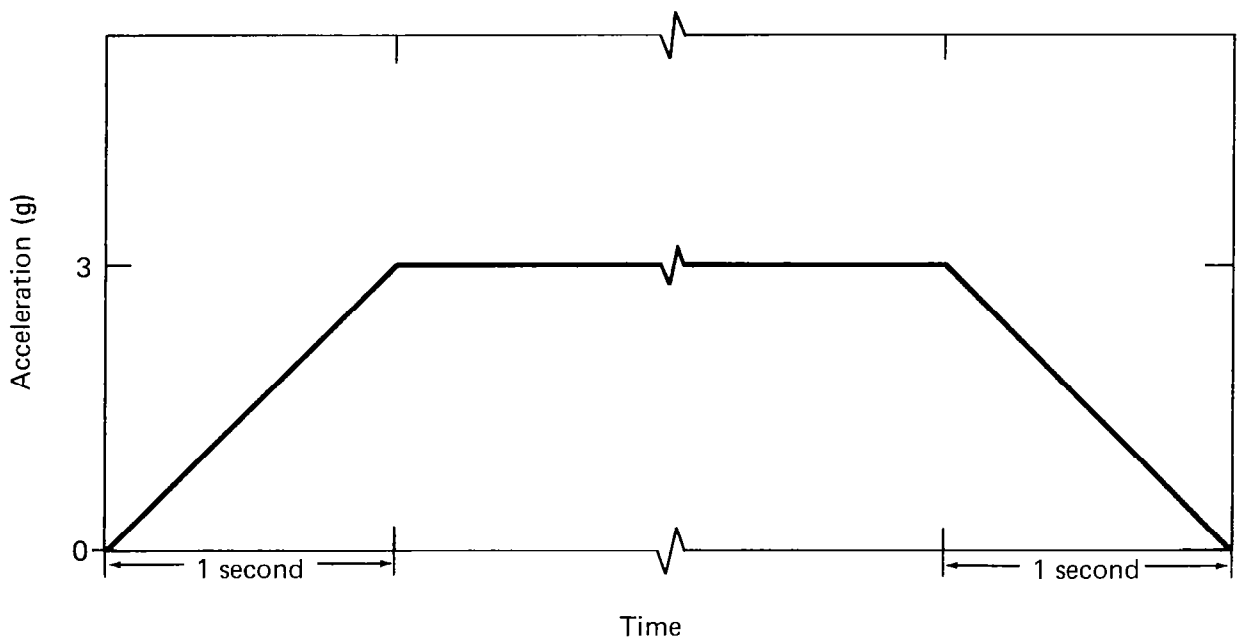

Fig. 10.2 Threat acceleration profile.

problems of launch time determination, optimization of midcourse-guidance algorithms, as well as terminal homing performance. The resulting system should be able to adapt the midcourse trajectory as a function of target position at the time of launch. This would increase the likelihood of a successful intercept over the entire target trajectory. However, for this study it is not necessary to compare performance over the entire trajectory. Instead, the engagement may be simulated by starting the interceptor at the same starting point along a fixed midcourse trajectory for each case. Thus, performance in the vicinity of the interceptor starting point is used as the basis for comparison of the various configurations.

Two interceptor midcourse profiles are considered in this study. The first profile corresponds to a launch site which is coplanar with the threat and the threat's objective. The starting point of the interceptor for simulation purposes is located at 40 kft (12.19 km) downrange and at 60 kft (18.29 km) altitude. The interceptor velocity corresponds to MACH 4.5 with a flight-path angle (angle referred to the horizontal) of 15 degrees. The second launch site corresponds to a position outside of the vertical plane containing the threat and objective. Figure 10.3 illustrates the three-dimensional crossing aspect of this profile. The starting point for this crossing engagement is determined by rotating the first profile by 10 degrees, about the threat's turn-down point. The coordinates of the starting point are approximately 42 kft (12.8 km) downrange, 20 kft (6.1 km) crossrange and 60 kft (18.29 km) altitude. Again the velocity corresponds to MACH 4.5 with a flight-path angle of 15 degrees and a heading angle of 10 degrees. In both cases the interceptor is assumed to be flying a fixed ballistic trajectory until terminal homing begins. In this study an acquisition range of 10 nmi (18.52 km) is assumed.

10.2 Area Defense Performance Criterion

The performance measure used for this part of the study is the portion of the target trajectory along which intercept occurs with less than 50 foot (15.24 meter) miss. The performance measure is computed as follows. For a given initial target position, the simulation is run and the resulting

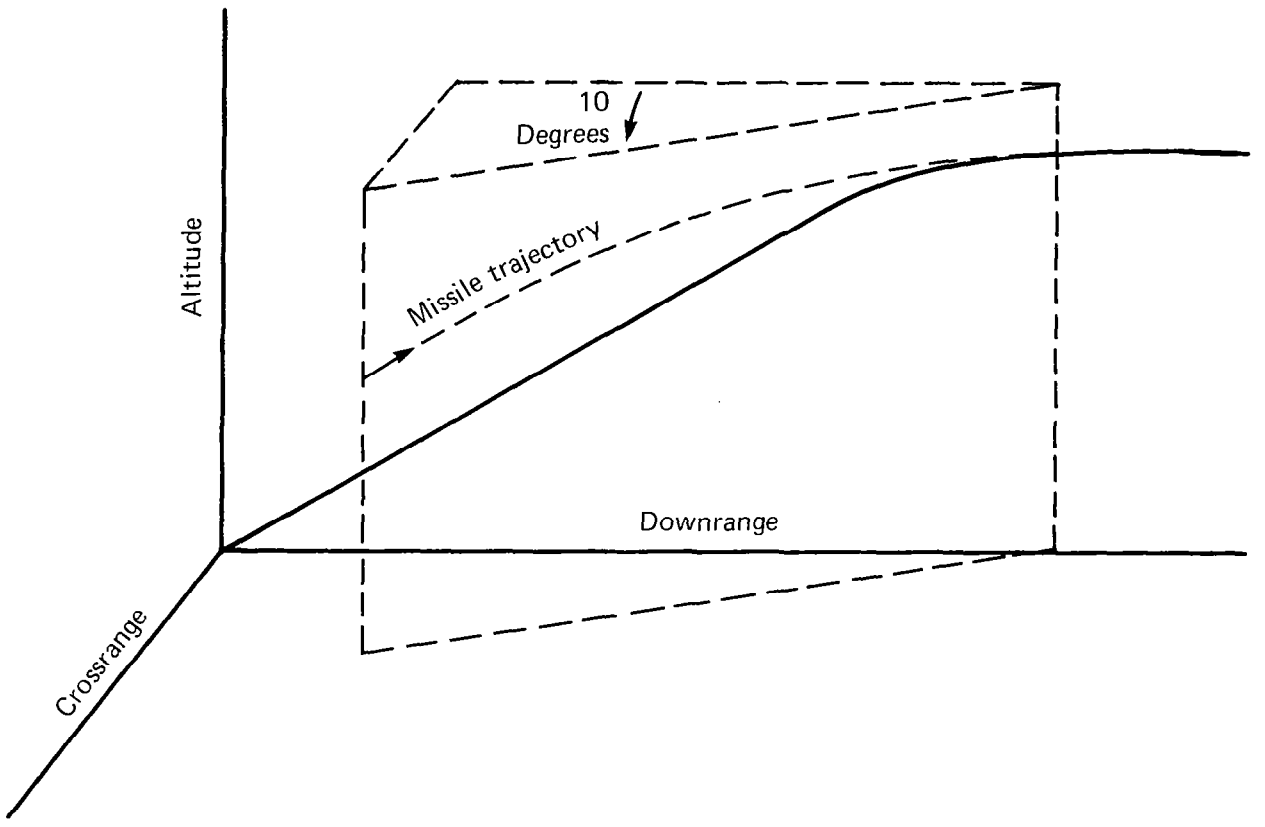

Fig. 10.3 Area defense crossing engagement geometry.

miss distance and intercept location are recorded. This procedure is repeated for a number of different target initiation points. From these data the portion of the target trajectory on which successful intercept occurs may be identified.

Since performance is to be compared in the vicinity of the interceptor starting point on its midcourse profile, bounds must be placed on the target initiation points to be considered. A minimum starting point corresponding to the 10 nmi (18.52 km) acquisition range is selected since it would not be valid to begin the simulated engagement from a point already within the acquisition range. A point located 40 nmi (74.08 km) downrange of the target's objective is chosen as the maximum initiation point for the target.

Figure 10.4 illustrates a representative intercept profile for this area defense engagement. The solid curve represents the trajectory flown by the target. The segments of dashed lines, offset from the target trajectory, indicate the portion of the target trajectory on which intercept occurs with less than 50 foot (15.24 meter) miss. Breaks between the segments occur in the regions where the interceptor was unable to successfully intercept the target. The right-most intercept point on each profile corresponds to the engagement with the target starting at its maximum downrange initiation point. The left-most intercept point on each profile may or may not correspond to the target starting at its minimum downrange initiation point. For those configurations which exhibit poor maneuverability, this last point will correspond to a target initiation point greater than the minimum.

Intercept profiles are generated for each of the configurations investigated in this study. A qualitative method of comparison is to present the regions of successful intercept superimposed on the same graph, thereby allowing for comparison on a one-to-one basis. A more desirable, quantitative method is to compare the percent of target trajectory successfully intercepted by each configuration. A 100-percent rating corresponds to successful intercepts between the end points corresponding to the maximum

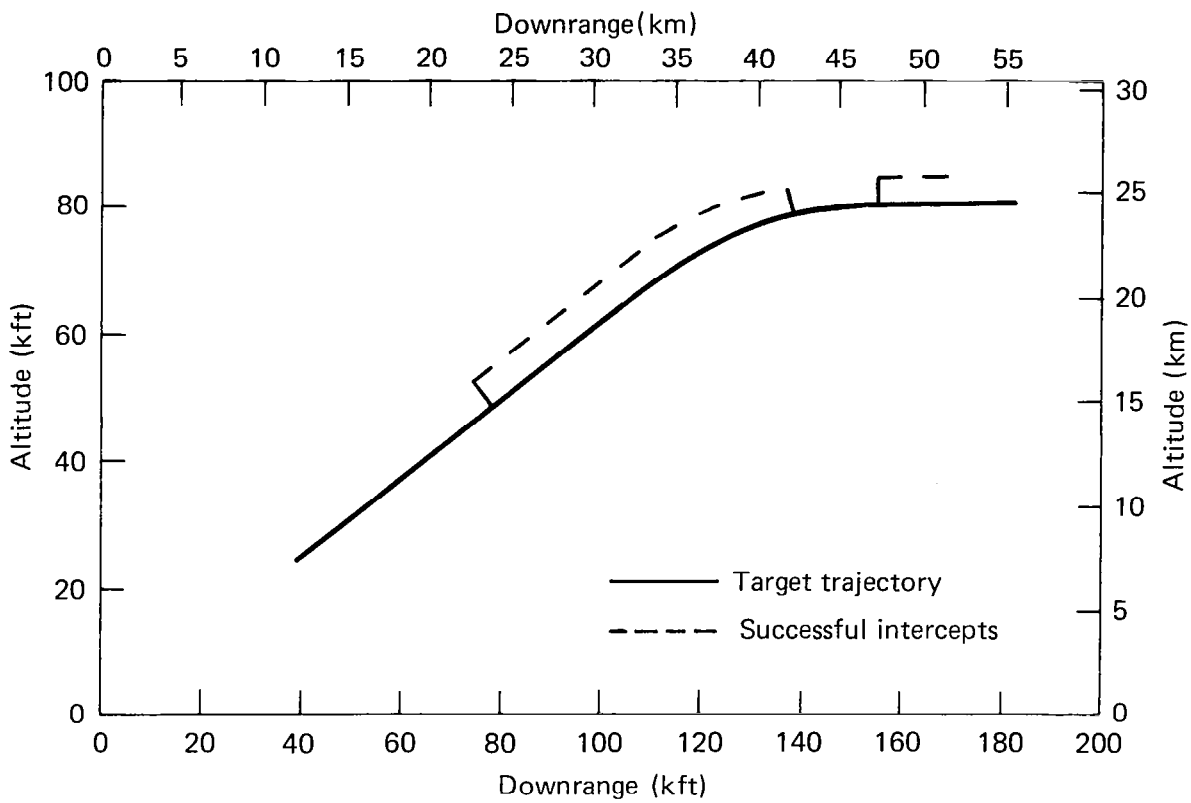

Fig. 10.4 Representative area defense intercept profile.

and minimum target initiation points. To provide additional information, the target trajectory may be broken down into three distinct regions and percent success compared in each region. The first region, called the cruise region, is over the portion of target trajectory which is flat. This is the region before the target initiates a turndown maneuver. The second region, called turndown, is the portion of trajectory on which the target is accelerating. The final region, called descent, corresponds to the portion of trajectory on which the target is no longer accelerating. Figure 10.5 illustrates the three regions for the area defense engagement described in Section 10.1. The percent success in each region is compared for the various configurations to reach the conclusions of this study.

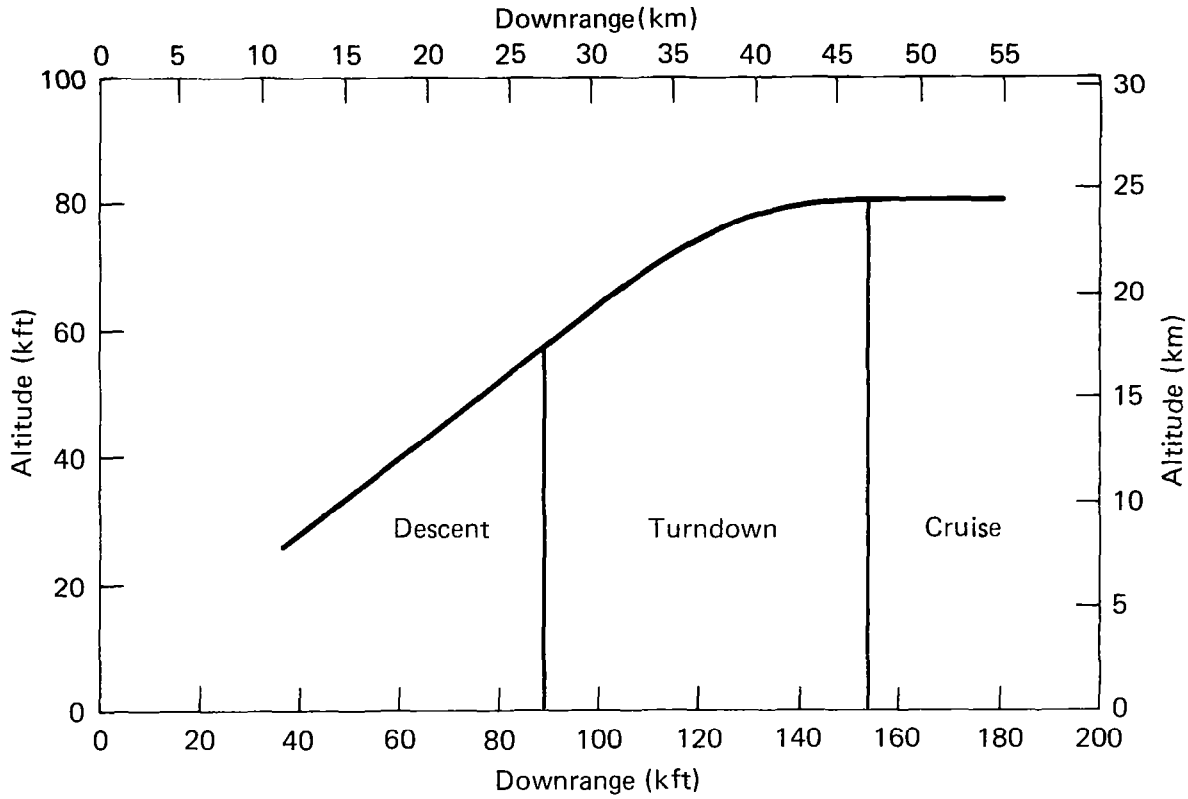

Fig. 10.5 Target trajectory regions.

11.0 AREA DEFENSE INTERCEPTOR MODELLING CHARACTERISTICS

Simplified 6 degree-of-freedom trim aerodynamic simulation models of the STT and various BTT control configurations have been developed and documented in Section 7 of this report. It is assumed that the line-of-sight angular rotation rate, required for implementation of proportional navigation, is measured perfectly. That is, corruption of the measurements by error sources such as radome aberration effects or inadequate seeker stabilization is not included. Furthermore, an acquisition range of 10 nmi (18.52 km) is imposed in all cases. For separation ranges greater than this, no signals are presented to the guidance signal processing subsystem. In addition, it is assumed that first order lags are sufficient to represent the low frequency characteristics of the guidance signal processing subsystem, aero/control and roll subsystems. Values assigned to these control subsystem parameters (e.g., time constants, limits, etc.) are chosen to be representative of an area defense interceptor. Table 11.1 contains a list of the parameters and values assigned to each. Two sets of subsystem time constants are selected to be representative of a fast and a slow system response. This is done in order that the effect of parameter variations may be assessed.

TABLE 11.1 SYSTEM PARAMETER VALUES

PARAMETER	FAST SYSTEM	SLOW SYSTEM
Guidance filter lag	0.3 sec	0.6 sec
Roll system lag	0.2 sec	0.2 sec
Acceleration limit	30 g	30 g
Angle-of-attack limit	25 deg	25 deg
Aero/control lag	see Figure 11.1	
Roll rate limit	see Figure 11.2	

It is anticipated that the interceptor steering dynamics will be dependent upon the flight condition. This dynamic relationship is often modelled by a functional dependency on dynamic pressure, q, in lb/ft^2(kP) Figure 11.1 illustrates the functional forms of the aero/control lag chosen for this study. The fast system time constant is given by $K_1/\sqrt{q}$, and the slow system time constant is $K_2/\sqrt{q}$, where K_1 and K_2 are given in Figure 11.1.

For a coordinated turn, the yaw rotation rate (r) and roll rate ($\dot{\phi}$) must be related according to $r = \dot{\phi} \tan\alpha$, where α is the angle-of-attack. One method to effect a coordinated turn for the BTT-90 and BTT-180 policies considered here is to control the yaw channel to develop the required rotation rate. Since the yaw channel response time increases with decreasing dynamic pressure, it may be unable to respond quickly to a rapid change in roll orientation when the dynamic pressure is low. As a result, excessive sideslip may occur. In order to avoid this condition the response of the roll system is made slower, so that the maneuver could be coordinated with smaller yaw rotation rates. For the first order roll model used in this study, the roll rate limit has a more predominant effect on responsiveness than does the roll system time constant. The effect which flight condition has on roll system responsiveness is modelled by varying roll rate limit as a function of dynamic pressure as illustrated in Figure 11.2. For dynamic pressures less than 800 lb/ft^2 (38.3 kP) the limit is fixed at 150 degrees per second and above 5000 lb/ft^2 (239.5 kP) the limit is fixed at 250 degrees per second. The roll rate limit increases linearly between these values. A dynamic pressure of 800 lb/ft^2 (38.3 kP) corresponds to a flight condition where the interceptor speed is MACH 4.5 at an altitude of approximately 80 kft (24.4 km); whereas, a dynamic pressure of 5000 lb/ft^2 (239.5 kP) corresponds to an interceptor velocity of MACH 4.25 at an altitude of approximately 40 kft (12.2 km).

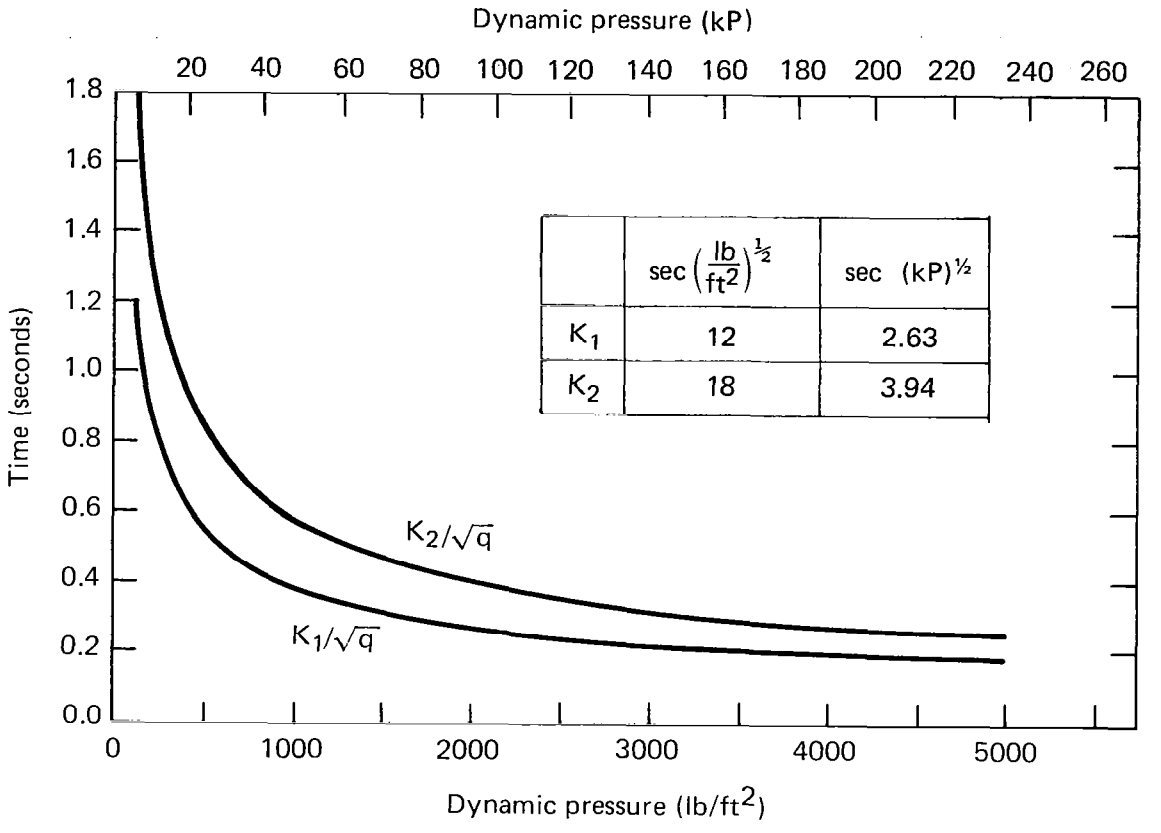

	$\sec\left(\frac{lb}{ft^2}\right)^{\frac{1}{2}}$	sec $(kP)^{\frac{1}{2}}$
K_1	12	2.63
K_2	18	3.94

Fig. 11.1 Aero/control time constant.

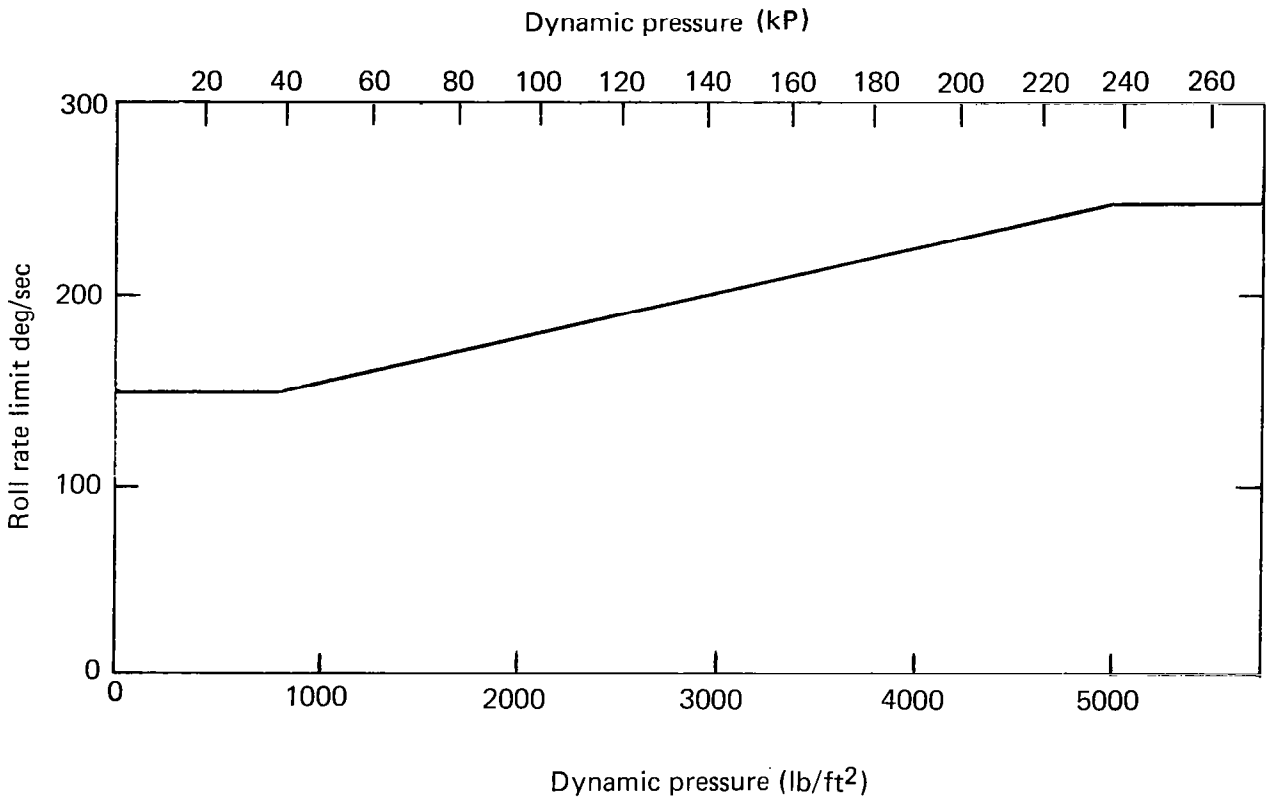

Fig. 11.2 Roll rate limit.

12.0 RESULTS OF THE AREA DEFENSE PERFORMANCE COMPARISON

The objective of the performance comparison study, as stated in the introduction, is to compare the high-lift planar airframe with the moderate-lift cruciform airframe and to assess the differences between steering policies and the effects of system parameter variations. In the second part of this study an area defense engagement, described in Section 10, has been selected as a representative mission for the basis of comparison. The performance measure is defined as the portion of the target trajectory along which intercept occurs with less than 50 foot (15.24 meter) miss distance. The best airframe and steering policy combination is that which is capable of successfully intercepting the target over the largest section of the target trajectory.

The results which are presented in this section are separated into three categories as follows

1. Comparison of steering policies
2. Comparison of airframe configurations
3. System parameter effects.

Within each category, data are presented for both the in-plane and cross-plane engagement geometries.

In the first category, all four steering policies are assessed using the moderate-lift airframe. Each steering policy is ranked relative to the others based upon the chosen performance criterion. The effect which system parameter values and engagement geometry dependencies have upon the ranking are investigated. In addition, the BTT-90 and BTT-180 steering policies are assessed using the high-lift airframe. This is done to assure that the relative performance ranking between steering policies is not different between the airframe configurations considered in this study.

In the second category, the airframe configurations are compared using both BTT-90 and BTT-180 steering policies. Again, the effect of system parameter values and engagement geometry dependencies are examined.

In the final category, the effects which system parameter values have upon the performance comparison are investigated. Rather than performing an

exhaustive parametric study, only selected sets are chosen in order to illustrate the important effects.

12.1 Comparison of Steering Policies

The performance of the STT, BTT-45, BTT-90 and BTT-180 steering policies has been assessed using the moderate-lift airframe configuration. These policies are ranked according to the performance measure discussed in Section 10.2.

12.1.1 In-Plane Geometry

The performance of the various steering policies is evaluated for the in-plane engagement described in Section 10.1. In each case the interceptor's midcourse trajectory is selected such that all configurations achieve successful intercept over the cruise region of the target trajectory. For this reason results will be presented which compare performance in the turndown and descent regions of the target trajectory only. The intercept profiles from which the following results were generated are contained in Appendix E.

Figure 12.1 illustrates the comparison of steering policies for the moderate-lift system configured with the fast set of system parameters. The STT, BTT-45, and BTT-90 steering policies exhibit the same level of performance, whereas the BTT-180 policy exhibits slightly poorer performance. In each case the systems exhibit more success over the turndown region. The limited success in the descent region is due to the limited maneuver capability of the moderate-lift airframe.

The similarity of performance for STT, BTT-45, and BTT-90 is a direct result of the similarity in response to commanded maneuvers for this in-plane engagement. At the initiation of homing, the interceptor responds to an initial heading error which requires a reduction in flight-path angle. For the STT vehicle, this is carried out by developing a negative load factor. The BTT-45 vehicle rolls to the combined plane while developing the required acceleration. The initial roll maneuver has negligible effect on performance.

In Section 8 it was observed that the response of the BTT-90 steering policy to commanded acceleration reversals is governed by the level of guidance filtering and abruptness of the command to reverse the maneuver direction. When the guidance filter lag is small or when the maneuver is abrupt the BTT-90 system carries out a maneuver reversal by maintaining its present roll attitude and reversing the direction of the pitch acceleration. This is identical to the response of an STT system. For this in-plane engagement the initial response of the BTT-90 vehicle is characterized by this type of maneuver. For subsequent maneuvers, all of which are commanded acceleration reversals for the in-plane engagement, the STT, BTT-45, and BTT-90 steering policies respond similarly. Therefore, performance is comparable.

The BTT-180 vehicle, which is restricted to positive load factors only, is required to bank the airframe by 180 degrees to reverse the maneuver direction. While banking, the interceptor has some out-of-plane component of acceleration resulting in an out-of-plane excursion that must be corrected by the guidance loop. If the bank system is fast relative to the pitch system, the out-of-plane excursion is small and the acceleration direction can be reversed faster than by an STT steering policy (see Appendix D). This is not true for the fast system parameters investigated here, resulting in the slightly poorer performance observed by the BTT-180 system.

Figure 12.2 illustrates the comparison of steering policies for the moderate-lift airframe using the set of slow system parameters. In this case none of these steering policies is able to achieve successful intercept in the descent region due to sluggish response and limited maneuver capability. However, in the turndown region the performance of STT, BTT-45, and BTT-90 are comparable and slightly better than the BTT-180 configuration. Although the roll system responsiveness is unchanged from the fast to slow parameter set, it remains relatively slower than the pitch system for both BTT-90 and BTT-180. Therefore, the BTT-90 system performance is comparable to STT and BTT-45, and the BTT-180 system performance is slightly poorer.

Figures 12.5 and 12.6 illustrate the comparison of BTT-90 and BTT-180 steering policies for the high-lift airframe configured with fast and slow parameter sets respectively. While the overall level of performance is greater than for the moderate-lift configuration (see Section 10.3) the ranking of steering policies is unchanged by the lift capability of the airframe used for comparison.

For the in-plane engagement and system configurations investigated in this study the ranking of steering policies according to the selected performance criterion is as follows:

1. STT, BTT-45, and BTT-90 are equivalent
2. BTT-180.

12.1.2 Cross-plane Geometry

The larger initial heading errors combined with the crossing aspect of the geometry presents a more difficult engagement for the area defense interceptor, which unlike the in-plane engagement exercises the banking capabilities of all BTT steering policies. Figures 12.3 and 12.4 illustrate the performance of the various steering policies configured with the moderate-lift airframe along with fast and slow parameter sets, respectively. Each of these configurations is able to achieve success over the cruise region of the target trajectory investigated in this study; whereas, none of these configurations is capable of successful intercept in the descent region of the target trajectory investigated here. The lack of success in the descent region is attributed to the lower maneuver capability of the moderate-lift airframe.

STT and BTT-45 exhibit similar performance, as they did against the in-plane target. For the fast set of system parameters (Figure 12.3) performance is similar for all of the steering policies; whereas, BTT-90 and BTT-180 outperform STT and BTT-45 when configured with the slow set of parameters (Figure 12.4). The relative improvement, over the results of in-plane geometry, of BTT-180 and BTT-90 in relationship to STT and BTT-45 is due to the decrease in effective maneuver response time for the crossing geometry.

The effective maneuver time constant of a coordinated BTT system is governed not only by the subsystem responses, but also by the amount the airframe must be banked to achieve the commanded orientation (see Appendix D). It is obvious that with a finite response time bank subsystem, the further the airframe must be banked the longer it will take to achieve the desired orientation. Thus, the effective time constant of the response in the plane of the maneuver is smaller when the desired maneuver plane is closer to the initial orientation of the interceptor's preferred maneuver plane. For the in-plane engagement, the BTT-180 interceptor is forced to bank 180 degrees to reach the desired orientation; whereas in the cross-plane engagement the desired orientation is achieved with less than 180-degrees bank motion. The result is a relatively faster response for the BTT system engaged against the crossing target; hence, performance compares more favorably with STT and BTT-45. In fact, for the slow set of system parameters, BTT-180 and BTT-90 (which executes similar maneuvers) outperform the STT and BTT-45 configurations.

Figures 12.7 and 12.8 illustrate the performance of the BTT-90 and BTT-180 steering policies configured with the high-lift airframe along with fast and slow parameter sets, respectively. The performance of these two configurations is similar over the turndown region for both sets of parameters, and BTT-90 is slightly better than BTT-180 over the descent region of the target trajectory. These results are consistent with those for the moderate-lift configuration. Notice that the slow configuration (Figure 12.8) can intercept the target over a slightly larger percent of the descent part of the trajectory than the fast configuration (Figure 12.7). (See also Figure E.12.) This result reflects the slower average velocity of the slow configuration. The time of flight for the closest intercept of the slow system is approximately one second longer than for the closest intercept for the fast system.

12.2 Airframe Configuration Comparison

The airframe configurations modelled in this study differ primarily in lift characteristics. As dynamic pressure decreases due to aerodynamic drag and increases in altitude, maneuverability is curtailed by the imposed

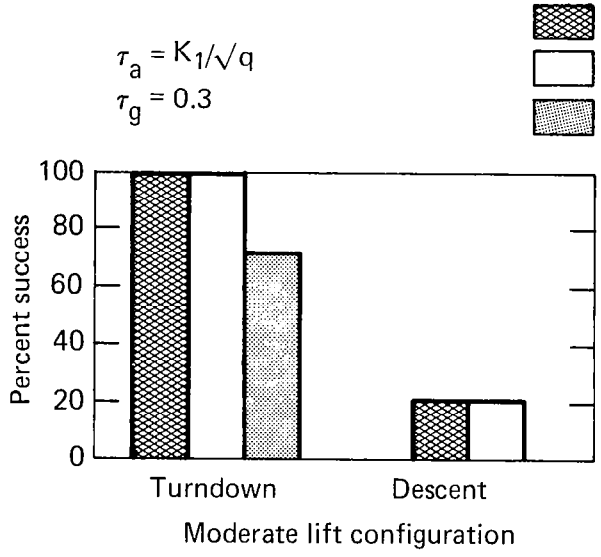

Fig. 12.1 **Steering policy comparison for the inplane engagement.**

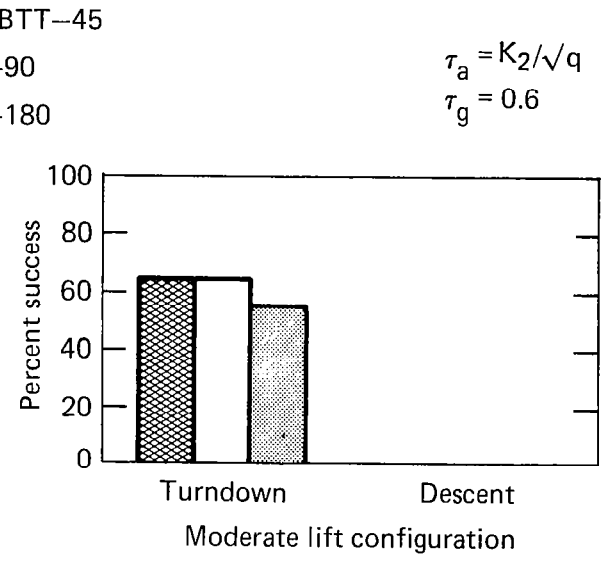

Fig. 12.2 **Steering policy comparison for the inplane engagement.**

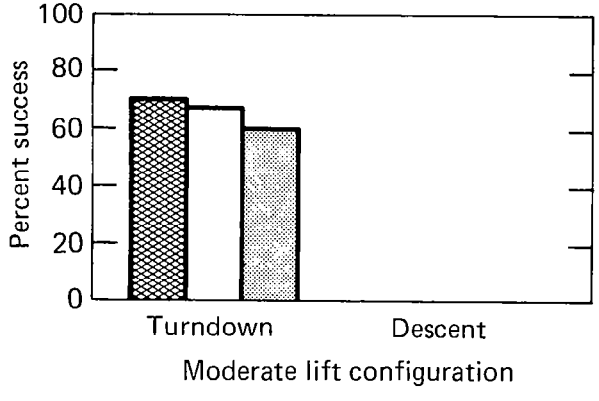

Fig. 12.3 **Steering policy comparison for the crossplane engagement.**

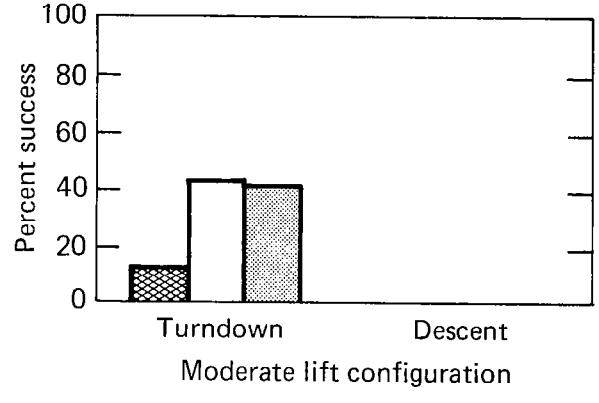

Fig. 12.4 **Steering policy comparison for the crossplane engagement.**

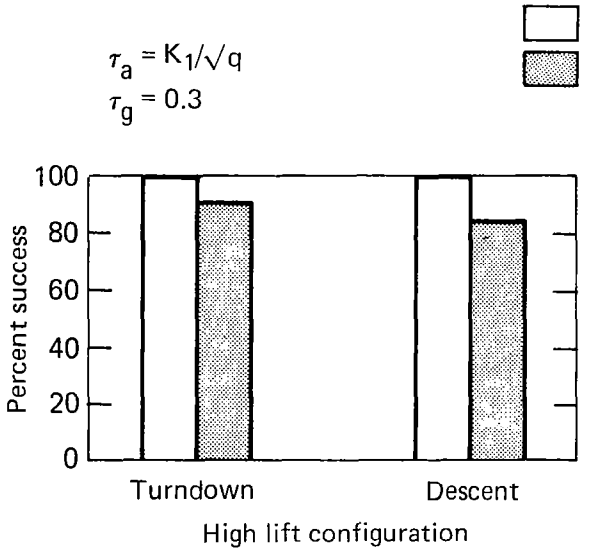

Fig. 12.5 **Steering policy comparison for the inplane engagement.**

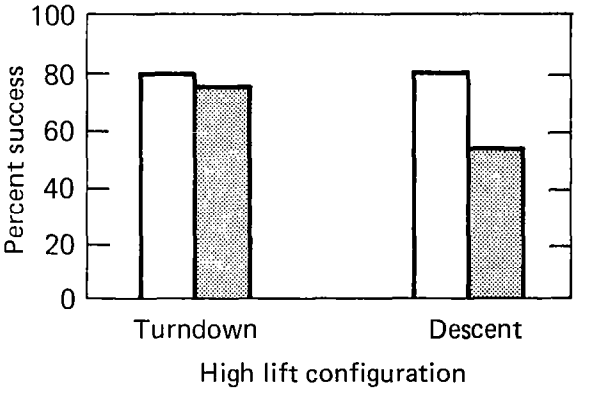

Fig. 12.6 **Steering policy comparison for the inplane engagement.**

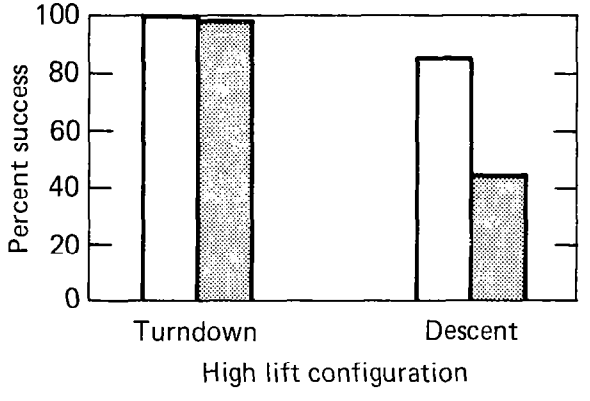

Fig. 12.7 **Steering policy comparison for the crossplane engagement.**

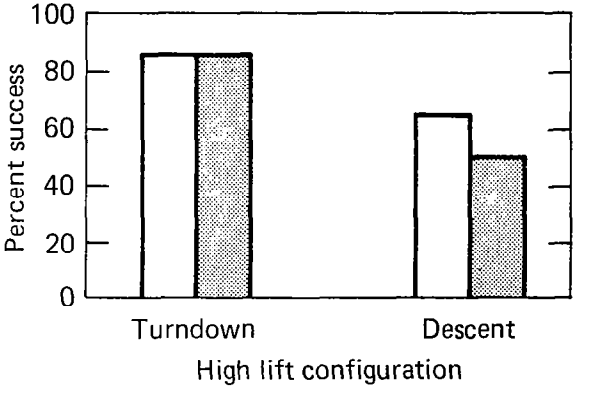

Fig. 12.8 **Steering policy comparison for the crossplane engagement.**

25 degree angle-of-attack limit. Since the planar configuration has higher lift capability, the 25 degrees of angle-of-attack translate into more acceleration capability and better performance.

12.2.1 In-plane Geometry

Figures 12.9 and 12.10 illustrate the comparison of airframes for the systems configured with BTT-90 steering along with fast and slow parameter sets respectively. The high-lift airframe exhibits much better performance over the descent region of the target trajectory. Figures 12.13 and 12.14 illustrate the comparison for the system configured with BTT-180 steering along with fast and slow parameter sets, respectively. Again the high lift airframe exhibits superior performance against the in-plane target.

12.2.2 Cross-plane Geometry

Figures 12.11 and 12.12 illustrate the comparison of airframes against the cross-plane target for systems configured with BTT-90 steering along with fast and slow parameter sets respectively. The difference in performance is slightly greater for the more difficult crossing engagement with the high-lift configuration showing the better performance. Similar results, contained in Figures 12.15 and 12.16, illustrate the comparison for the BTT-180 steering policy against the crossing target. Again the high-lift planar configuration is superior.

12.3 Effect of System Parameters on the Performance Comparison

Some of the effects which system parameter variations may have upon performance of the various configurations have been demonstrated in the previous sections. In each case, the set of smaller system lags resulted in the best performance. However, the relative ranking of steering policies depended upon the level of system lags. Table 12.1 contains a list of the rankings for the in-plane and cross-plane engagement illustrating the effect of the level of system lags. For the in-plane geometry STT, BTT-45, and BTT-90 all exhibit similar performance with BTT-180 slightly worse. The poorer performance of BTT-180 is caused by the slowness of

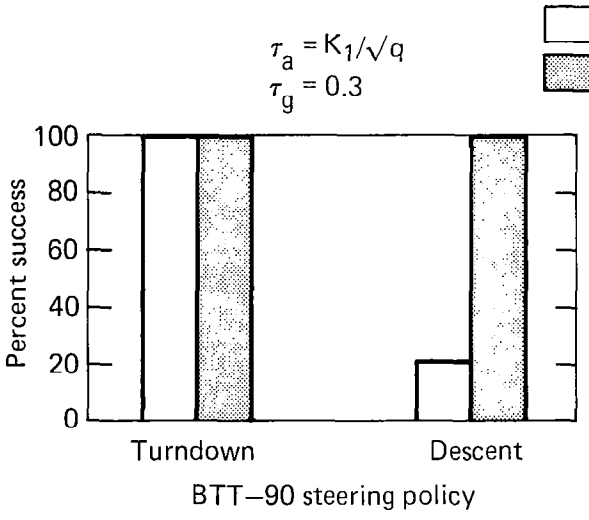

Fig. 12.9 Airframe comparison for the inplane engagement.

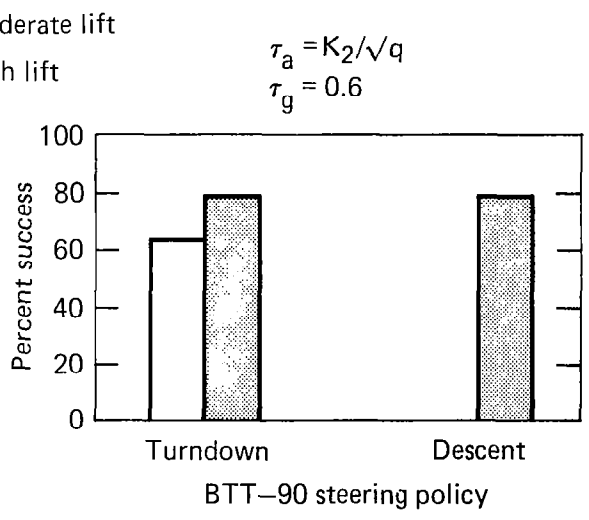

Fig. 12.10 Airframe comparison for the inplane engagement.

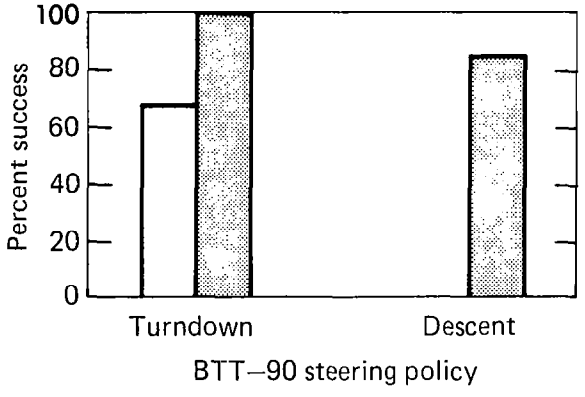

Fig. 12.11 Airframe comparison for the crossplane engagement.

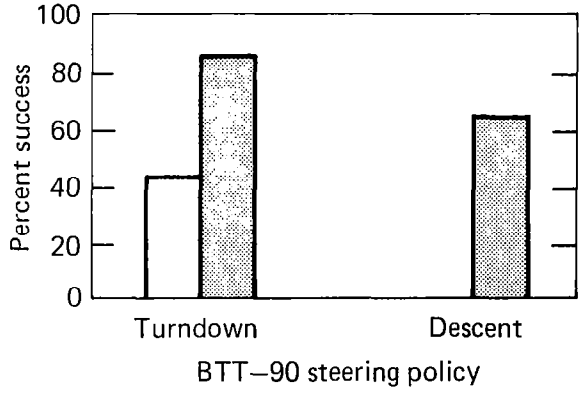

Fig. 12.12 Airframe comparison for the crossplane engagement.

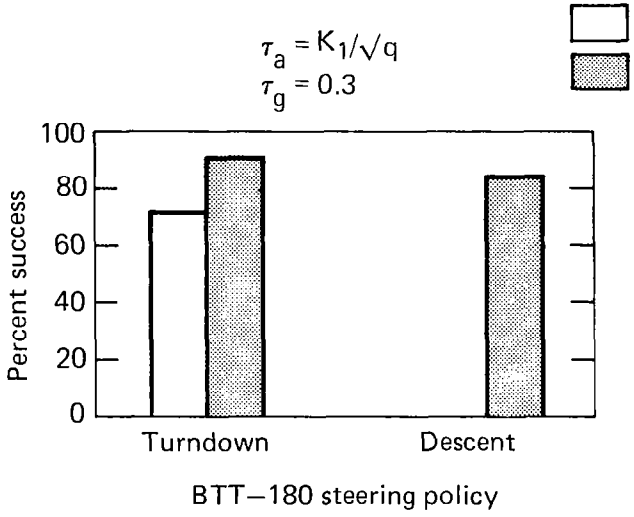

Fig. 12.13 **Airframe comparison for the inplane engagement.**

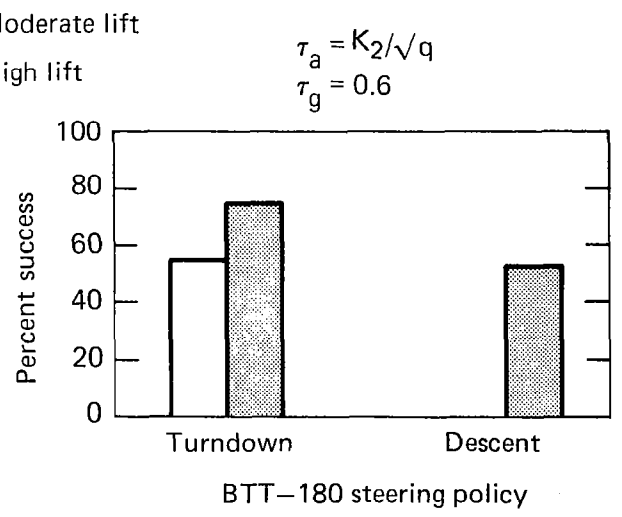

Fig. 12.14 **Airframe comparison for the inplane engagemant**

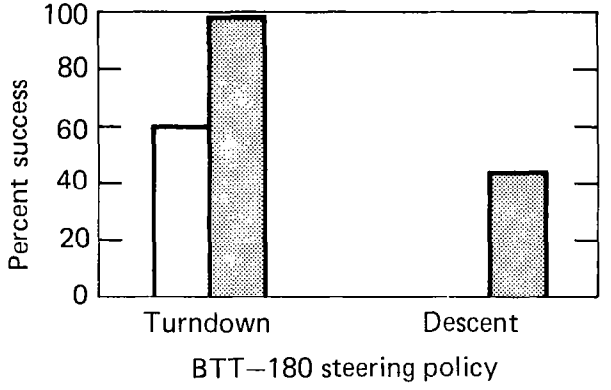

Fig. 12.15 **Airframe comparison for the crossplane engagement.**

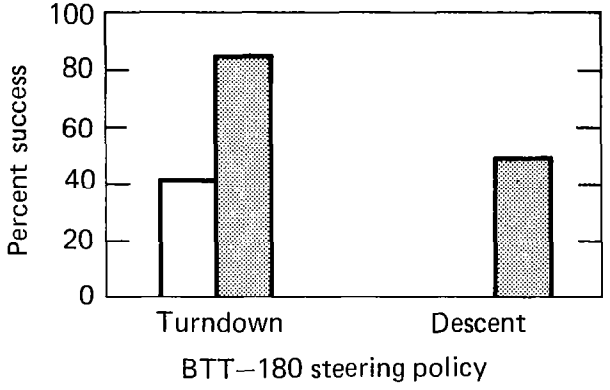

Fig. 12.16 **Airframe comparison for the crossplane engagement.**

the bank control system in relationship to the pitch control system. Additional studies have shown that a fixed roll rate capability of approximately 250 degrees per second is sufficient for the performance of the BTT-180 system configured with the slow set of parameters to equal the performance of the other steering configurations against the in-plane target.

TABLE 12.1 RANKING OF STEERING POLICIES FOR THE FAST AND SLOW SYSTEM PARAMETER SETS OF THE AREA DEFENSE ENGAGEMENT

IN-PLANE ENGAGEMENT		CROSS-PLANE ENGAGEMENT	
fast	slow	fast	slow
STT BTT-45 BTT-90	STT BTT-45 BTT-90	STT BTT-45	BTT-90
BTT-180	BTT-180	BTT-90	BTT-180
		BTT-180	STT BTT-45

The results of the cross-plane engagement show that both BTT-90 and BTT-180 are performance-limited by the lack of sufficiently high roll rate capability when configured with the fast set of system parameters. However, for the slow set of system parameters BTT-90 and BTT-180 both outperform STT and BTT-45. Since the maneuver response time of these BTT configurations is affected by the amount the airframe must be rolled to achieve the commanded orientation (see Section 12.1.2), the performance is relatively better in relationship to STT and BTT-45 for the cross-plane engagement.

13.0 CONCLUSIONS - AREA DEFENSE ASSESSMENTS

Comparative performance assessments have been made of a moderate-lift cruciform airframe (with low aspect ratio wings) configured with both skid-to-turn and bank-to-turn steering, and a high lift planar airframe (with larger wings) configured with bank-to-turn steering. A medium range or area defense engagement against a high altitude air-to-surface enemy missile was selected as the basis for comparison in this study. Both in-plane and cross-plane engagement geometries were considered. The measure of performance selected was the amount of the target trajectory on which the target can be successfully intercepted, where a successful intercept is defined as an intercept with a miss of less than 50 feet (15.24 meter). Simplified six degree-of-freedom trim aerodynamic terminal homing models of each configuration, described in Section 7 of this report, were used to assess the performance. In order to facilitate comparison of these configurations, the weight and reference areas for aerodynamic coefficients were made equal. The two configurations differ aerodynamically primarily in their trim lift and drag characteristics.

The control features of the steering policies investigated in this study are summarized in Table 2.1. The performance of the moderate-lift cruciform airframe was assessed for all four policies while the high-lift planar airframe was evaluated for BTT-90 and BTT-180. Two sets of system parameter values were considered for each configuration. The results of this study are separated into three categories as follows:

- Comparison of steering policies
- Comparison of airframe configurations
- Subsystem parameters effects.

Figure 13.1 contains a summary of performance results of this area defense engagement. The performance measure expressed here as percent success, corresponds to the ratio of the length of target trajectory which is successfully intercepted to the total length of target trajectory investigated (see Appendix E). Two sets of results which compare the performance of the various configurations for the in-plane and cross-plane

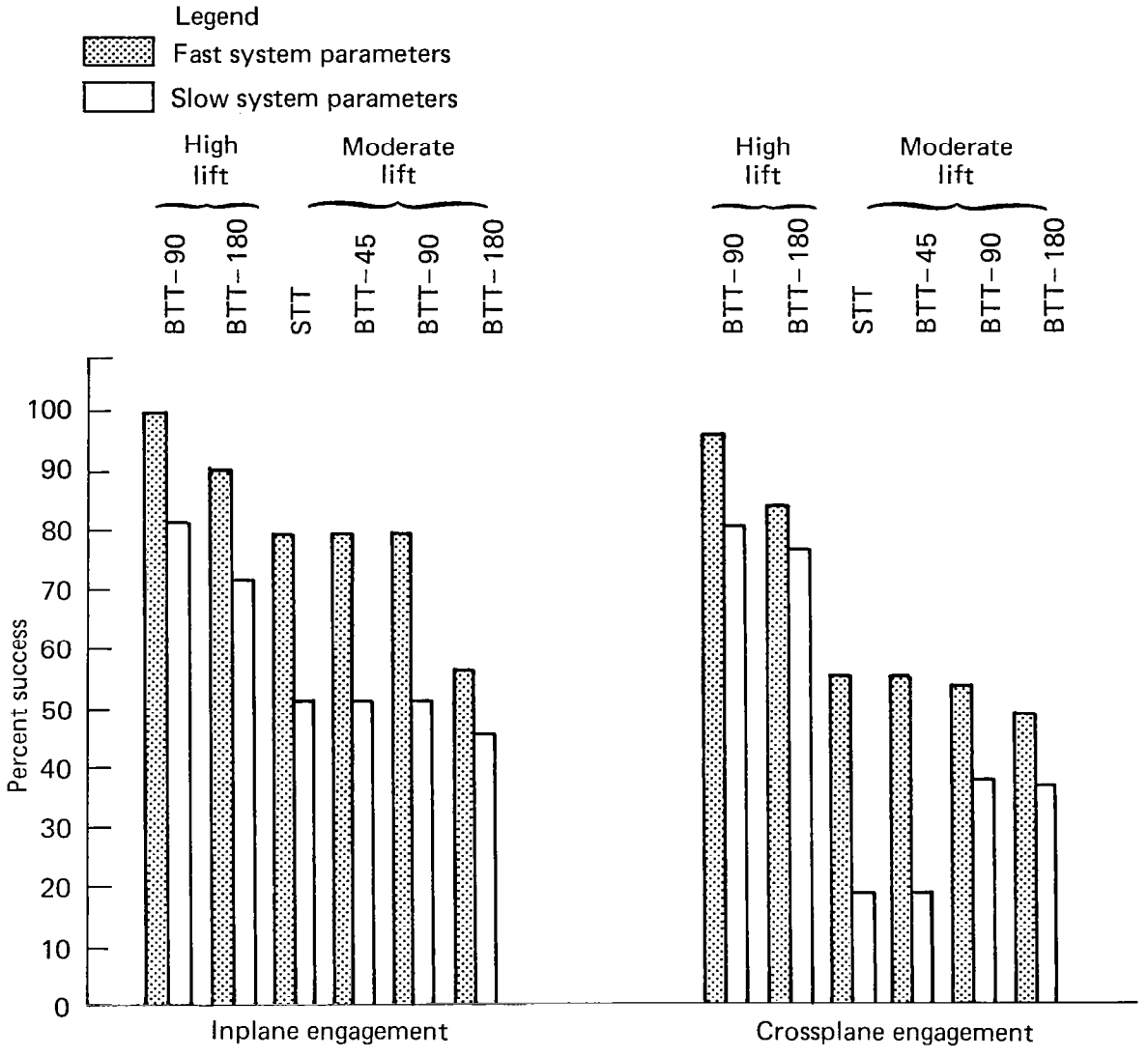

Fig. 13.1 Summary of area defense results.

enagagement geometries are shown. Interpretation of these results follows.

13.1 Steering Policy Comparison

For the in-plane engagement geometry, performance of STT, BTT-45, and BTT-90 are similar and better than BTT-180 for both sets of system parameters investigated. The BTT-180 interceptor performance is limited by the slow response time associated with the bank system, relative to the pitch system, at the conditions for this engagement.

For the cross-plane engagement, the performance of STT and BTT-45 are nearly identical. When configured with the set of system parameters corresponding to a fast system response, the performance ranking of steering policies is as follows

1. STT and BTT-45 are equivalent (55.7%)
2. BTT-90 (54.1%)
3. BTT-180 (49.3%)

For the slow set of system parameters the ranking is

1. BTT-90 (38.3%)
2. BTT-180 (37.5%)
3. STT and BTT-45 are equivalent (19.3%)

The change in performance ranking for the two sets of system parameters investigated is associated with the larger degradation in performance exhibited by STT and BTT-45 in shifting from the in-plane to cross-plane engagement geometry. Since the BTT interceptors do not have to bank as much to achieve the commanded maneuver orientation in the cross-plane engagement, the effective response time is relatively faster and performance does not degrade as rapidly as for STT and BTT-45 whose response times are unaffected by the engagement geometry. In general, it is recommended that the maximum allowable roll rate capability be strived for when designing a bank-to-turn system.

13.2 Airframe Comparison

When configured with the same steering policy, the high-lift planar airframe exhibits better performance than the moderate-lift cruciform configuration. This difference is greater for the cross-plane engagement

geometry. For the sets of parameters investigated in this study, the performance of the high-lift airframe configured with its best steering policy exceeded the performance of the moderate-lift cruciform airframe configured with its best steering policy.

13.3 Subsystem Parameter Effects

For each case, the smaller set of system lags resulted in the best performance. Increasing the maximum roll rate capability of the BTT-90 and BTT-180 configurations improves the performance of these systems by reducing the overall maneuver response time. In addition, the effective response time in the plane of the desired maneuver is not only affected by subsystem responses, but also by the amount the airframe must bank to achieve the commanded orientation. For the cross-plane engagement, the effective time constant of the response in the plane of maneuver is smaller than for the in-plane engagement since the commanded maneuver plane is closer to the initial orientation of the interceptor's maneuver plane.

APPENDIX A

AIRFRAME DESCRIPTION

Edward T. Marley

The airframes chosen for this investigation are representative of interceptor airframes that could be developed for the two selected missions, the Raid Suppression Mission and the Area Defense Mission. The Raid Suppression Mission calls for intercepting "jamming" aircraft flying at medium altitudes; this requires intercepts at long range. The Area Defense Mission requires intercepting air-to-surface missiles. These air-to-surface missiles cruise during their midcourse flight at high altitudes and then descend during terminal flight enroute to their intended surface targets. The maximum range boundaries for the Area Defense Mission are considerably shorter than for the Raid Suppression Mission, and therefore a smaller missile can be used for the Area Defense Mission since the volume required for fuel or propellant is not as large.

Two aerodynamic configurations, applicable to either mission, were chosen for comparison. They are designated in this investigation as a high-lift configuration and a moderate-lift configuration. The high-lift configuration, Figure A.1, is a planar configuration symmetric about its wing plane and, like an airplane, banks as needed to perform the bulk of its required maneuvers in a direction normal to the plane of its wings. This is referred to as a Bank-to-Turn Configuration (BTT). The two all-movable tail surfaces, inline with the wings, are used for both pitch and roll control. Tail stabilizers provide directional stability, and trailing-edge flaps on the stabilizers provide control. The moderate-lift configuration, Figure A.2, has the same body as the high-lift configuration, four low aspect-ratio wings in cruciform arrangement, and four tail control surfaces inline with the wings. The tail surfaces are used for both steering and roll control. This configuration, like the high-lift configuration, can bank-to-turn like an airplane so as to maneuver in a preferred direction normal to its longitudinal axis. The preferred maneuver can take place in a plane coincident with either set of wing planes or mid-way between these wing planes. The moderate-lift configuration can also be

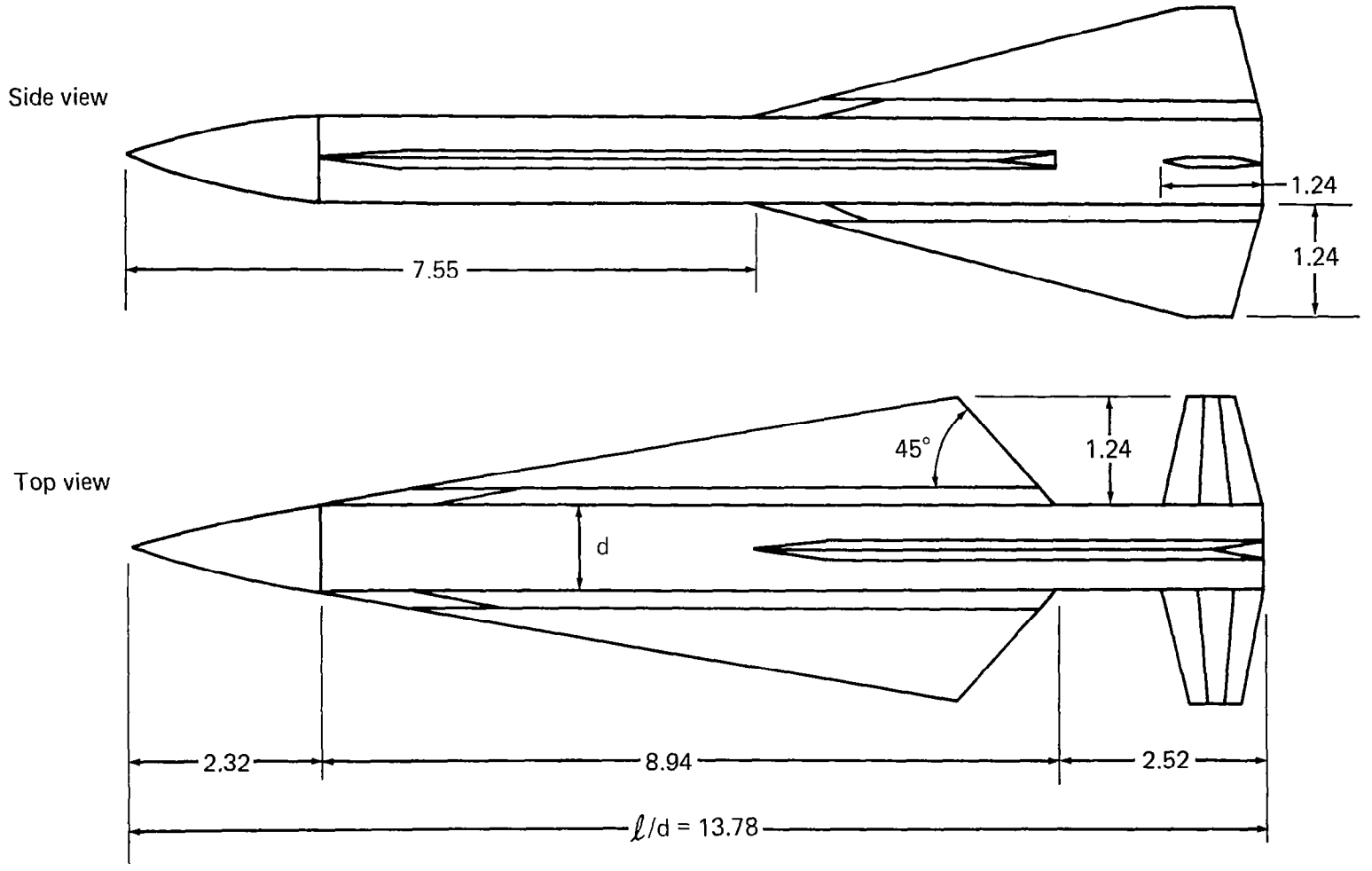

All dimensions are in missile diameters.

Fig. A.1 High lift configuration.

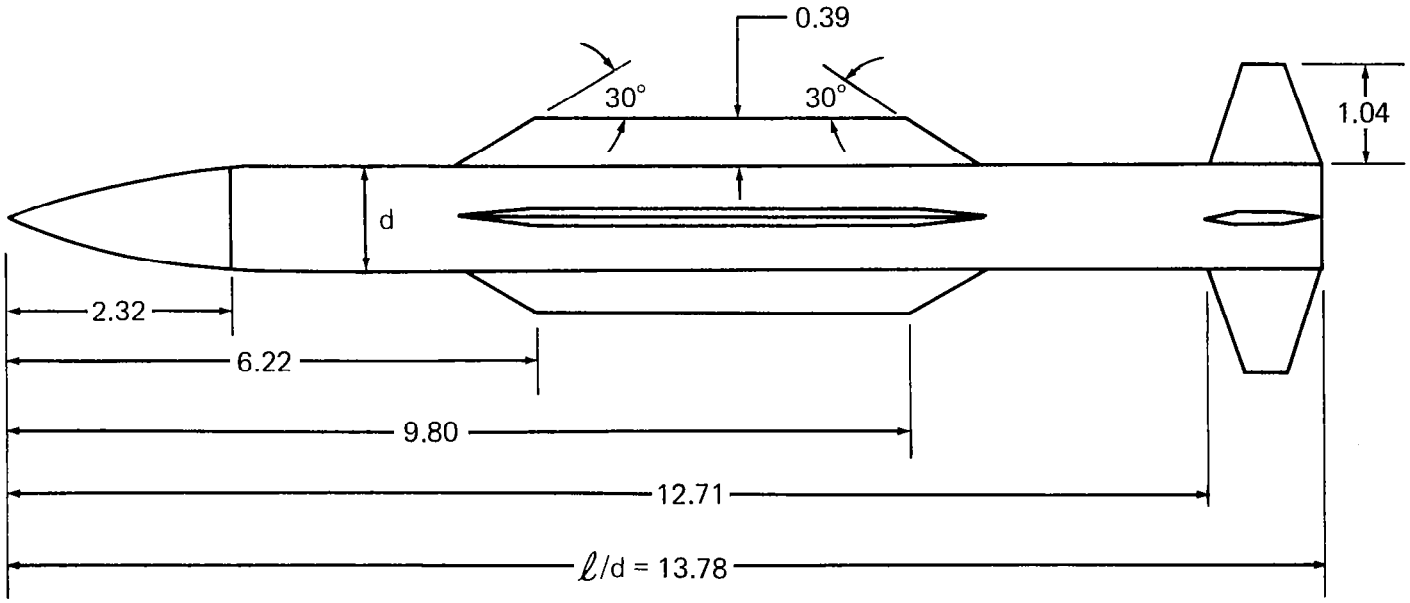

All dimensions are in missile diameters.

Fig. A.2 Moderate lift configuration.

roll stabilized in space and be required to maneuver in a preferred radial direction normal to its longitudinal axis regardless of the orientation of its wings. This later operation is called Skid-to-Turn (STT). The linear dimensions of high-lift and moderate-lift missiles used in the Raid Suppression Mission are 18.5 percent greater than the corresponding dimensions of the missiles used in the Area Defense Mission.

The simulation of trajectories for this investigation required a representation of the trim normal force and axial drag associated with the interceptors. The trim normal force coefficients versus angle of attack, at $M = 3.5$, for the Raid Suppression interceptors are presented in Figure 5.1. These coefficients are associated with a center of gravity located at 55% of the body length aft of the nose vertex. In order to simplify the simulation the trim coefficients at $M = 3.5$ were used for the complete Mach number range covered in this investigation, $3.0 < M < 4.5$. Aerodynamic data indicate that the largest deviation in trim normal force coefficients with Mach number occurs at the higher angles of attack; this deviation is less than $\pm 7\%$ of the values in Figure 5.1. The trim normal force coefficients shown for the moderate-lift interceptor are representative of all aerodynamic roll orientations. The corresponding curves for the Area Defense Mission are shown in Figure 5.2; these curves are for a missile center of gravity located at 51.6% of the body length which is the center of gravity associated with fuel-depleted flight conditions. The axial drag characteristics for the moderate-lift configuration are presented in Figure 5.3; these coefficients, associated with fuel-depleted flight, were extrapolated to $M = 4.5$ for use in the simulation. The corresponding axial drag coefficients of the high-lift configurations used in this investigation are 20 percent higher than the values in Figure 5.3.

An extensive body of wind-tunnel data is available on the normal force and the lateral and longitudinal stability and control characteristics of both configurations. It is deduced from these data that both configurations have sufficient aerodynamic control to perform maneuvers over the angle-of-attack range considered herein. This aerodynamic information can be used

for design investigations leading to the development of aero/control systems once specific missile control requirements are established.

APPENDIX B

LOW LEVEL SIGNAL ROLL CONTROL

Formation of the bank command for the roll system ($\phi_c = \arctan \frac{\eta_{az_c}}{\eta_{elv_c}}$) may present anomalous results in the presence of noise. The effect that this noise can have on resolution of the bank command may be envisioned as shown in Figure B.1. As the magnitude of commanded acceleration approaches zero, bank command resolution is severely degraded. In the limiting case where commanded acceleration is zero the roll system command becomes undefined. This behavior has been simulated in the computer model with results as shown in Figure B.2. Note that when the commanded acceleration is sufficiently close to zero the bank command angle traverses between +180° and -180°.

Low level signal roll control logic has been developed to improve the roll system response under these anomalous conditions. Figure B.3 illustrates the roll control system model implemented with this logic. The first section of the system is noise suppression processing. The relationship of the output ϕ_c' to input, is implemented in the simulation by the the following difference equation, $\phi_c'(i) = K\phi_c(i) + (1-K)\phi_c'(i-1)$ where K is a gain selected by the threshold function shown in the diagram. When commanded acceleration is below a specified level, K becomes zero and ϕ_c' holds its last value. When commanded acceleration is above this threshold K becomes unity and ϕ_c' is equal to ϕ_c. The characteristic form of the nonlinear gain K may be altered to meet the requirements of noise immunity for the roll control system. In addition to a dead zone in the roll channel, it may also be desirable to have a dead zone in the pitch steering channel. Since the corrupted bank angle command may position the airframe at an unfavorable attitude, excessive out-of-plane motion could occur if the system were allowed to develop acceleration during this time.

In a complete design of a BTT system, the selection of dead zone width would be based on expected noise levels, autopilot stability and required performance. Noise and autopilot stability are not considered in this per-

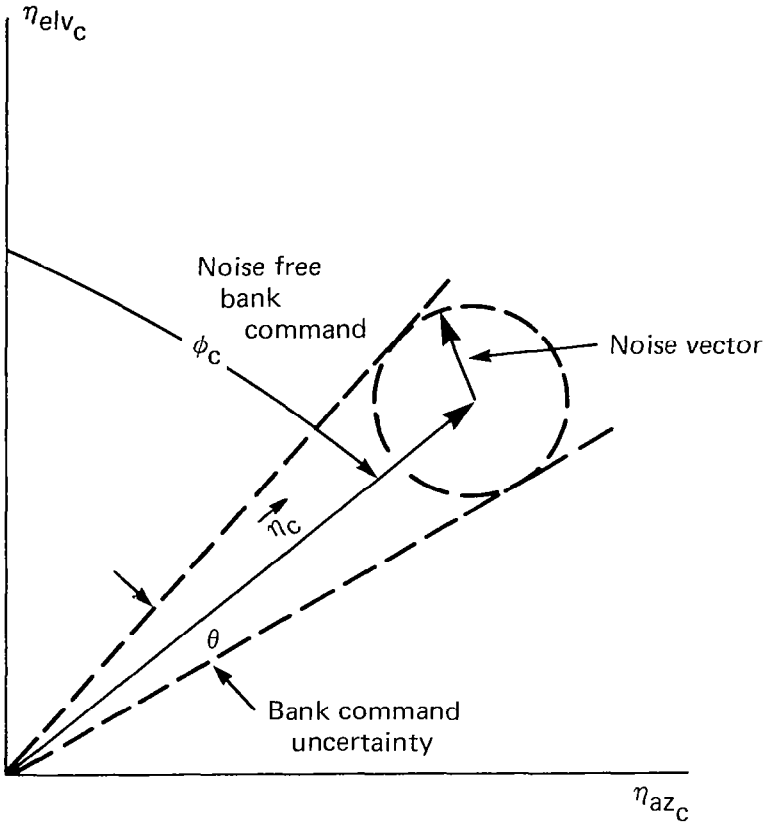

Fig. B.1 Resolution of the bank command in the presence of noise.

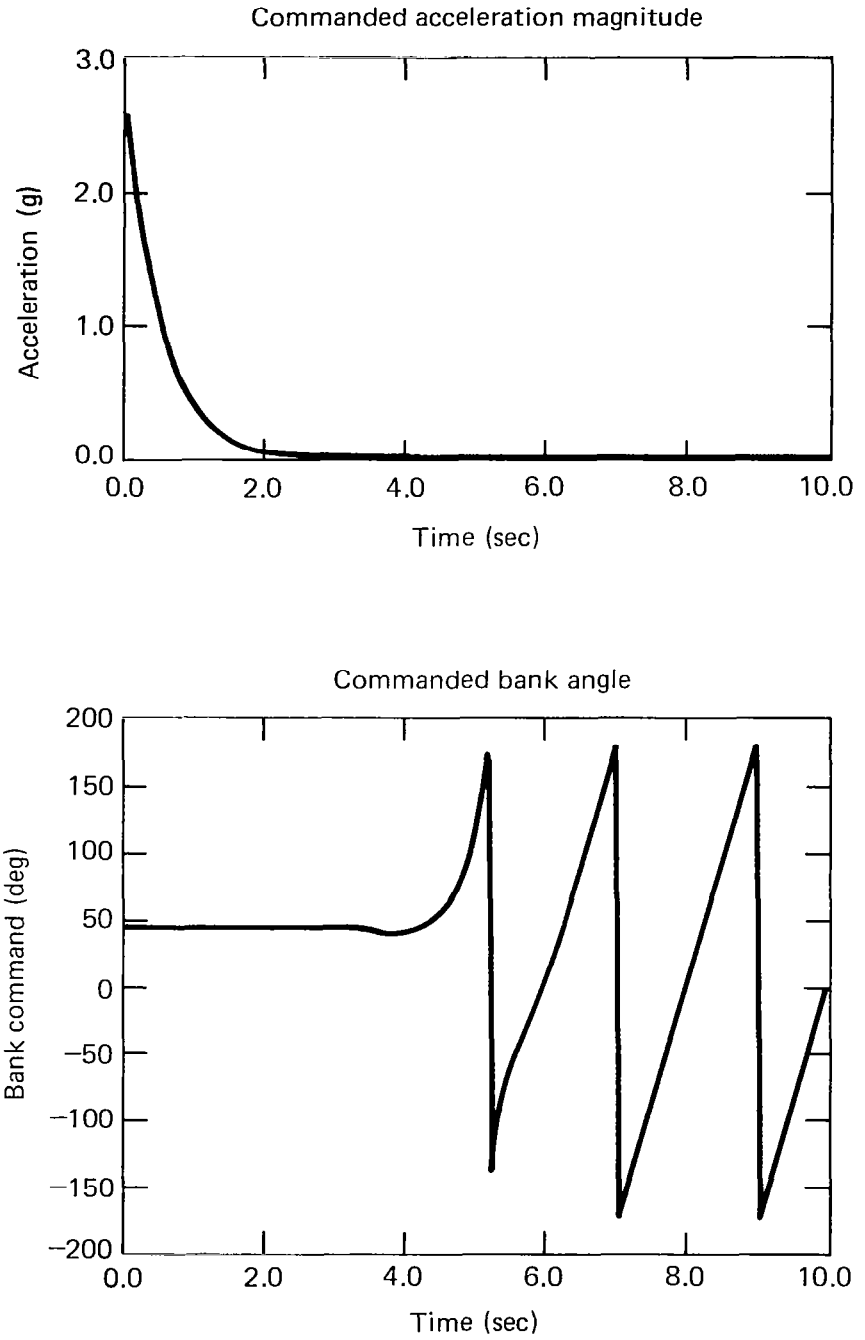

Fig. B.2 Illustration of roll system response to the arctangent roll control function in the presence of low level commanded acceleration and noise.

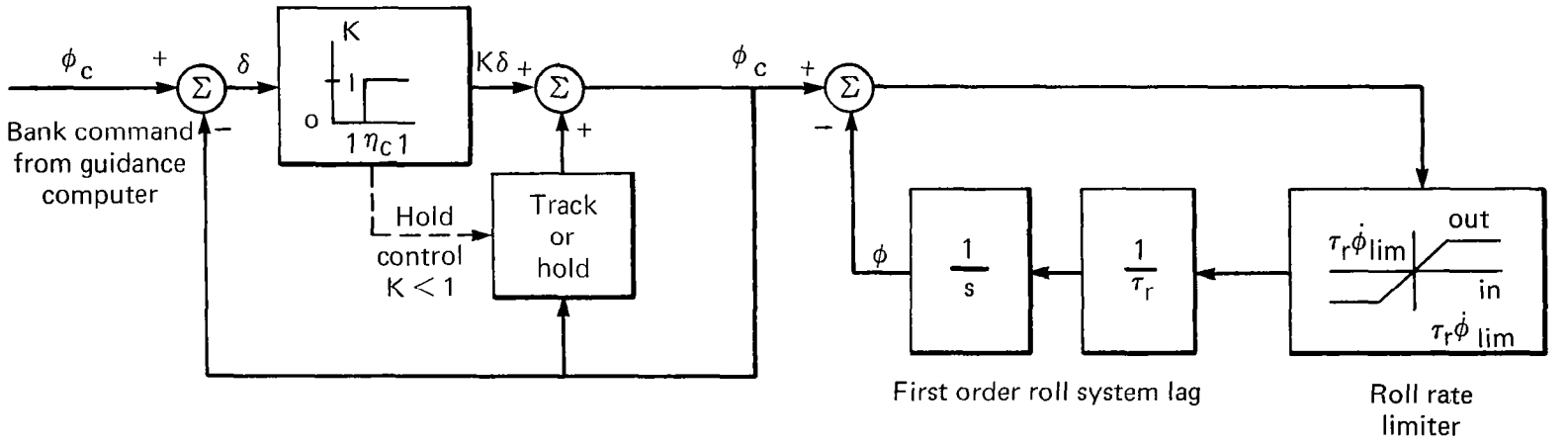

Figure B.3 Roll system configured with low level signal roll control logic.

formance study. Figure B.4 illustrates the miss distance performance of a representative raid suppression engagement (10 degree initial heading error) as a function of the dead zone width expressed in commanded acceleration g. The data for several initial ranges-to-go are presented. Some degradation in performance is expected as the dead zone width is increased because this tends to increase the response time of the system. However, the results in Figure B.4 indicate that the performance degradation is not dramatic. This is because the commanded acceleration is rarely less than about 2 g. Thus the increase in response time due to the dead zone delay is quite small.

Since the selection of dead zone does not significantly alter performance, a value of 0.05 g was selected for the study. This small value is sufficient to avoid any undesirable roll excursions that might be caused by computer round-off errors.

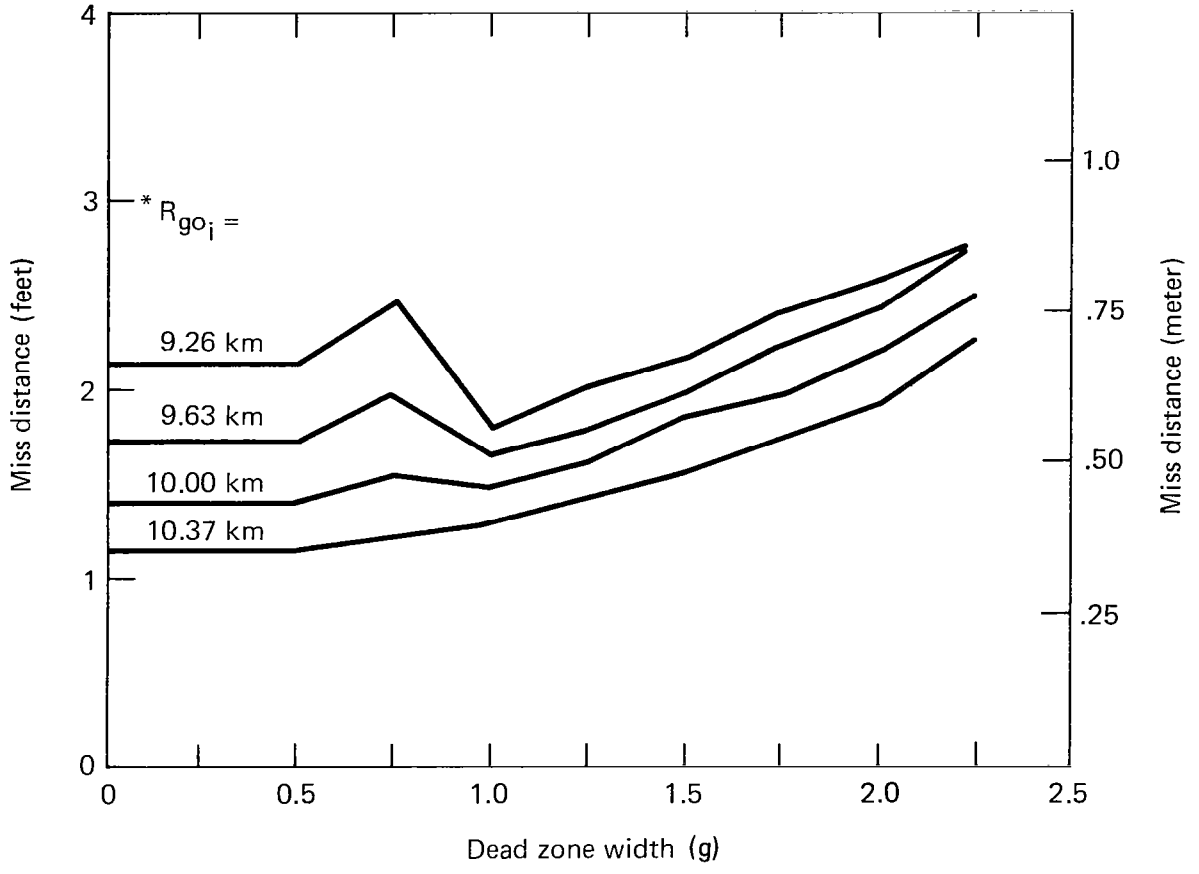

* R_{go_i} is range-to-go at homing initiation

Fig. B.4 Effect of roll control dead zone nonlinearity on performance.

APPENDIX C

COMPARISON OF 5 DEGREE-OF-FREEDOM AND 6 DEGREE-OF-FREEDOM TURN COORDINATION MODELS

A coordinated turn requires the missile to rotate the airframe about the missile velocity vector. This motion results in a rapid turn with minimum induced sideslip. Both a 6 degree-of-freedom (DOF) and a 5 DOF model of a bank-to-turn (BTT) system which executes coordinated turns have been developed (Section 7.5.3). The 6 DOF model utilizes a cross coupling of roll rotation rate and achieved pitch acceleration to formulate the yaw acceleration command resulting in turn coordination. With this technique, sideslip is regulated near zero. The 5 DOF model represents the characteristics of a perfectly coordinated autopilot. Since yaw acceleration is forced to be zero, sideslip is also maintained at zero.

Comparative performance results for a representative raid suppression engagement have been generated for both of these models. Figure C.1 contains a graph of the achieved miss distance versus initial range to go (acquisition range) for a 10-degree heading error case. Both systems were configured with a guidance filter lag of 0.3 seconds, aero/control lag of 0.3 seconds and roll rate limit of 250 degrees/seconds. Since the comparison of results was adequate, the simpler 5 DOF model representing ideal BTT coordination was selected for use.

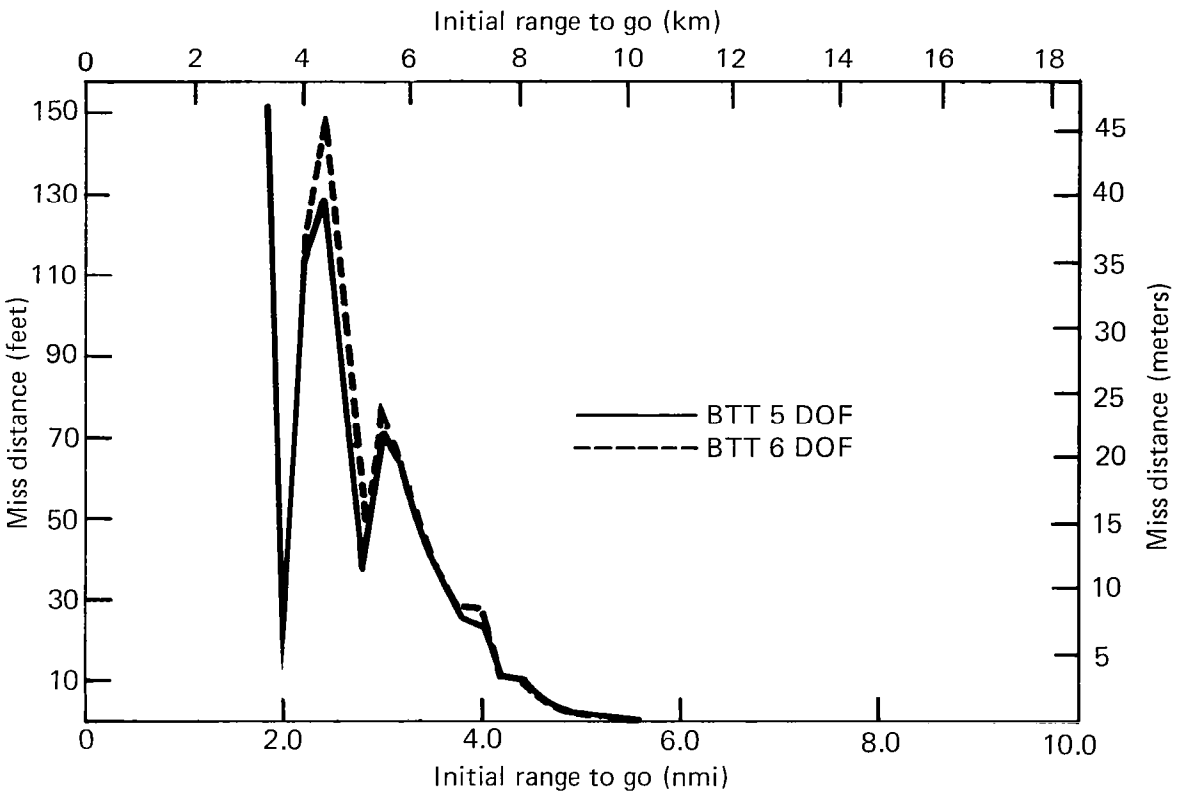

Fig. C.1 Comparison of 5 DOF and 6 DOF turn coordination models.

APPENDIX D

RESPONSE TIME COMPARISON OF STT AND COORDINATED BTT

The results contained in the body of this report indicate that, with appropriate parameter combinations, the performance of a BTT system can exceed that of STT. In order to demonstrate the plausibility of these results, the effective time constants of STT and BTT systems are compared in this appendix. Three factors which influence the response time of the aero/control subsystem and ultimately affect terminal homing performance are considered. These factors are:

1. aero/control time constants
2. commanded maneuver orientation
3. initial conditions.

D.1 COMPUTING RESPONSE TIME

The aero/control subsystem input is a commanded maneuver of specified magnitude and spatial orientation. For a Cartesian steering policy, like STT, the inputs are orthogonal components of commanded acceleration. Since the STT system maintains a fixed roll attitude, the magnitude and polarity of the inputs are adjusted so that the achieved maneuver, which may be expressed as a vector sum of the two orthogonal components, will be of correct magnitude and orientation. For a polar steering policy, like BTT-90 or BTT-180, the inputs are the magnitude and spatial roll orientation of the commanded maneuver. The pitch steering channel of the coordinated BTT aero/control systems develops the required maneuver level while the roll system directs the achieved acceleration. For a minimum sideslip BTT configuration, as considered here, the yaw and roll systems follow a coordinated control policy which results in a maneuver with zero sideslip (yaw acceleration).

Response time is evaluated by exciting each control configuration with a step change in the commanded maneuver. It is assumed that initially the commanded maneuver level is zero and that the output of the aero/control system has some specified initial condition (residual acceleration level). Following the step change of the input, the output of each control policy

(i.e., achieved acceleration) is resolved (via vector projection) into the plane of the commanded maneuver. The response time in the plane of the commanded maneuver is determined by calculating the time required for the response to reach 63 percent of its final value. The equations describing the acceleration response in the plane of maneuver are developed next.

Figure D.1 illustrates the geometry used in evaluating response time. For both STT and BTT the initial roll attitude is referenced at ϕ=0 degrees. The commanded maneuver orientation is Φ_c and the maneuver level is N.

For the STT policy the aero/control commands are:

$$\eta_{p_c} = N \cos \Phi_c$$

$$\eta_{y_c} = N \sin \Phi_c$$

$$\phi_c = 0$$

where η_{p_c} and η_{y_c} are commanded pitch and yaw acceleration respectively. The response of these control channels may be expressed as:

$$\eta_p(t) = N (\cos \Phi_c) (1-e^{-t/\tau_a}) + \eta_p(0)e^{-t/\tau_a}$$

$$\eta_y(t) = N (\sin \Phi_c) (1-e^{-t/\tau_a}) + \eta_y(0)e^{-t/\tau_a}$$

$$\phi(t) = 0$$

where $\eta_p(0)$ and $\eta_y(0)$ are initial conditions on the pitch and yaw steering channels respectively. Forming the vector projection of the acceleration response yields:

$$\eta_m(t) = \eta_p(t) \cos \Phi_c + \eta_y(t) \sin \Phi_c$$

$$\eta_m(t) = (\eta_p(0) \cos \Phi_c + \eta_y(0) \sin \Phi_c)e^{-t/\tau_a} + N(1-e^{-t/\tau_a}) \quad .$$

For the BTT policy the aero/control commands are

$$\eta_{p_c} = N$$

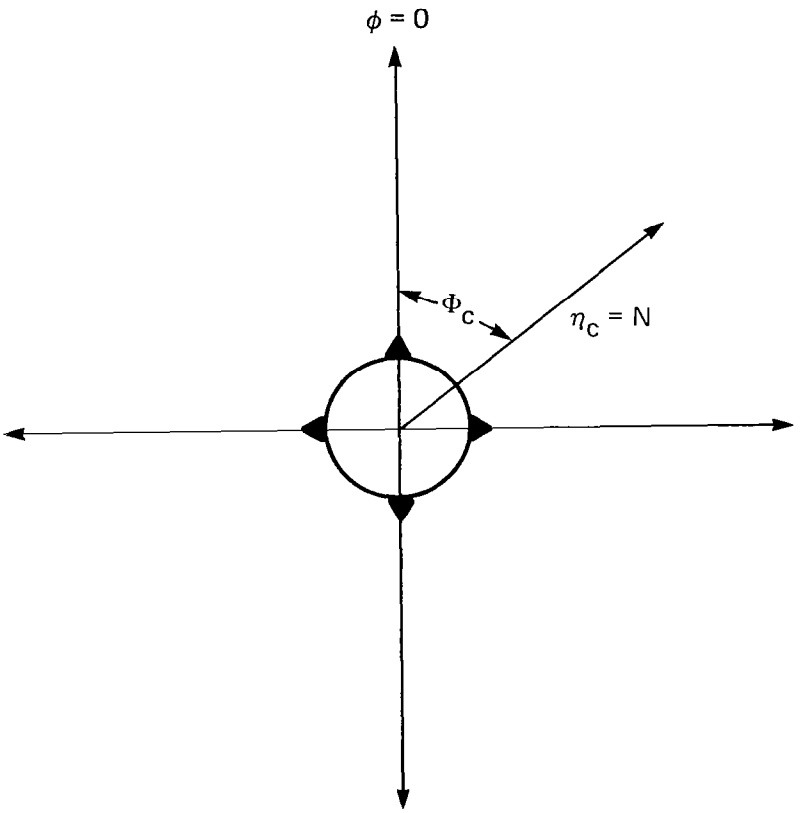

Fig. D.1 Response time geometry.

$$\eta_{y_c} = 0$$

$$\phi_c = \Phi_c$$

The response of these control channels may be expressed as:

$$\eta_p(t) = \eta_p(0)e^{-t/\tau_a} + N(1-e^{-t/\tau_a})$$

$$\eta_y(t) = 0$$

$$\phi(t) = \Phi_c(1-e^{-t/\tau_r})$$

Forming the vector projection of the acceleration response requires the definition of the angle between the BTT pitch plane and the maneuver plane, which is denoted as:

$$\Delta\phi(t) = \Phi_c - \phi(t)$$

$$\Delta\phi(t) = \Phi_c e^{-t/\tau_r} \quad .$$

Thus, the response in the maneuver plane is given by:

$$\eta_m(t) = \eta_p(t) \cos \Delta\phi(t)$$

$$\eta_m(t) = [\eta_p(0)e^{-t/\tau_a} + N(1-e^{-t/\tau_a})] \cos (\Phi_c e^{-t/\tau_r})$$

The next three sections discuss the effects which the aero/control time constants, commanded maneuver orientation and initial conditions have upon the response time.

D.2 EFFECT OF AERO/CONTROL TIME CONSTANTS

The effect of the aero/control time constants, which are τ_a (steering channel) for STT or τ_a (steering channel) and τ_r (roll channel) for BTT, on response time are evaluated. It is assumed that all initial conditions are zero and that the commanded maneuver orientation is given as Φ_c = 90 degrees.

For the STT policy, the response is given by

$$\eta_m(t) = N(1-e^{-t/\tau_a})$$

The time to reach 63 percent of the final value is computed as follows:

$$\eta_m(t_{63}) = N(1-e^{-t_{63}/\tau_a}) = .63N$$

Solving for t_{63} yields:

$$t_{63} = \tau_a \quad .$$

Thus the response time in the plane of the maneuver is equal to the steering channel time constant for STT.

For the BTT policy, the response is given by:

$$\eta_m(t) = N(1-e^{-t/\tau_a}) \cos (\Phi_c e^{-t/\tau_r}), \text{ with } \Phi_c = \frac{\pi}{2} \quad .$$

Evaluation of the time to reach 63 percent of the final value may be accomplished by simulating the response of this equation on a digital computer, and by observing the time when $\eta_m(t)$ reaches .63N for several combinations of parameters (τ_a, τ_r). Figure D.2 contains a set of curves which show the response time as a function of both τ_a and τ_r. For a given steering system time constant (τ_a) the response time increases as the roll system time constant is increased. Similarly, for a given roll system time constant the response time increases as the steering system time constant increases. It should be noted that, under the conditions investigated here, the response time of the BTT policy is always greater than or equal to the steering system time constant (τ_a). Thus, if both BTT and STT are configured with identical steering lags and the maneuver is initiated with zero initial conditions, the response of BTT will never be faster than STT.

The next section investigates sensitivity of response time to the commanded maneuver orientation.

D.3 EFFECT OF COMMANDED MANEUVER ORIENTATION

The commanded maneuver orientation is given by the angle Φ_c, as defined in Figure D.1. In the previous section, response time was evaluated for a commanded maneuver orientation given by Φ_c = 90 degrees. In this section, it is assumed that initial conditions are zero and that Φ_c = 180 degrees. For purposes of comparison with results in the previ-

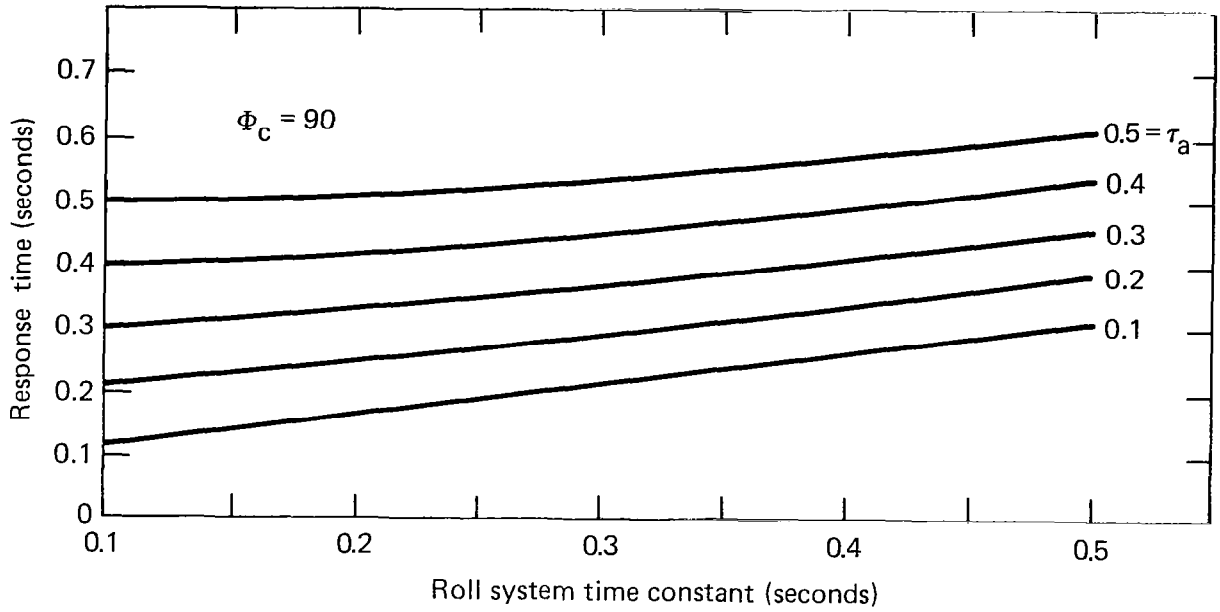

Fig. D.2 Effect of system time constants on maneuver response time.

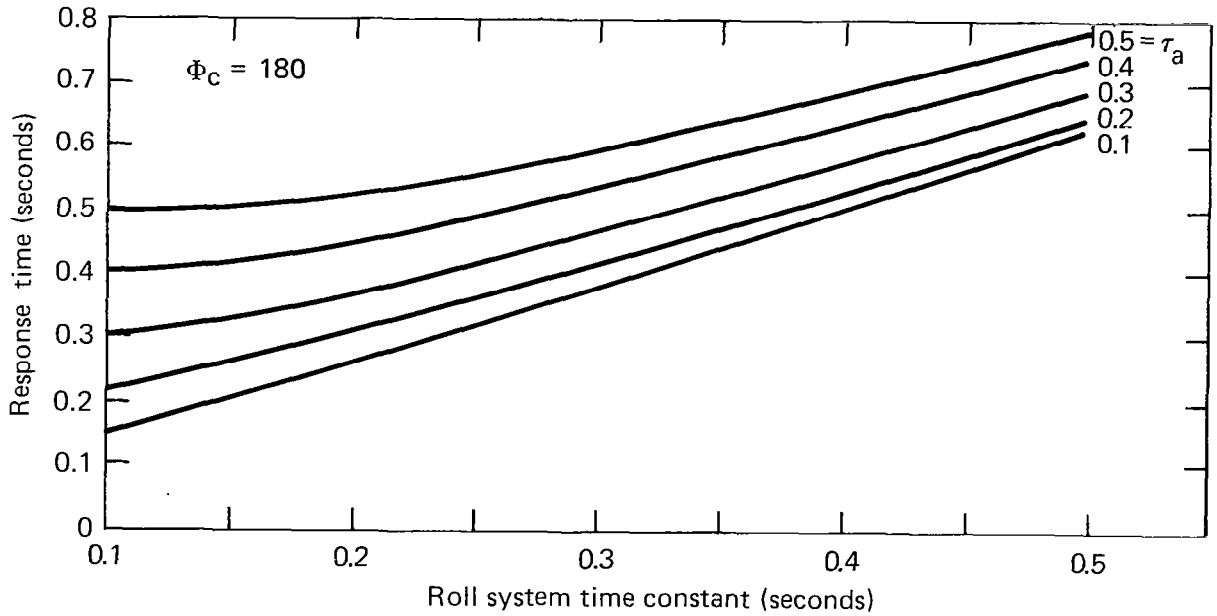

Fig. D.3 Effect of system time constants on maneuver response time.

ous section, response time is evaluated as a function of aero/control time constants.

For the STT policy, the response in the plane of the maneuver is given by:

$$\eta_m(t) = N(1-e^{-t/\tau_a})$$

The time to reach 63 percent of the final value is computed as follows

$$\eta_m(t_{63}) = N(1-e^{-t_{63}/\tau_a}) = .63N$$

Solving for t_{63} yields:

$$t_{63} = \tau_a.$$

This is the same value as computed in the previous section. The STT response time is independent of the commanded maneuver orientation.

The response for the BTT policy may be expressed as:

$$\eta_m(t) = N(1-e^{-t/\tau_a}) \cos(\pi e^{-t/\tau_r}).$$

The solution of this equation for the time when the response reaches 63 percent of the final value is accomplished with the same technique as in Section D.2. Figure D.3 contains a graph of the response time for the BTT policy as a function of steering system time constant (τ_a) and roll system time constant (τ_r). Comparison of these results with those shown in Figure D.2 (Φ_c = 90 degrees) indicates that the response time in the plane of maneuver is sensitive to the commanded maneuver orientation. The slope of the curves for Φ_c = 180 is approximately 50 percent larger than for Φ_c = 90. In general, larger required roll excursions (i.e., larger values of Φ_c) result in slower response time for the BTT policy.

D.4 EFFECT OF INITIAL CONDITIONS

In the previous sections it was assumed that initial conditions on the aero/control subsystem were zero. Under those conditions it was observed that the response time of the BTT policy was always greater than or equal to the STT response time. In this section it will be shown that the response time of STT is insensitive to the initial conditions imposed, while coordinated BTT response time is significantly reduced when some

initial maneuver level is present. The presence of some initial maneuver level in the aero/control subsystem is analogous to the conditions occurring when a roll reversal is initiated during a terminal homing engagement with some residual pitch acceleration.

Given some initial pitch channel acceleration, $\eta_p(0)$, and zero initial yaw channel acceleration, the time response in the maneuver plane for the STT policy is given by:

$$\eta_m(t) = \eta_p(0)\ (\cos\ \Phi_c)e^{-t/\tau_a} + N(1-e^{-t/\tau_a})$$

When $\Phi_c = 90$, the response time is $t_{63} = \tau_a$, regardless of the initial pitch acceleration level. Similarly it can be shown that for any maneuver orientation or initial pitch acceleration, the response time is equal to the steering system time constant for STT.

For the BTT policy, the response in the plane of the maneuver is given by:

$$\eta_m(t) = [\eta_p(0)e^{-t/\tau_a} + N(1-e^{-t/\tau_a})]\ \cos\ (\Phi_c e^{-t/\tau_r})$$

In general this equation may not be solved analytically for the independent variable (t). However, a special case where $\eta_p(0) = N$, leads to an analytic solution. The above equation reduces to:

$$\eta_m(t) = N\ \cos\ (\Phi_c e^{-t/\tau_r})$$

For a maneuver where $\eta_p(0) = N$ and $\Phi_c = 90$, the response time is given by:

$$t_{63} = -\tau_r\ \ell n\left[\frac{\cos^{-1}(.632)}{\pi/2}\right]$$

$$= 0.572\ \tau_r\ .$$

This result indicates that whenever the coordinated BTT maneuver is performed with the pitch system maneuver level initialized to the magnitude of the commanded maneuver, the response time is dependent only on roll system dynamics. Provided the roll system time constant is small enough

relative to the steering time constant (τ_a) of the STT aero/control system (i.e., $\tau_r < \tau_a/0.572$), response time of the BTT aero/control system will be less than that for STT under these conditions. The effect of other initial maneuver levels is examined next.

Figure D.4 illustrates the response time of the coordinated BTT aero/control subsystem as a function of roll system time constant and initial maneuver level for a steering time constant of 0.5 second and commanded roll orientation of 180 degrees. For a given roll system time constant, the response time decreases rapidly as the initial maneuver level is increased. The rate of decrease becomes smaller as the initial maneuver level approaches the commanded maneuver level. These data indicate that the response of the coordinated BTT policy may be faster than STT depending upon the response of the roll system and the level of residual pitch acceleration at the time the maneuver is initiated. A similar set of results is shown in Figure D.5 for a steering time constant of 0.2 second and commanded roll orientation of 180 degrees. When the steering system is fast, the curves are much closer together. In the limit, as the steering time constant approaches zero, only one curve remains which would correspond to the special case considered previously.

D.5 BODY ROTATION RATE REQUIREMENTS

The response time of the coordinated bank-to-turn aero/control subsystem has been shown to be sensitive to the value of the aero/control time constants as well as to commanded maneuver orientation and initial conditions. Results have been generated which express response time as a function of steering system time constant, roll system constant and ratio of initial maneuver level to commanded maneuver level for a given commanded roll orientation. From these data it is possible to compute the maximum roll rate capability required for the BTT response time to equal the STT response time when both systems are configured with identical steering system time constants (τ_a). The method of computing maximum roll rate requirement is described next.

Consider the BTT response time expressed as a function of roll system time constant and ratio of initial maneuver level to commanded maneuver

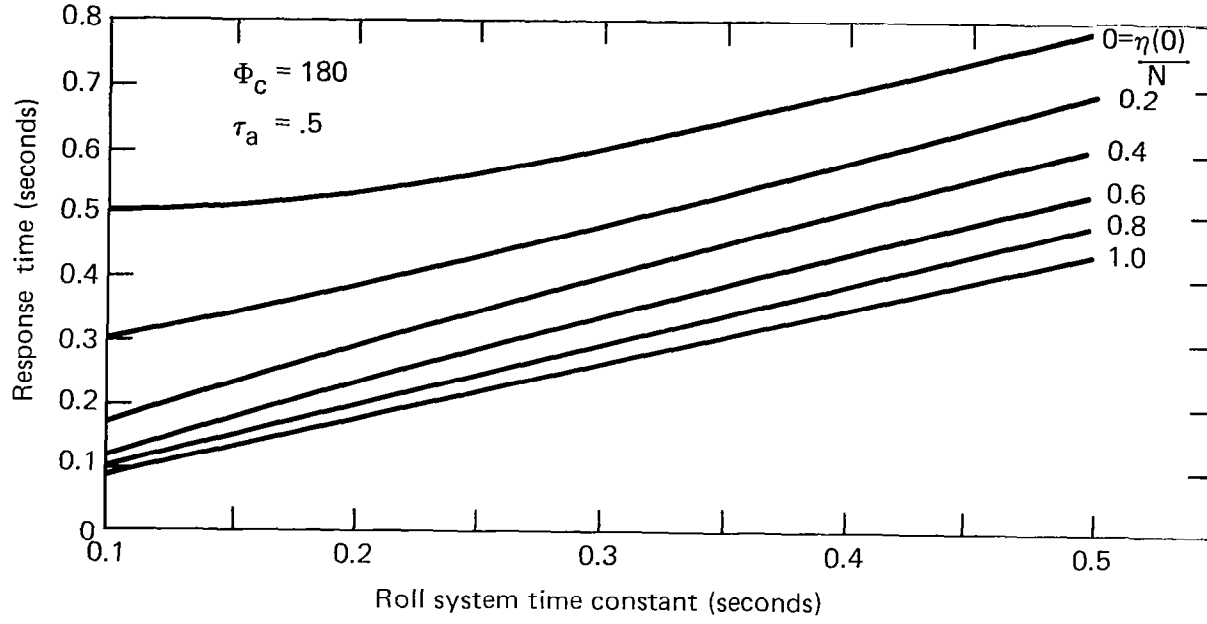

Fig. D.4 Effect of initial maneuver level on maneuver response time.

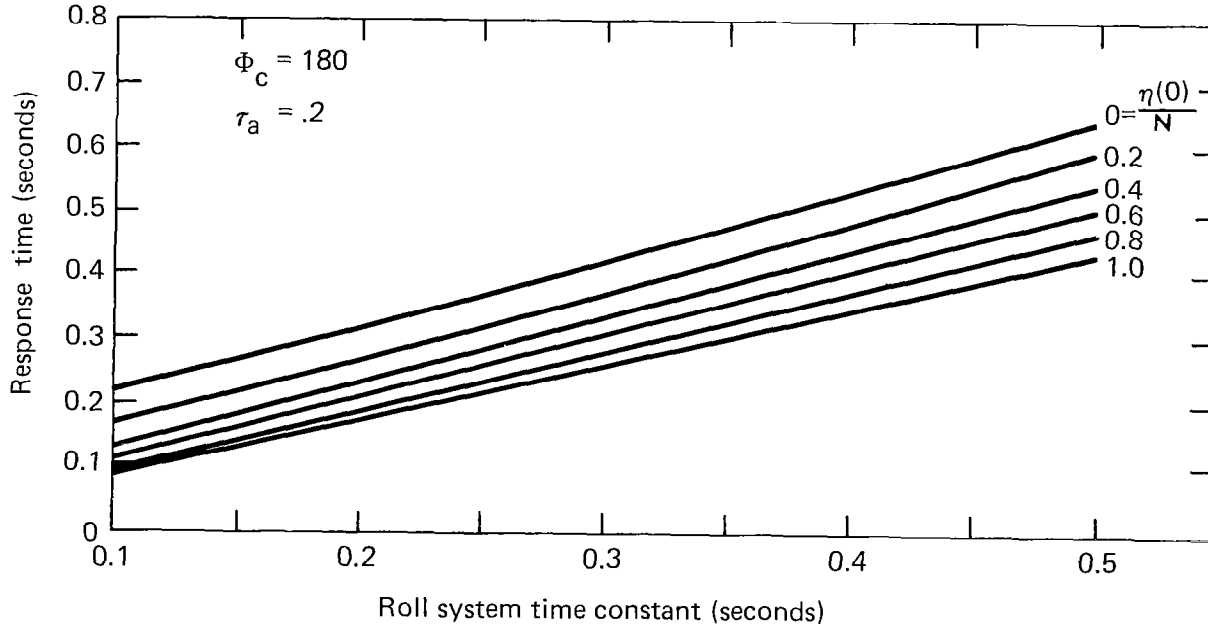

Fig. D.5 Effect of initial maneuver level on maneuver response time.

level for a given steering time constant as shown in Figure D.4. From this graph, the roll system time constant required for the response time to equal the steering time constant (τ_a = 0.5 sec) may be determined as a function of initial maneuver level as shown in Table D.1

TABLE D.1 REQUIRED ROLL SYSTEM TIME CONSTANT

INITIAL MANEUVER LEVEL RATIO	ROLL SYSTEM TIME CONSTANT (SEC)
0.0	0.10
0.2	0.32
0.4	0.40
0.6	0.46
0.8	0.52
1.0	0.57

For a first order roll system, as considered here, the maximum roll rate may be expressed in terms of the commanded roll orientation (Φ_c) and roll system time constant (τ_r) as follows:

$$\dot{\phi}_{max} = \frac{\Phi_c}{\tau_r} \text{ deg/sec}$$

Table D.2 shows the minimum roll rate required for the coordinated BTT response time to equal STT when both systems are configured with a steering time constant of 0.5 sec.

TABLE D.2 ROLL RATE REQUIREMENT

INITIAL MANEUVER LEVEL RATIO	ROLL RATE REQUIREMENT (DEG/SEC)
0.0	1800
0.2	563
0.4	450
0.6	391
0.8	346
1.0	316

In a similar procedure, the maximum roll rate requirement may be determined as a function of initial maneuver level ratio and steering system time constant. Figures D.6 and D.7 illustrate the maximum roll rate requirement for a commanded roll orientation of 90 degrees and 180 degrees respectively. These data indicate that required roll rate capability decreases as the initial maneuver level ratio is increased or as the steering system time constant is increased. In addition, roll rate requirement is larger for the 180 degree commanded maneuver orientation.

In addition to evaluating the maximum required roll rate, it is necessary to consider the yaw rotation required to coordinate the turn at the maximum roll rate. In Section 7 it was shown that a kinematic requirement for turn coordination may be approximated in terms of the missile body rotation rates as follows:

$$r = \dot{\phi} \tan \alpha$$

where

r = yaw rotation rate

$\dot{\phi}$ = roll rate

α = total angle-of-attack

Figure D.8 contains a graph of this equation which may be used in conjunction with the previous figures illustrating roll rate requirements in order to determine required yaw rate capability as a function of total angle-of-attack. Yaw rate requirement is an important quantity which ultimately impacts the design of a coordinated bank-to-turn autopilot.

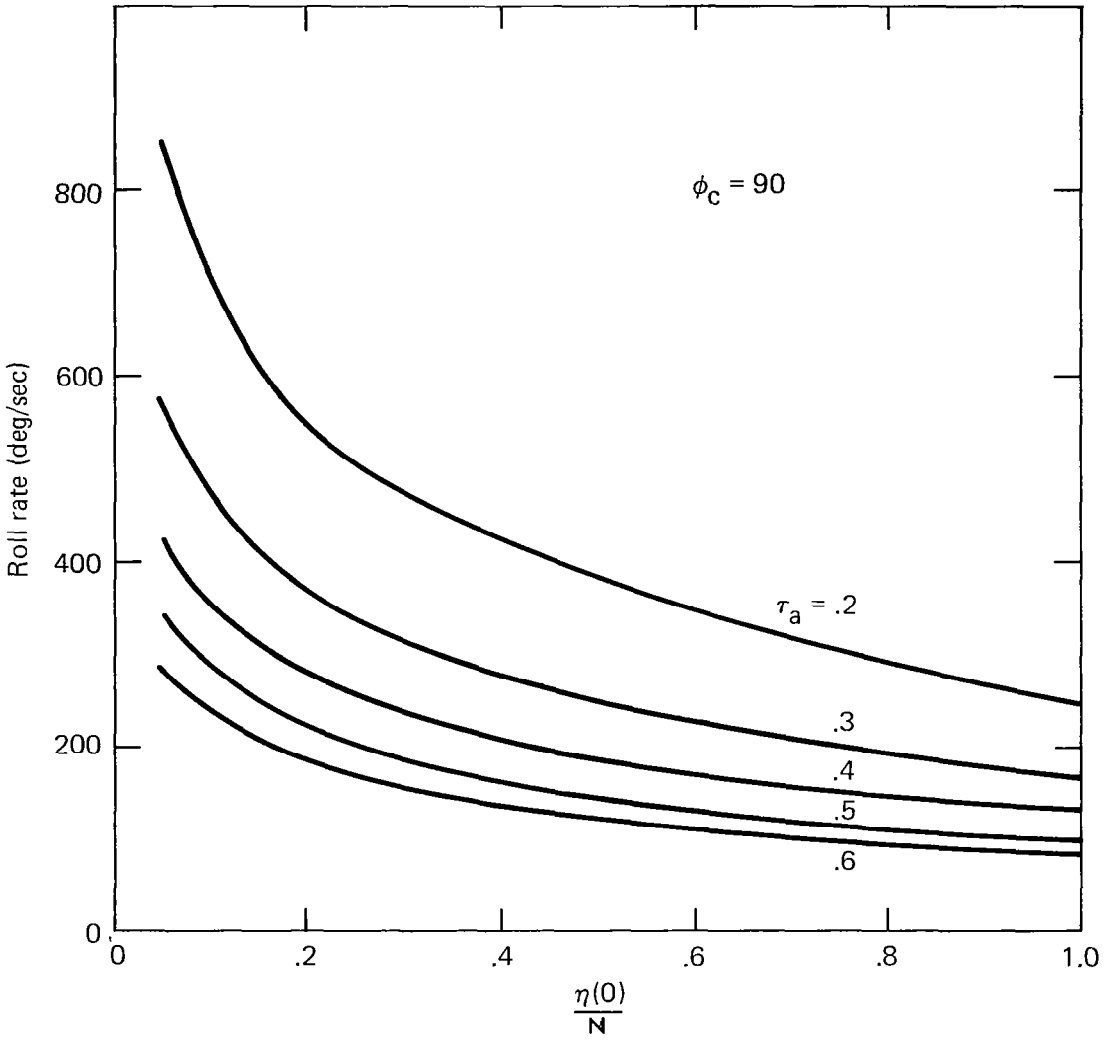

Fig. D.6 Required roll rate for BTT response time to equal STT.

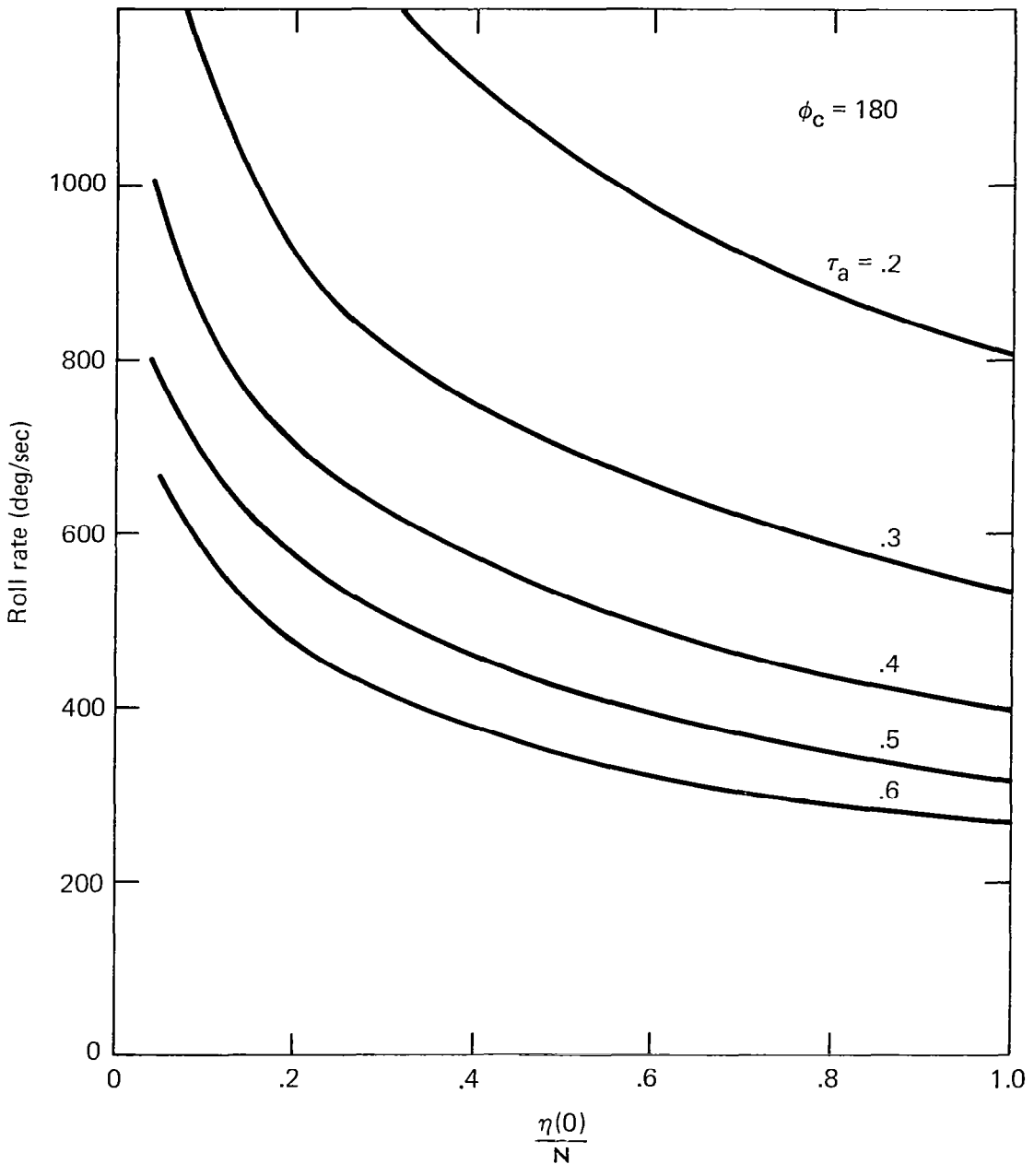

Fig. D.7 Required roll rate for BTT response time to equal STT.

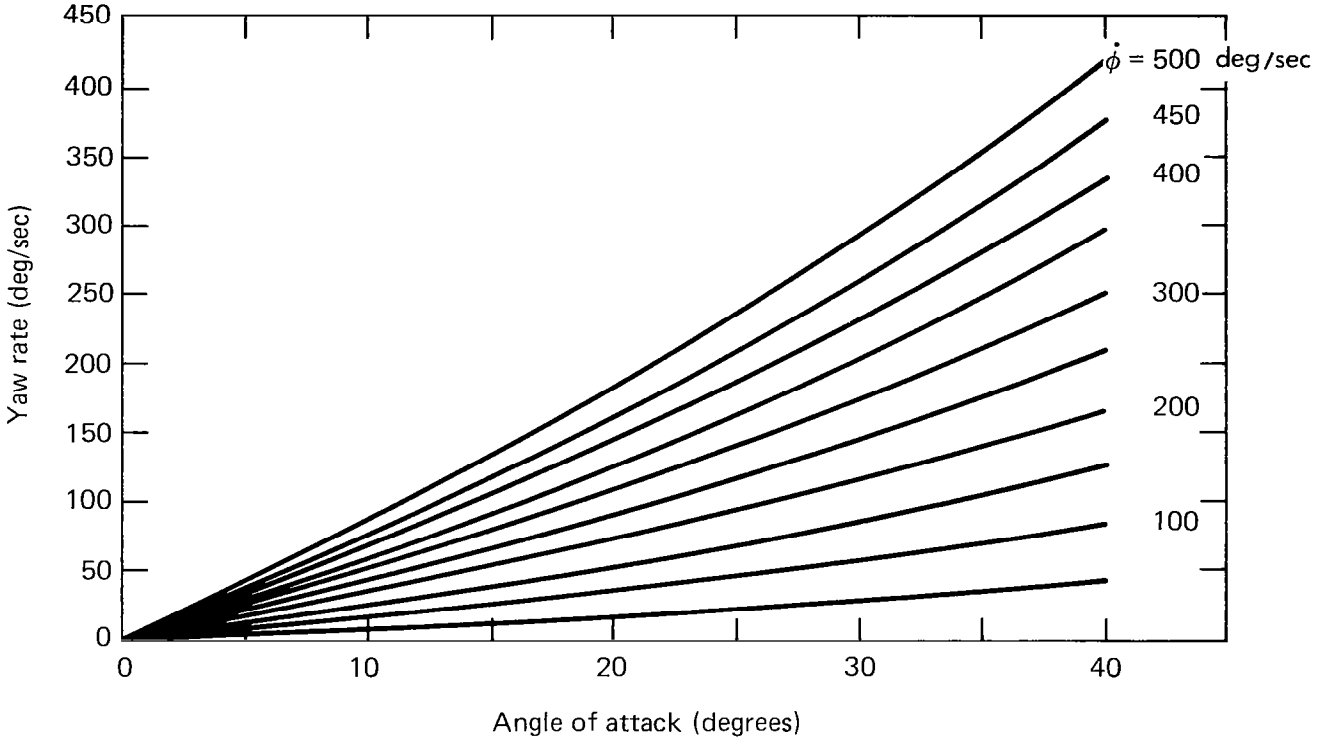

Fig. D.8 Required yaw rate for turn coordination.

APPENDIX E

INTERCEPT PROFILES FOR THE IN-PLANE AND CROSS-PLANE AREA DEFENSE ENGAGEMENTS

The performance measure used to assess the area defense interceptor is described in Section 3. This section contains graphs of the intercept profiles used to generate the comparative performance data shown in Section 5 of this report.

Figures E.1 through E.4 illustrate the results for the moderate-lift configurations against the in-plane target. Figures E.5 and E.6 contain the data for the high-lift configurations against the in-plane target. Figures E.7 through E.10 contain the data for the moderate-lift configurations against the cross-plane target. Figures E.11 and E.12 contain the data for the high-lift configurations against the cross-plane target.

In each figure two sets of results are shown which correspond to the given system configured with the fast and slow system parameter sets. The breakdown of the target trajectory investigated into the cruise, turndown and descent regions described in Section 5 is done as a function of target downrange position as follows:

Region	Downrange Position (dp)
Cruise	$51.5 \geq dp \geq 47.24$ km
Turndown	$47.24 > dp \geq 27.74$ km
Descent	$27.74 > dp \geq 20.36$ km

Percent success in a given region, which is used as the performance indicator in this study, is defined by the ratio of the length of target trajectory which is successfully intercepted in the given region to the total length of target trajectory in the region.

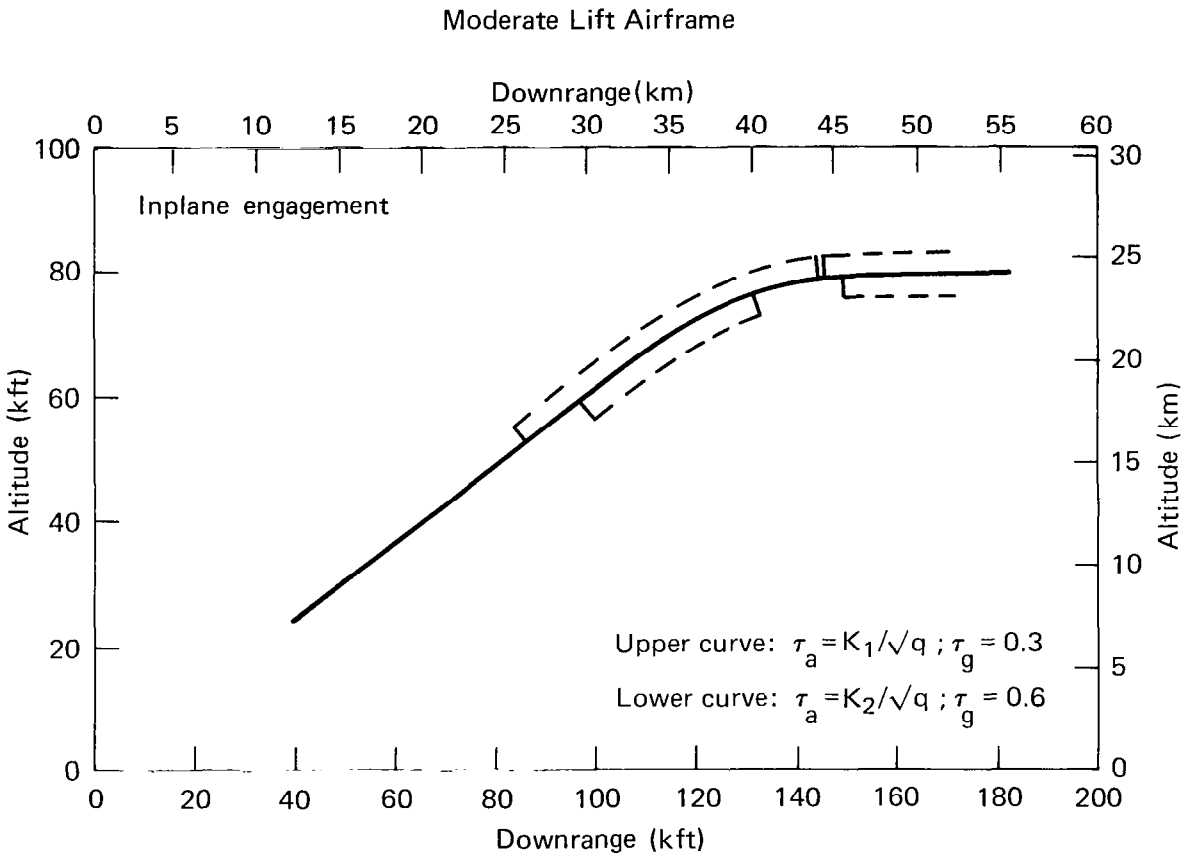

Fig. E.1 Intercept profile for the STT steering policy.

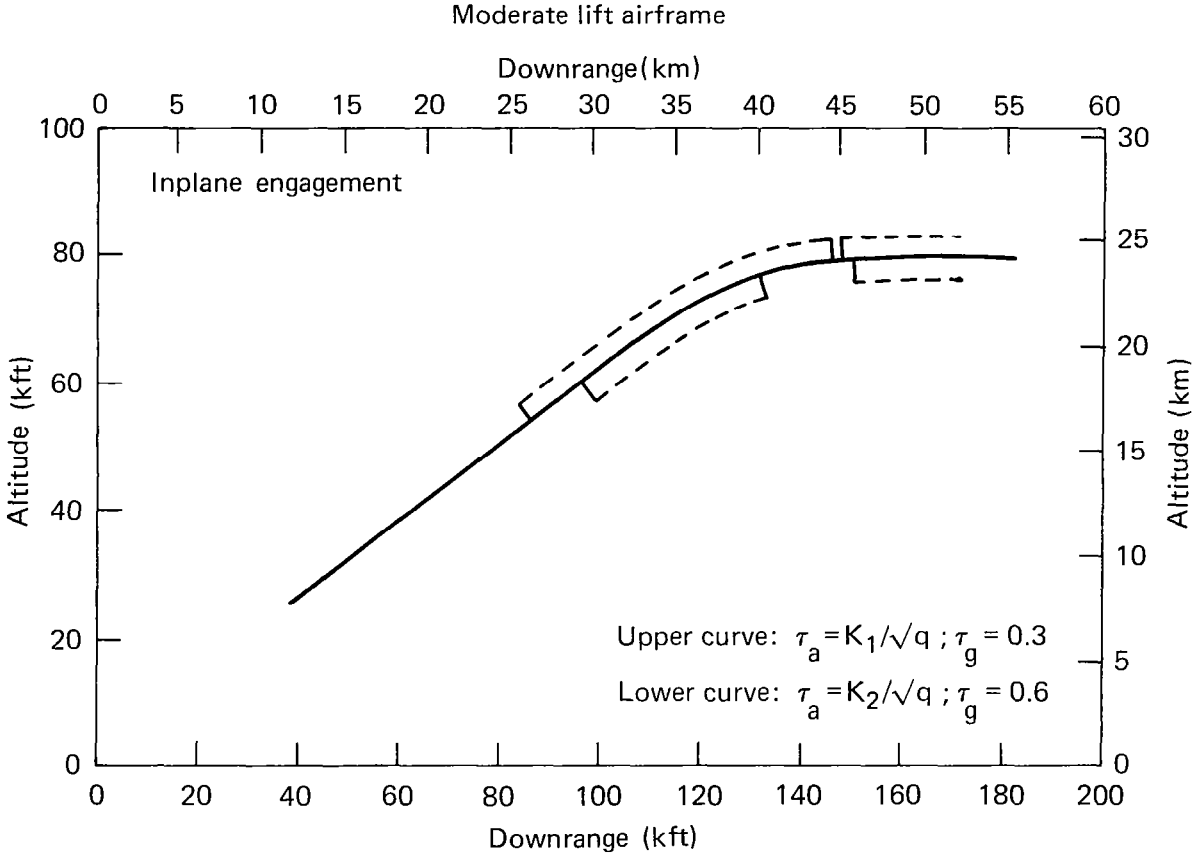

Fig. E.2 Intercept profile for the BTT–45 steering policy.

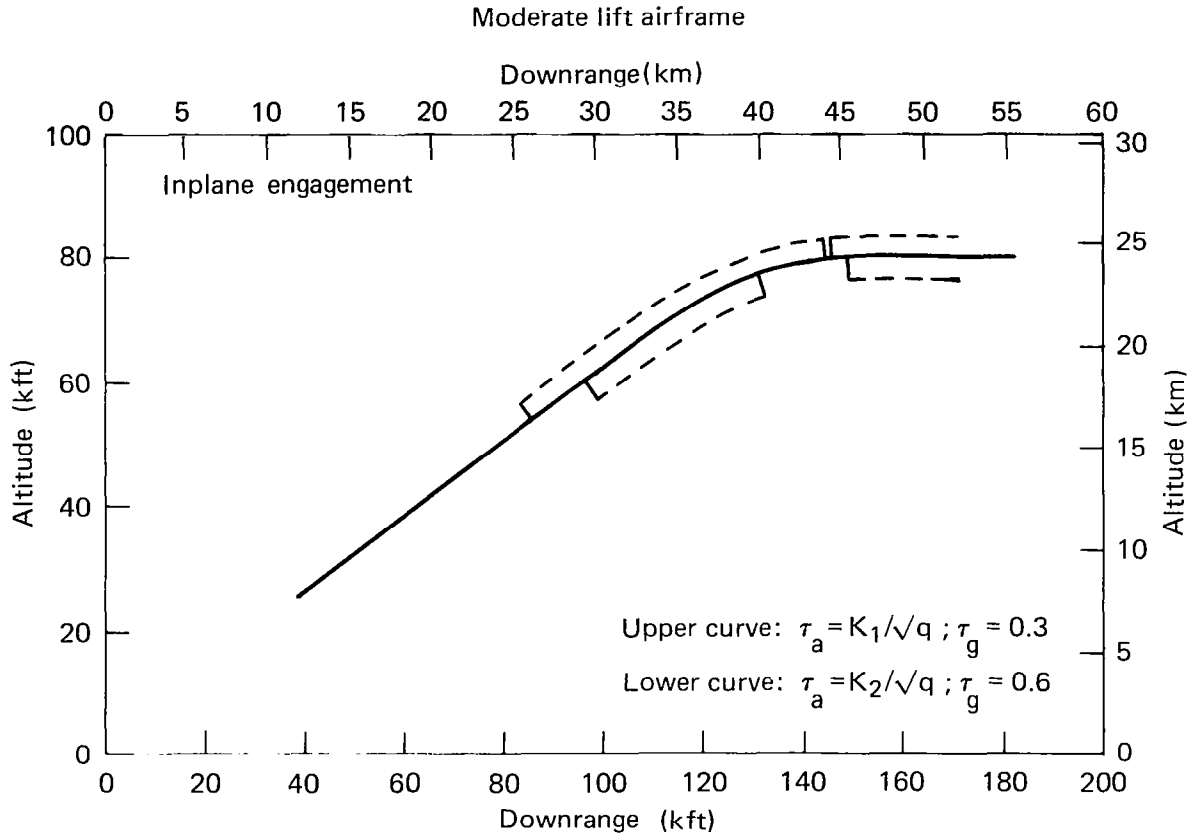

Fig. E.3 Intercept profile for the BTT–90 steering policy.

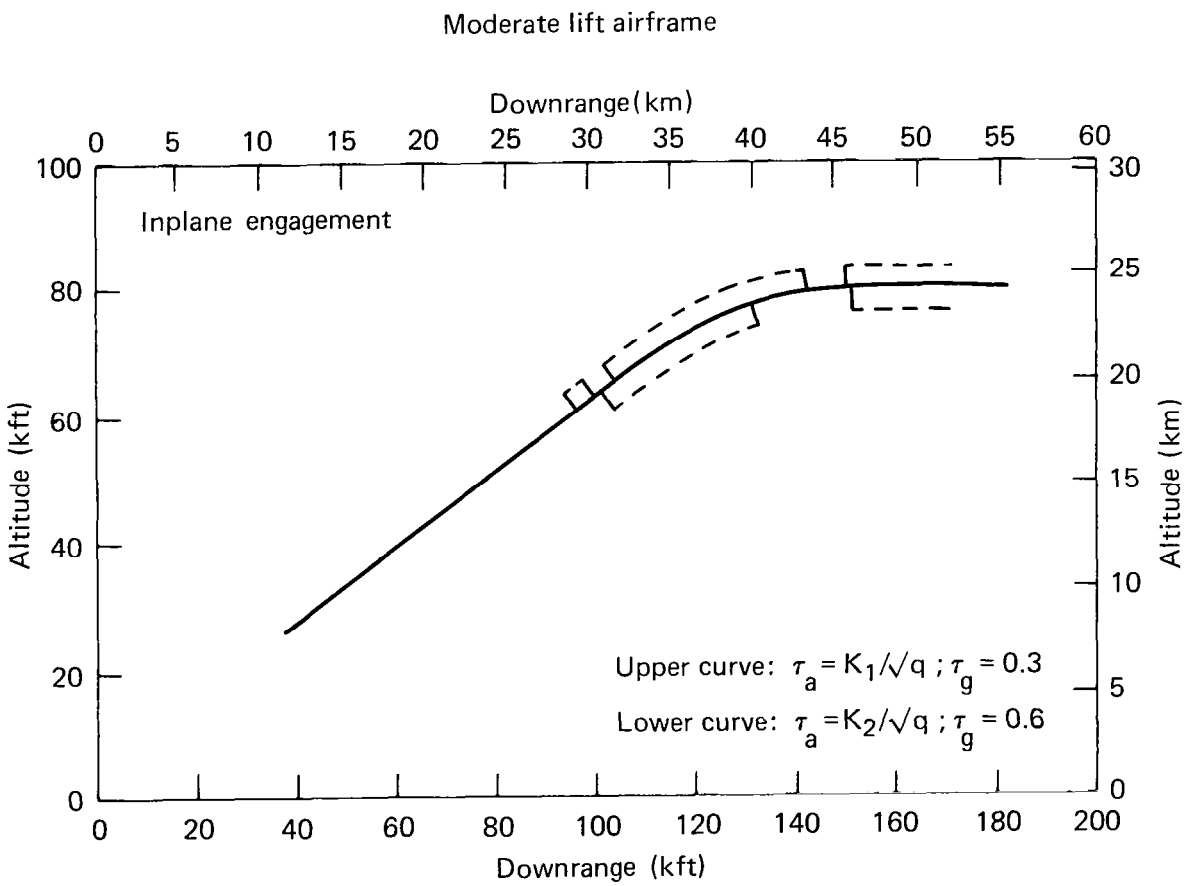

Fig. E.4 Intercept profile for the BTT–180 steering policy.

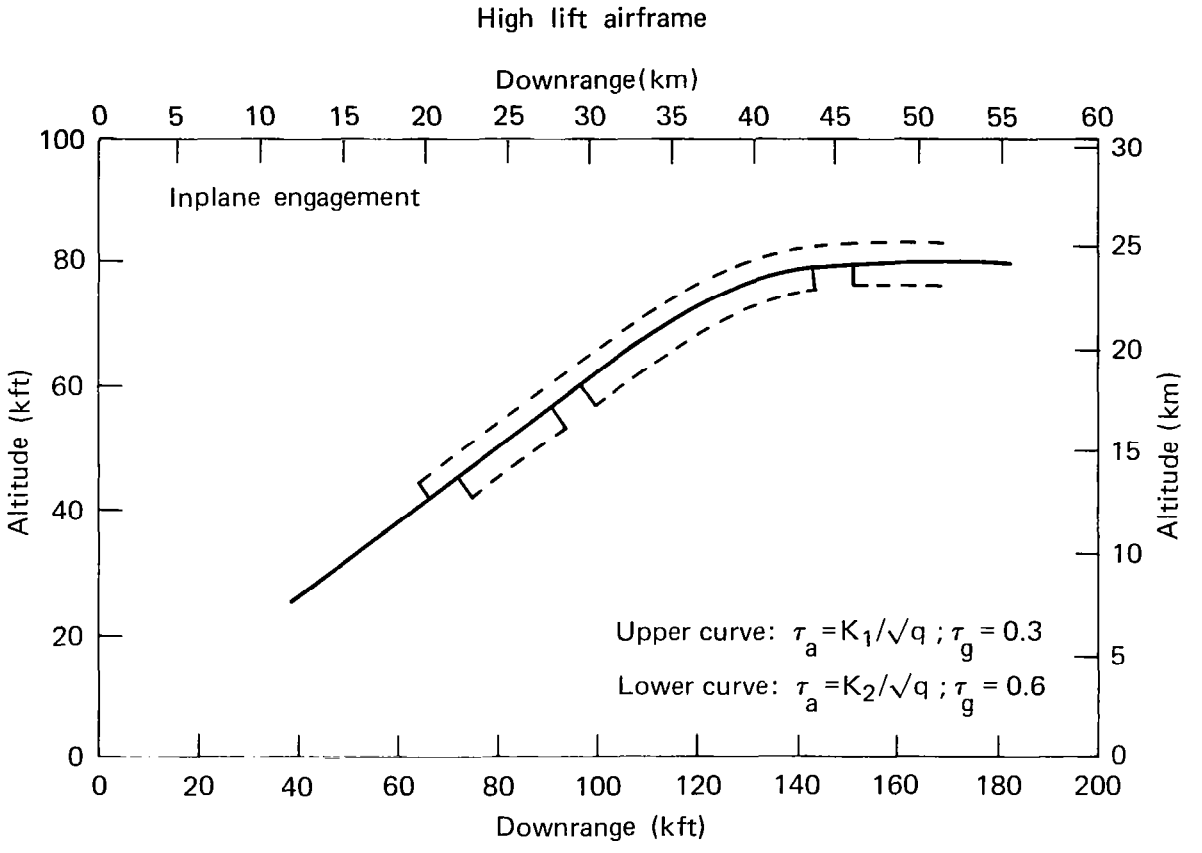

Fig. E.5 Intercept profile for the BTT–90 steering policy.

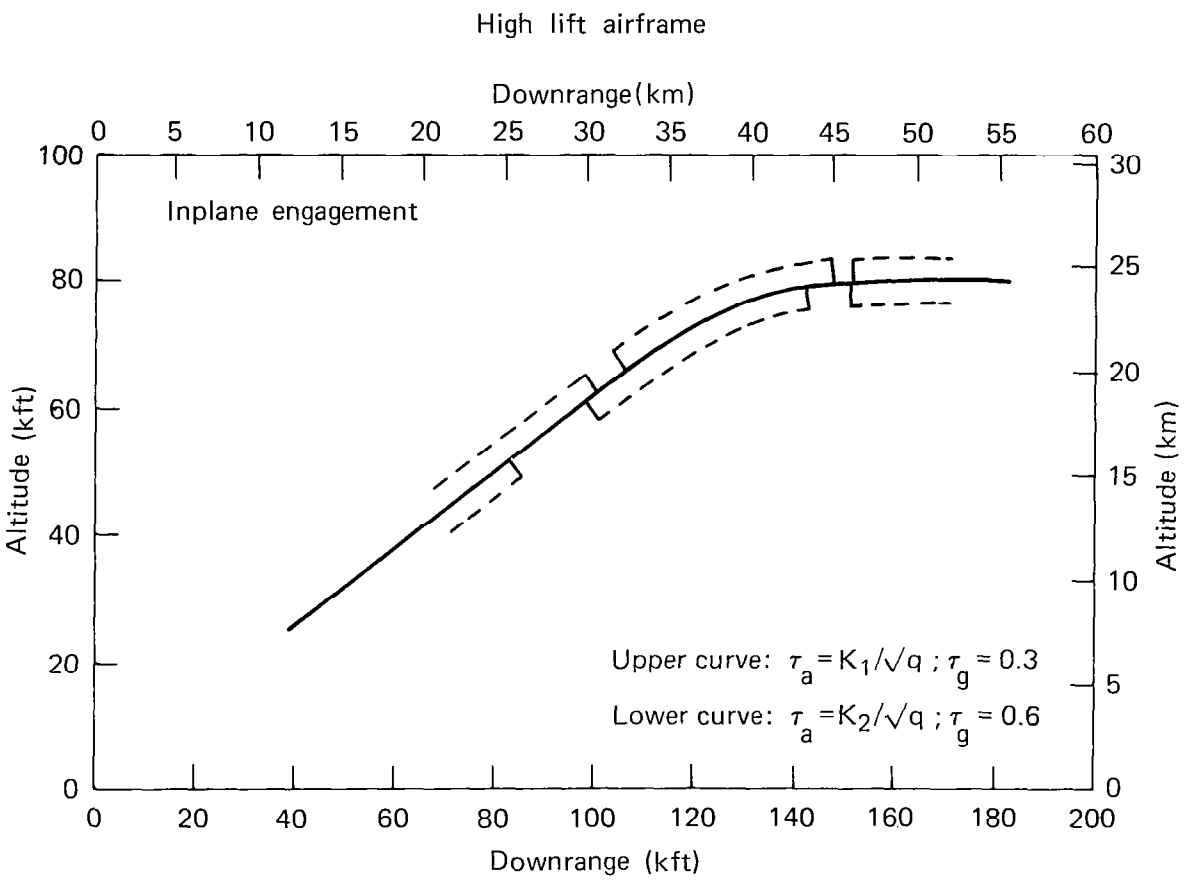

Fig. E.6 Intercept profile for the BTT–180 steering policy.

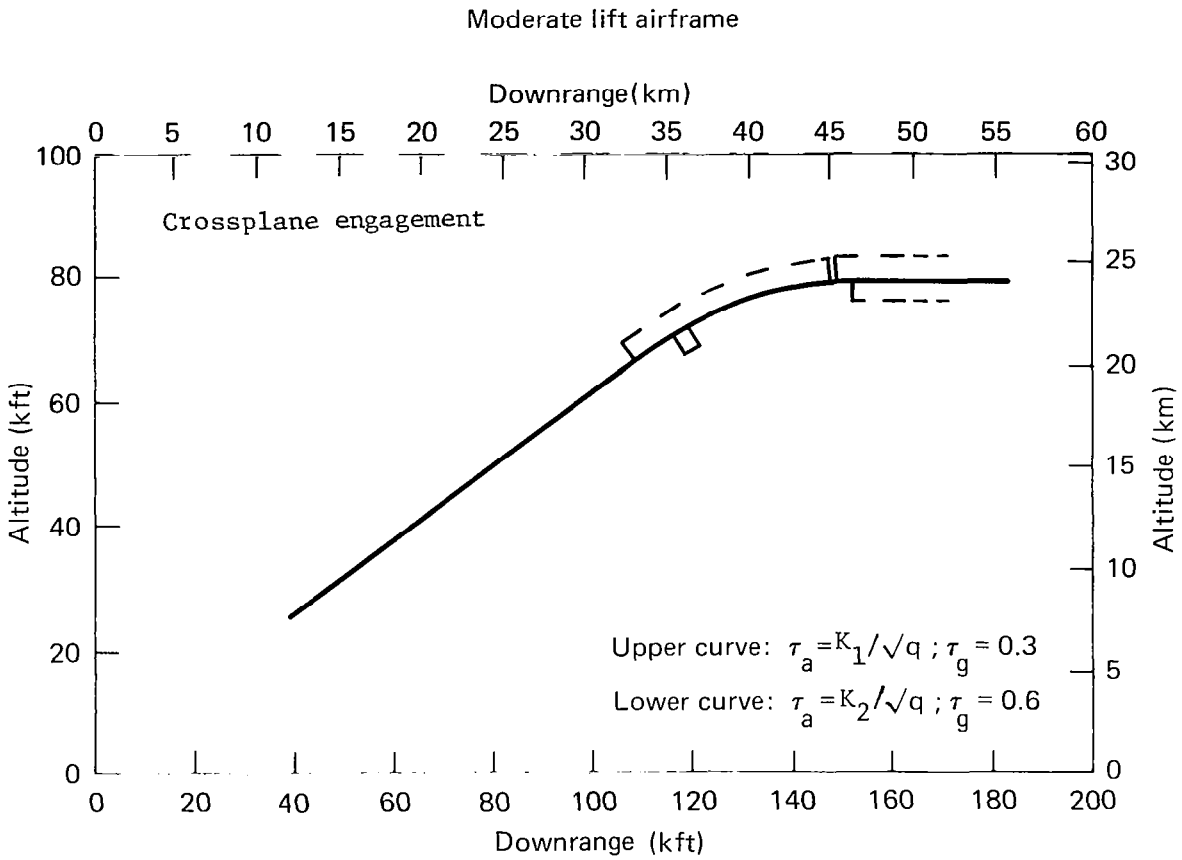

Fig. E.7 Intercept profile for the STT steering policy.

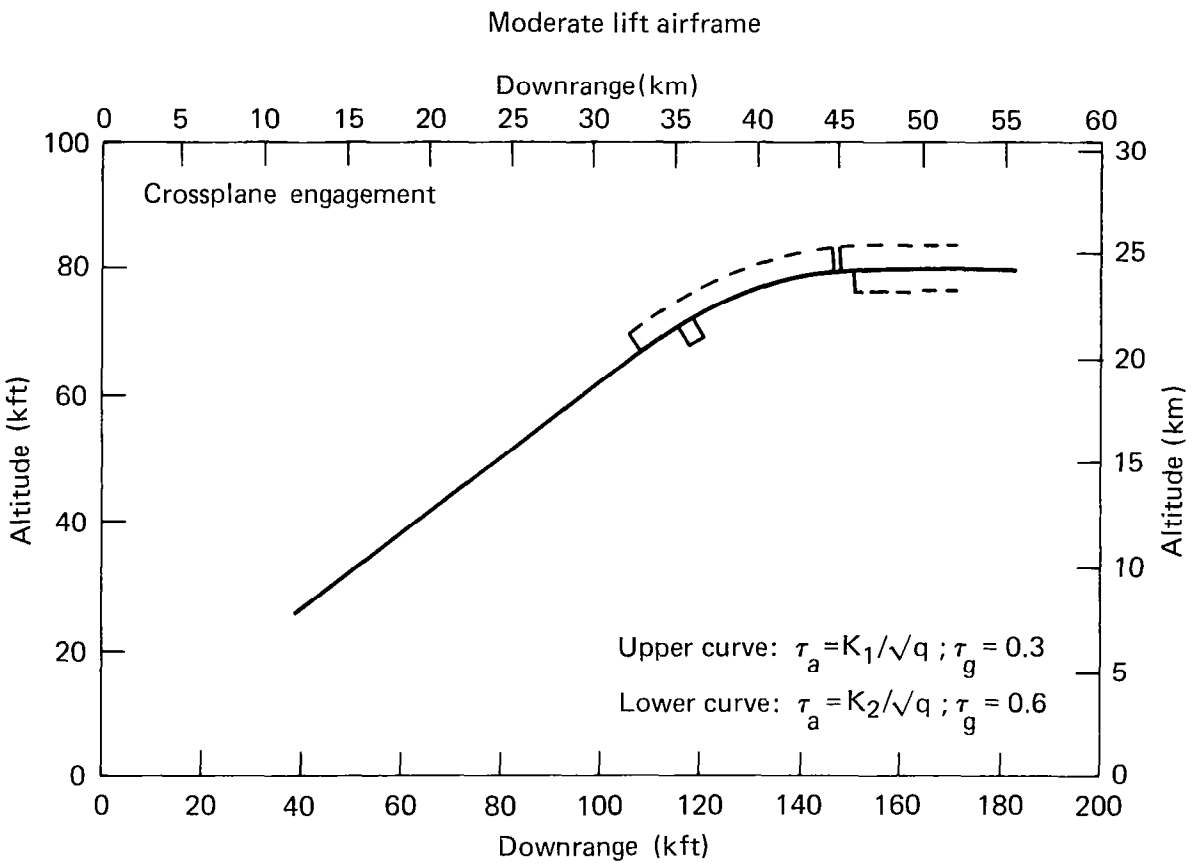

Fig. E.8 Intercept profile for the BTT–45 steering policy.

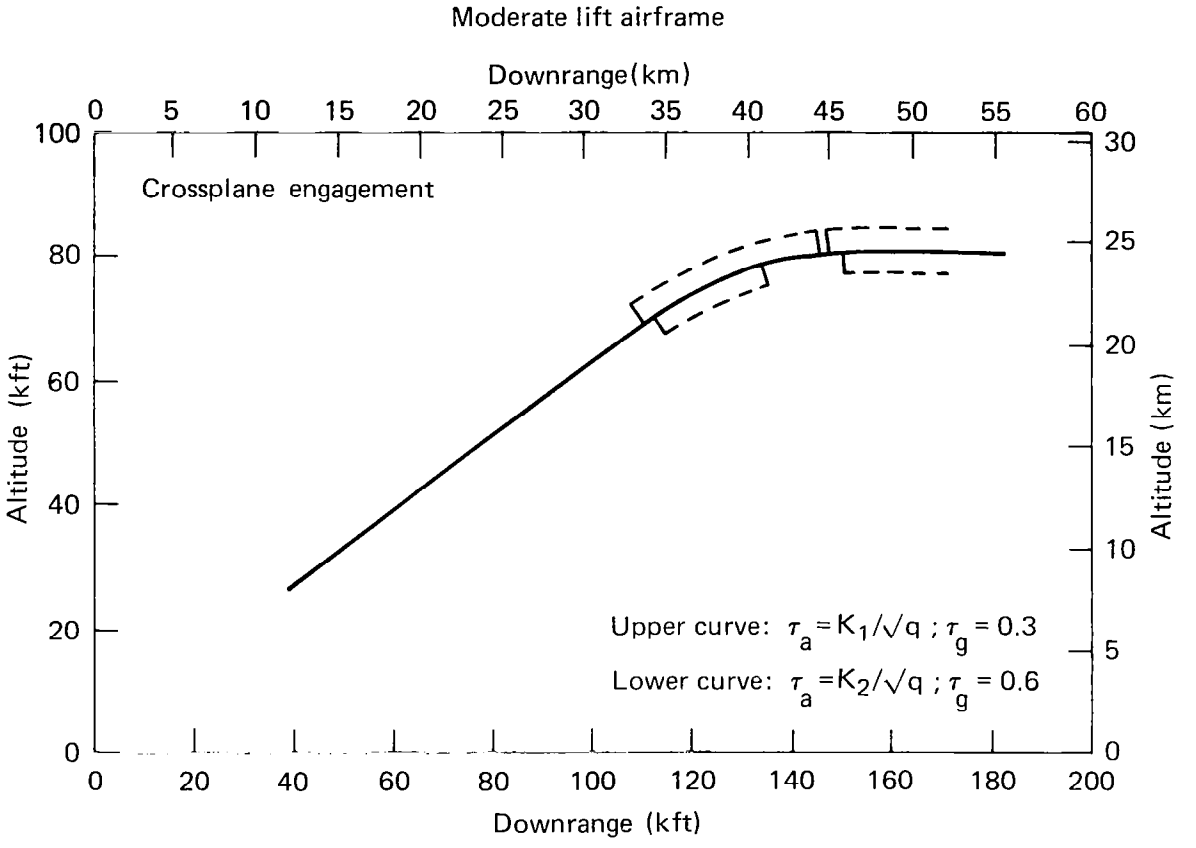

Fig. E.9 Intercept profile for the BTT–90 steering policy.

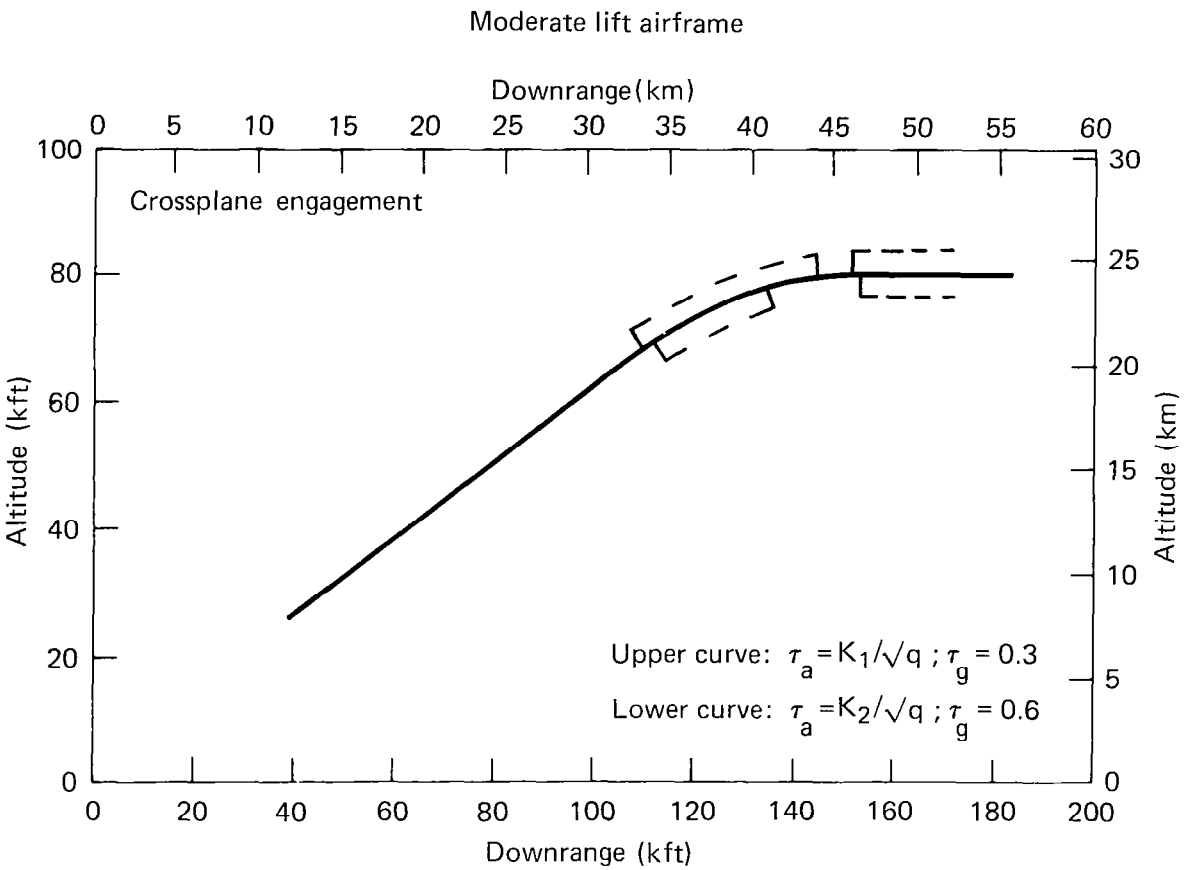

Fig. E.10 Intercept profile for the BTT—180 steering policy.

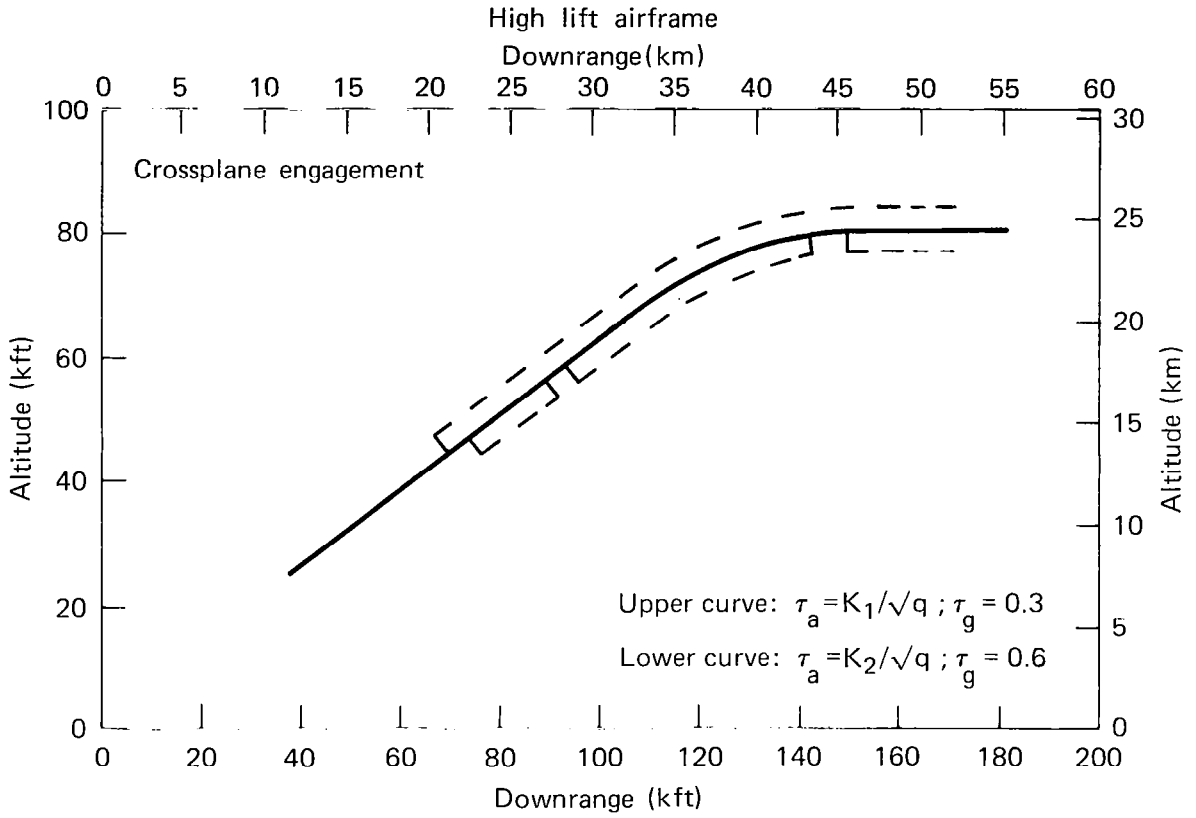

Fig. E.11 Intercept profile for the BTT–90 steering policy.

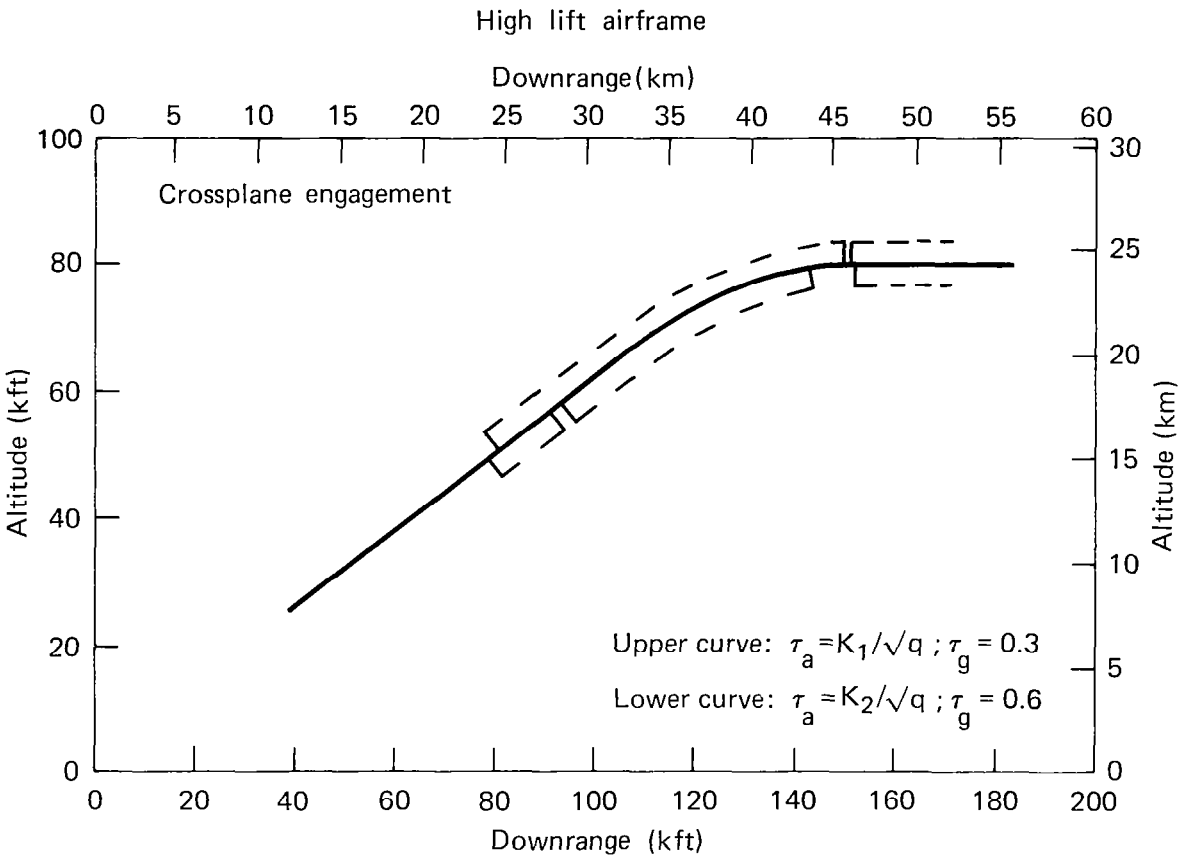

Fig. E.12 Intercept profile for the BTT–180 steering policy.

APPENDIX F

REPRESENTATIVE TRAJECTORY AND MISSILE ATTITUDE TIME HISTORY PROFILES

The end result, achieved miss distance, of a terminal homing engagement provides a measure from which comparative assessments of homing performance may be made. However, these comparisons do not provide an indication of how a missile system responds to the dynamic conditions of the homing engagement. This section provides representative trajectory and missile attitude time history profiles for both the raid suppression and area defense engagements.

Figures F.1 - F.8 present simulation results for the high-lift (planar) BTT-180 raid suppression interceptor configured with the slow set of system parameters. The parameters of the engagement geometry, described in Section 6, are an initial azimuthal heading error of 30 degrees and an initial range-to-go of 6 nmi (11.11 km). The trajectory profiles of the missile and target are shown in Figures F.1 and F.2. The markers on each curve are separated in time by one second each. Figures F.3 and F.4 show the command and response for the pitch steering channel and roll control system respectively. Figure F.5 contains the angle-of-attack time history. Figure F.6 shows how the missile speed decreases due to maneuver-induced drag throughout the engagement. Figures F.7 and F.8 illustrate the heading angle and flight-path angle of the missile velocity vector respectively. Flight-path angle is a measure of the angular deviation of the velocity vector from an inertial horizontal reference plane while the heading angle is a measure of angular deviation from a vertical plane aligned with the downrange axis shown in Figure F.1. The resulting miss distance for this engagement was 21.5 feet (6.55 meters).

Figures F.9 - F.15 present simulation results for the moderate-lift (cruciform) BTT-180 area defense interceptor configured with the slow set of system parameters. The target's initial downrange position, for the in-plane area defense engagement described in Section 10, is 23.93 nmi (44.32 km). Figure F.9 shows the trajectory profile of the missile and target. The markers on each curve are separated in time by 2 seconds

each. Figures F.10 and F.11 illustrate the command and response for the pitch steering channel and roll control system respectively. Figure F.12 contains the angle-of-attack time history. Figure F.13 illustrates how missile speed decreases due to maneuver induced and axial drag. Figures F.14 and F.15 contain the flight-path angle and heading angle of the missile velocity vector, respectively. For this engagement, target acquisition occurred at approximately 6.4 seconds and the resulting miss distance was 71.5 feet (21.8 meters).

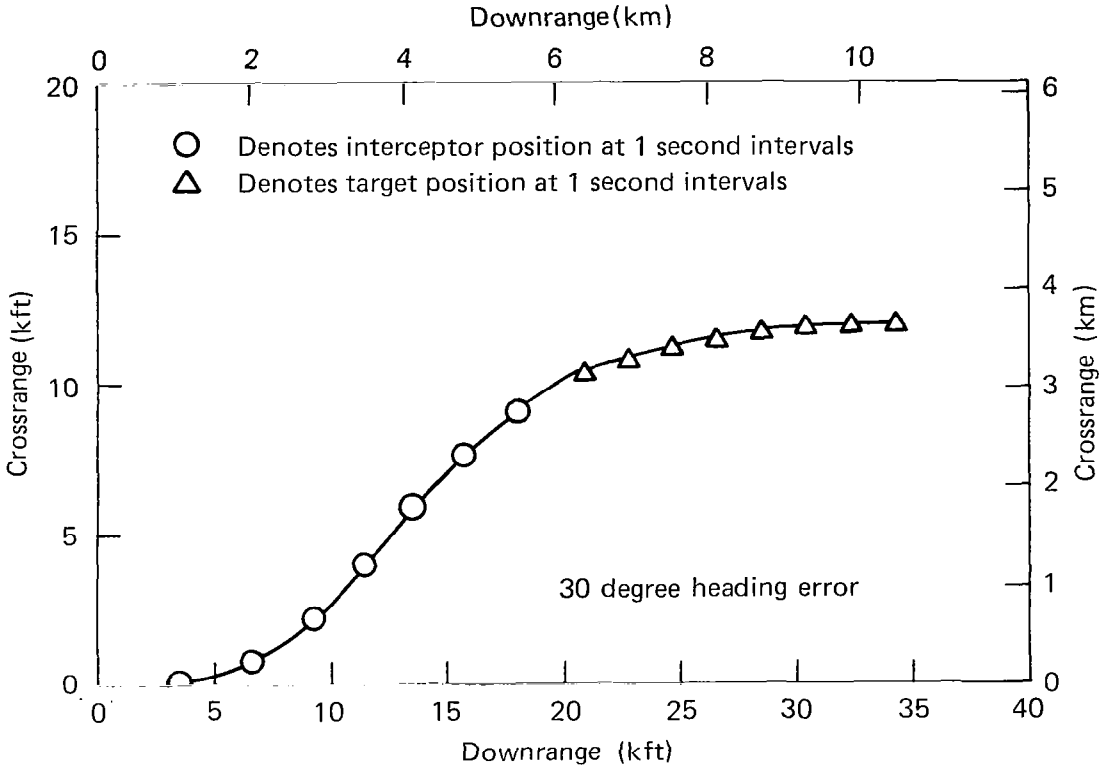

Fig. F.1 Raid suppression trajectory profile.

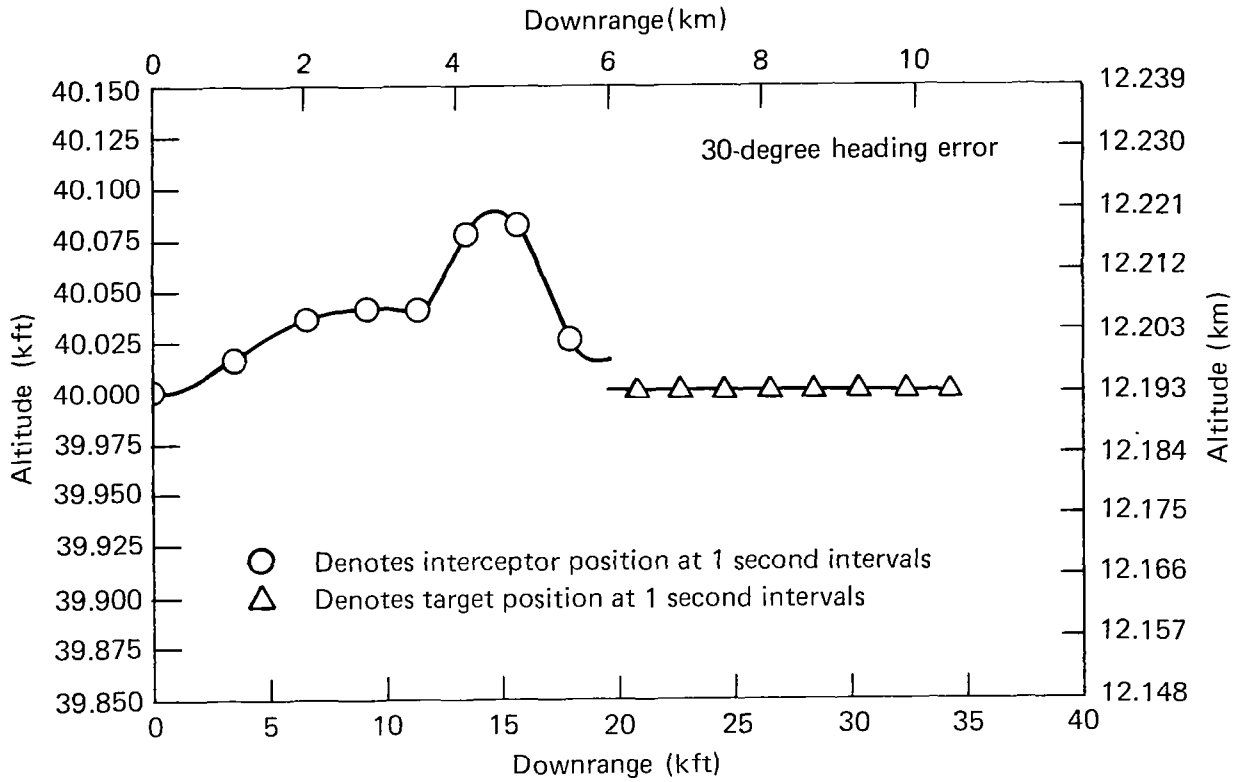

Fig. F.2 Raid suppression trajectory profile.

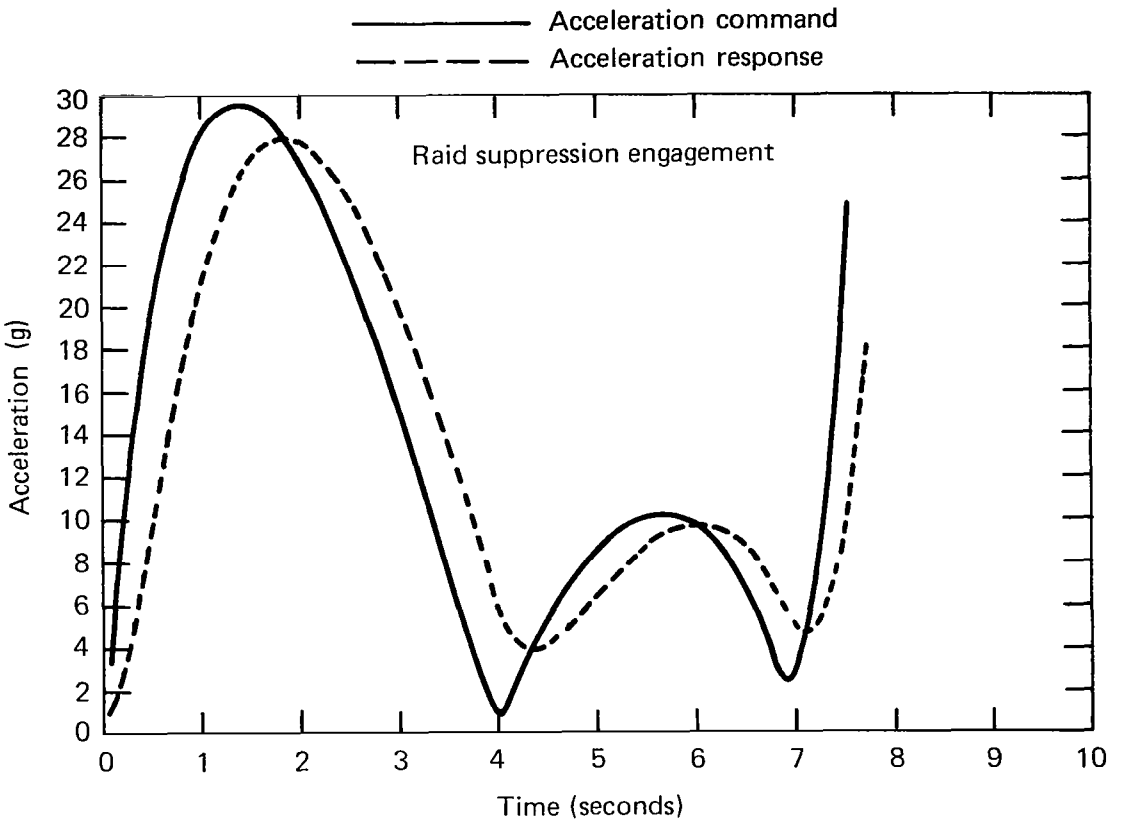

Fig. F.3 Pitch acceleration time history.

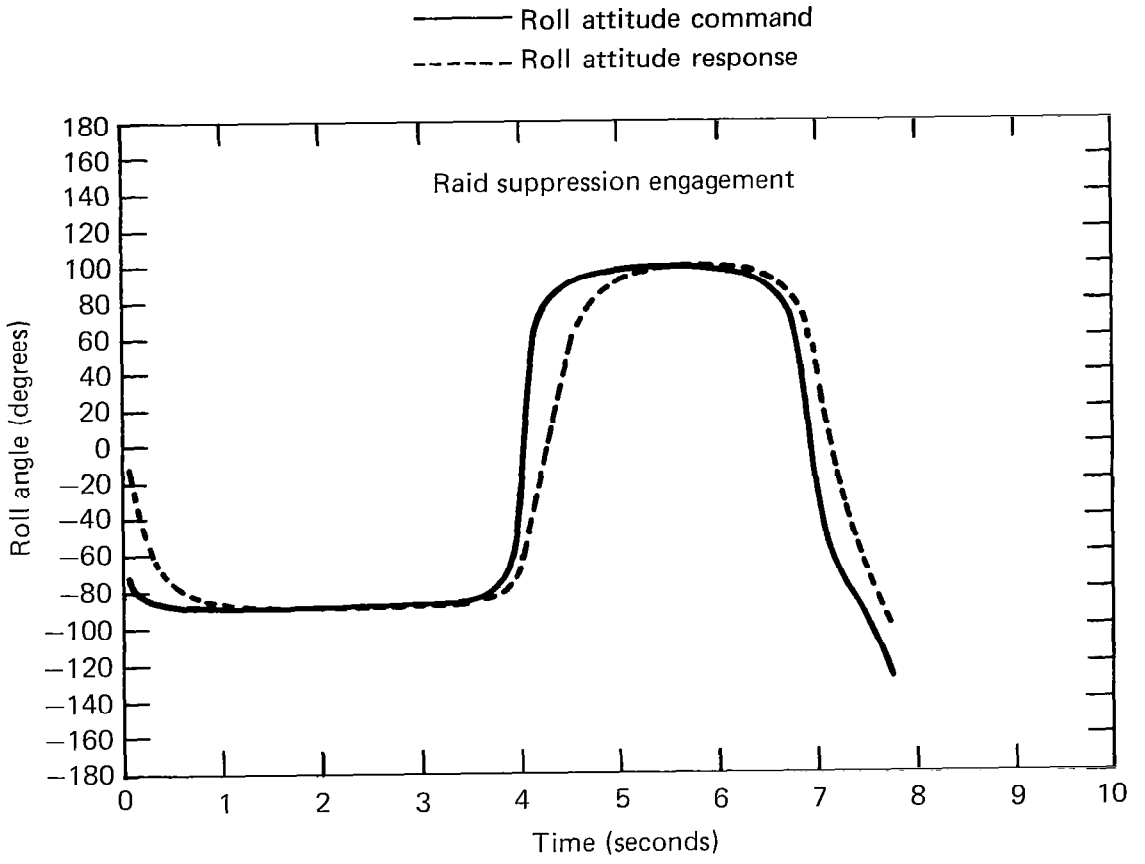

Fig. F.4 Roll attitude time history.

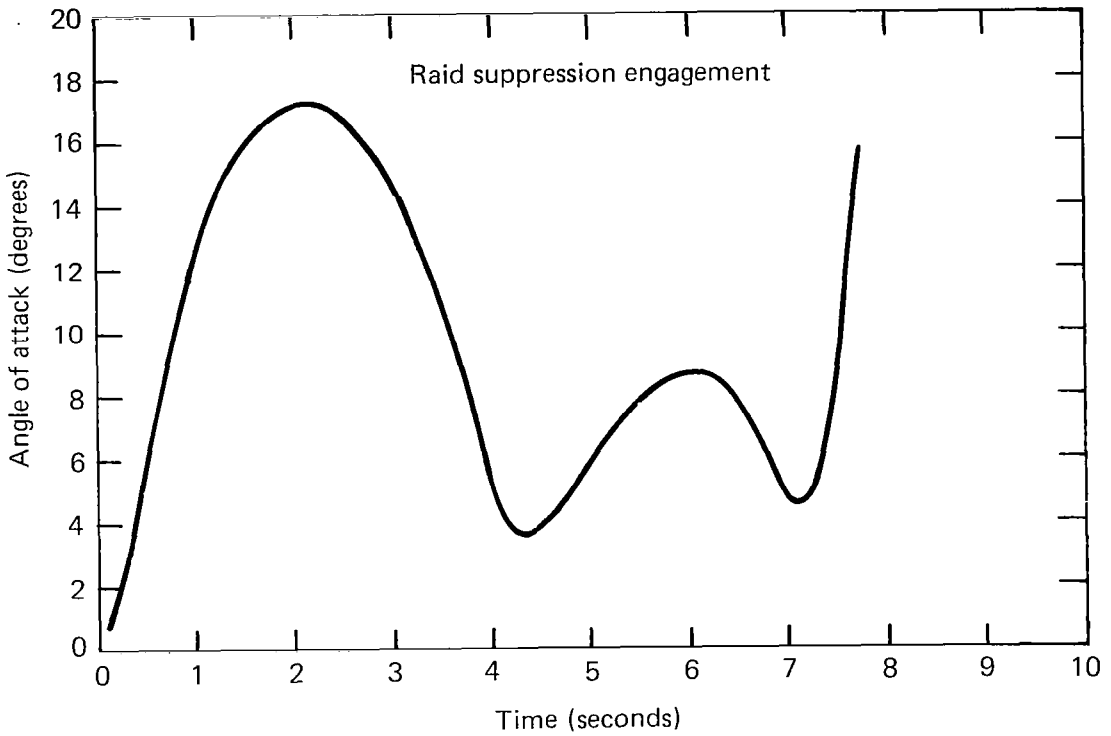

Fig. F.5 Angle-of-attack time history.

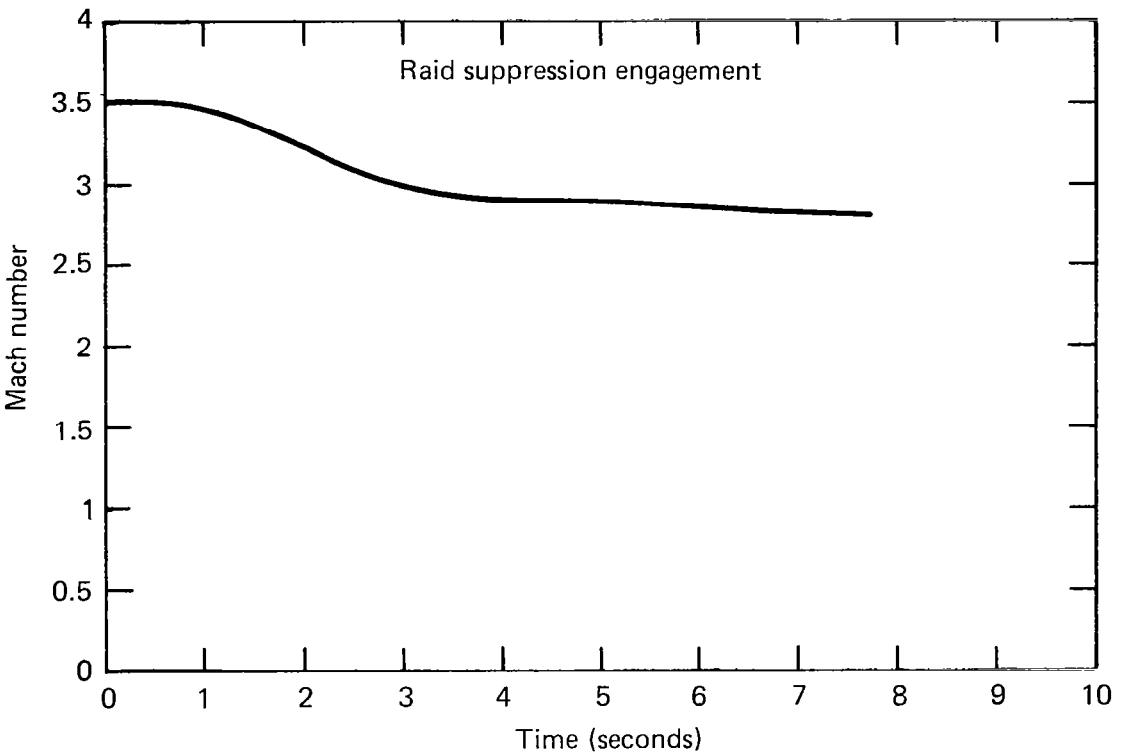

Fig. F.6 Mach number time history.

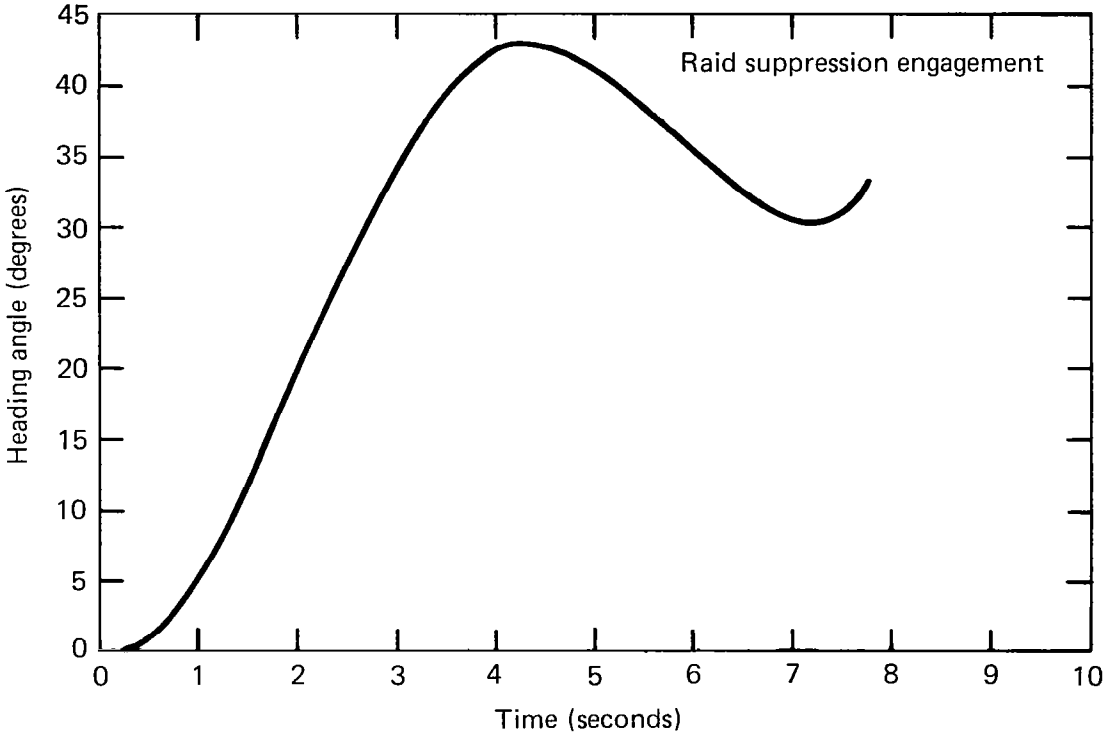

Fig. F.7 Heading angle time history.

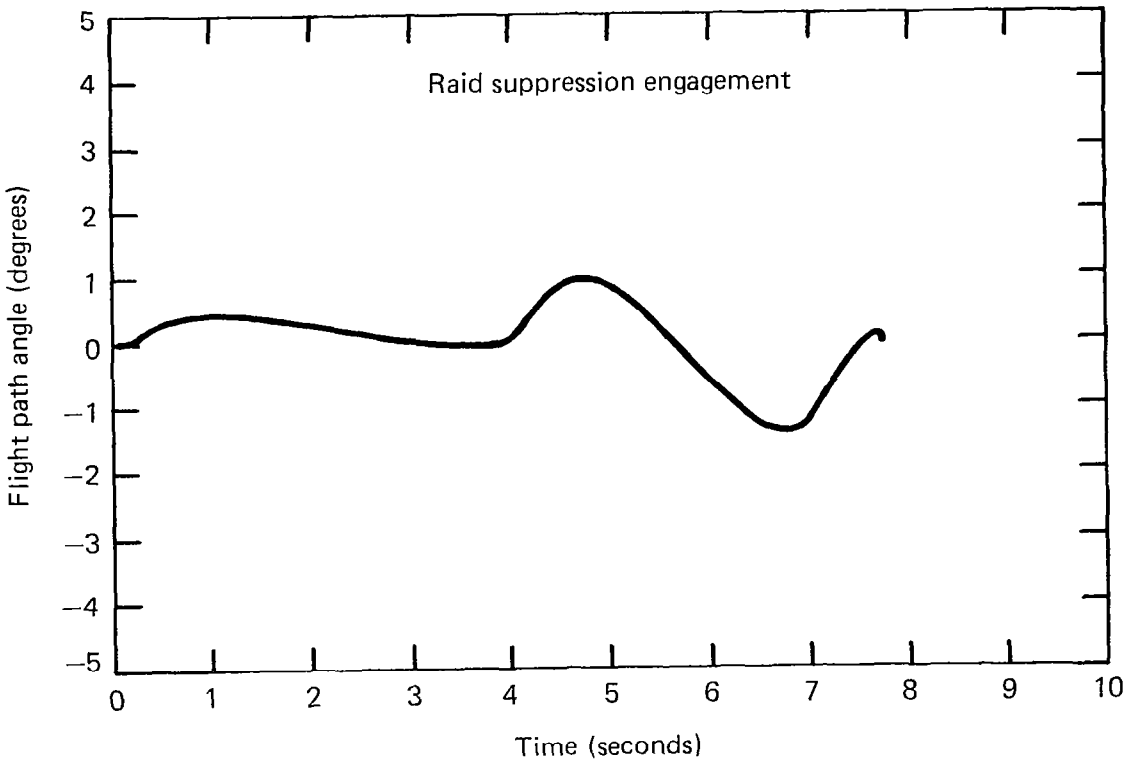

Fig. F.8 Flight path angle time history.

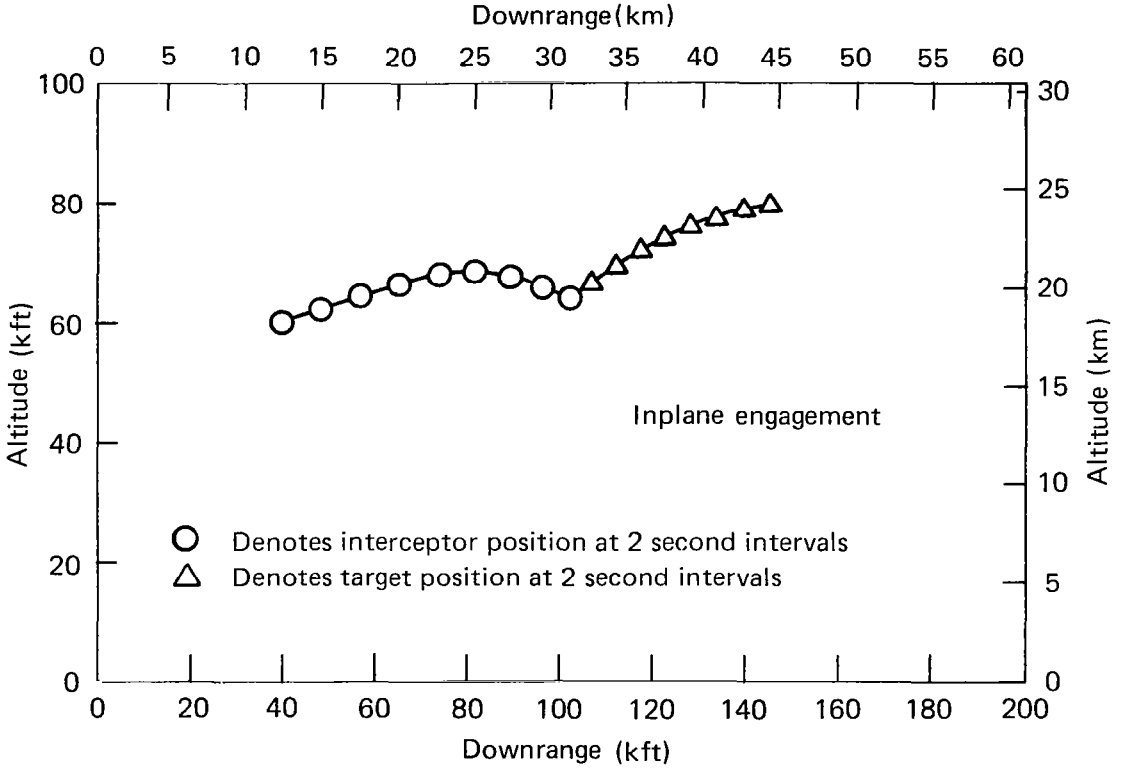

Fig. F.9 Area defense trajectory profile.

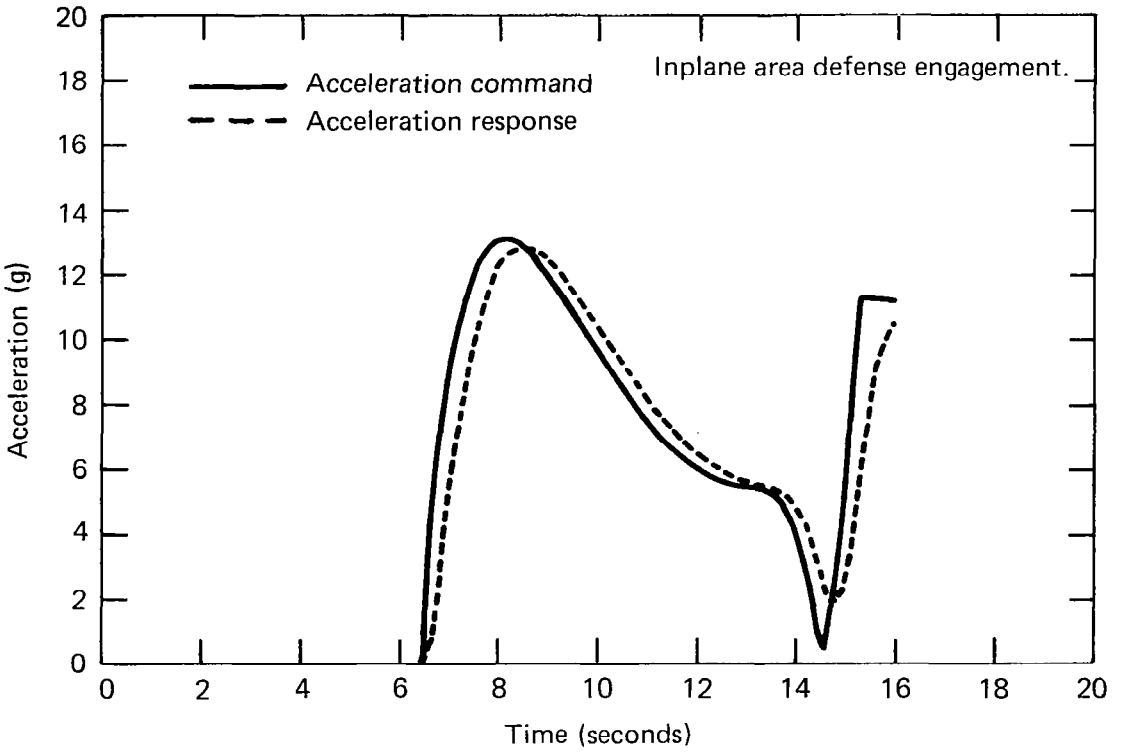

Fig. F.10 Pitch acceleration time history.

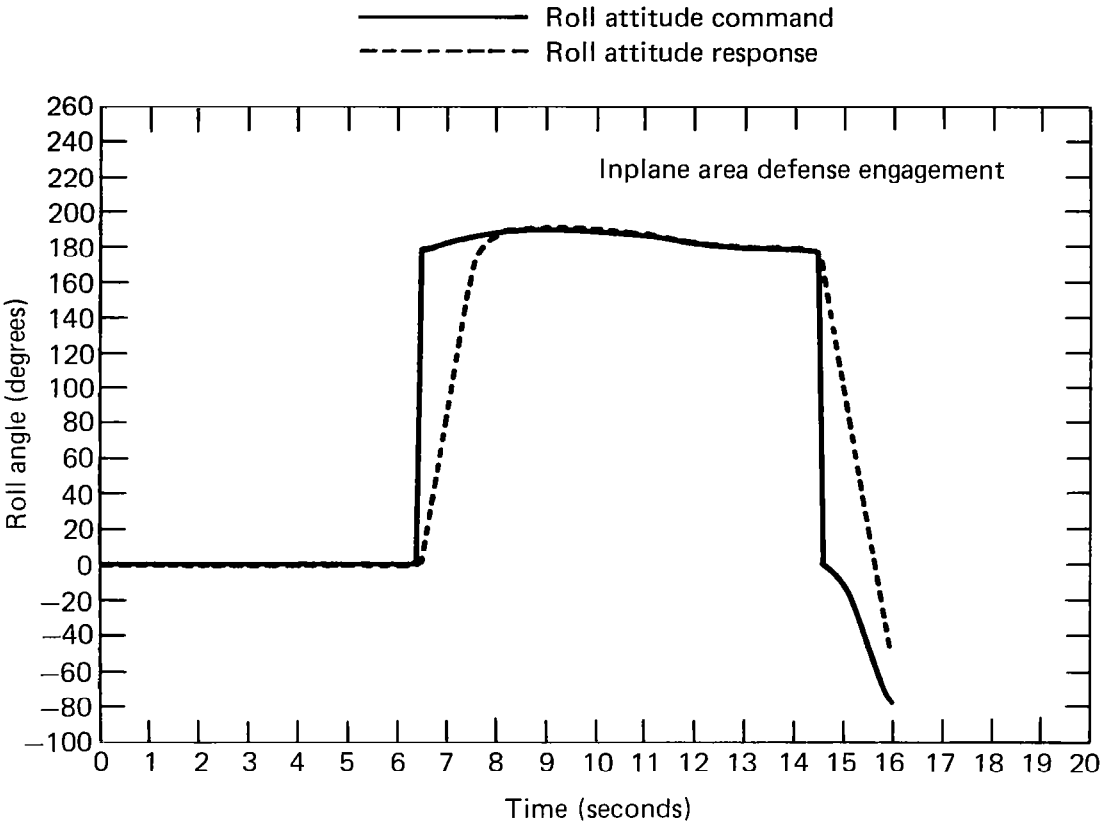

Fig. F.11 Roll attitude time history.

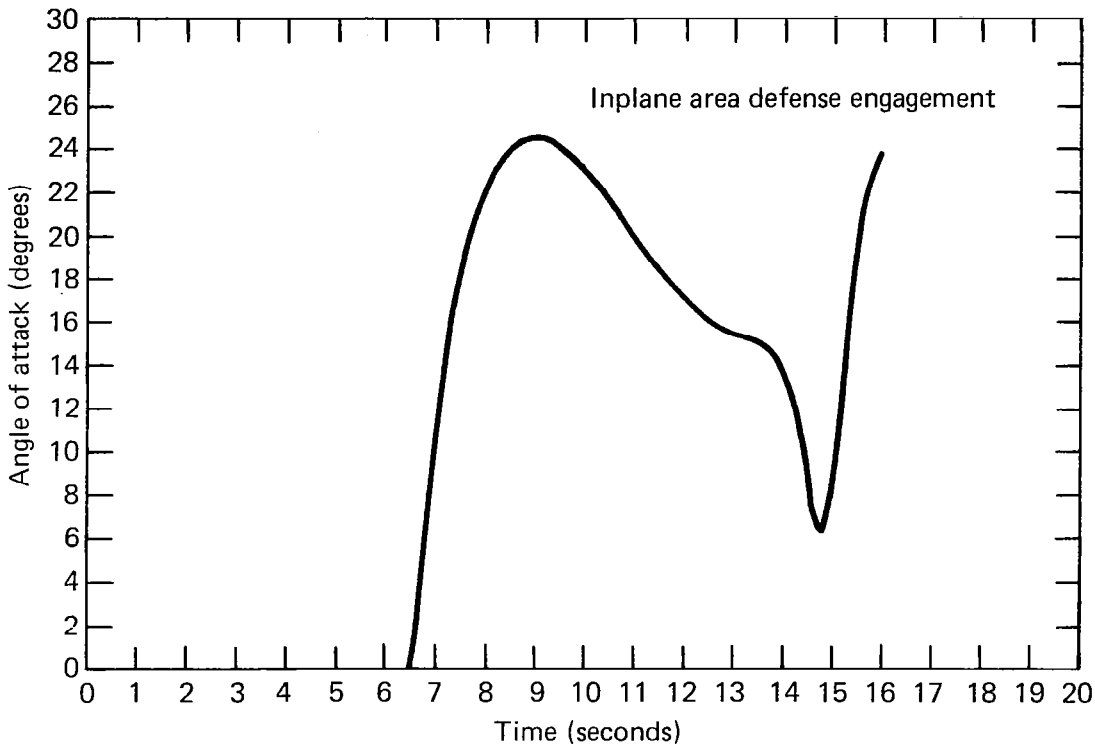

Fig. F.12 Angle of attack time history.

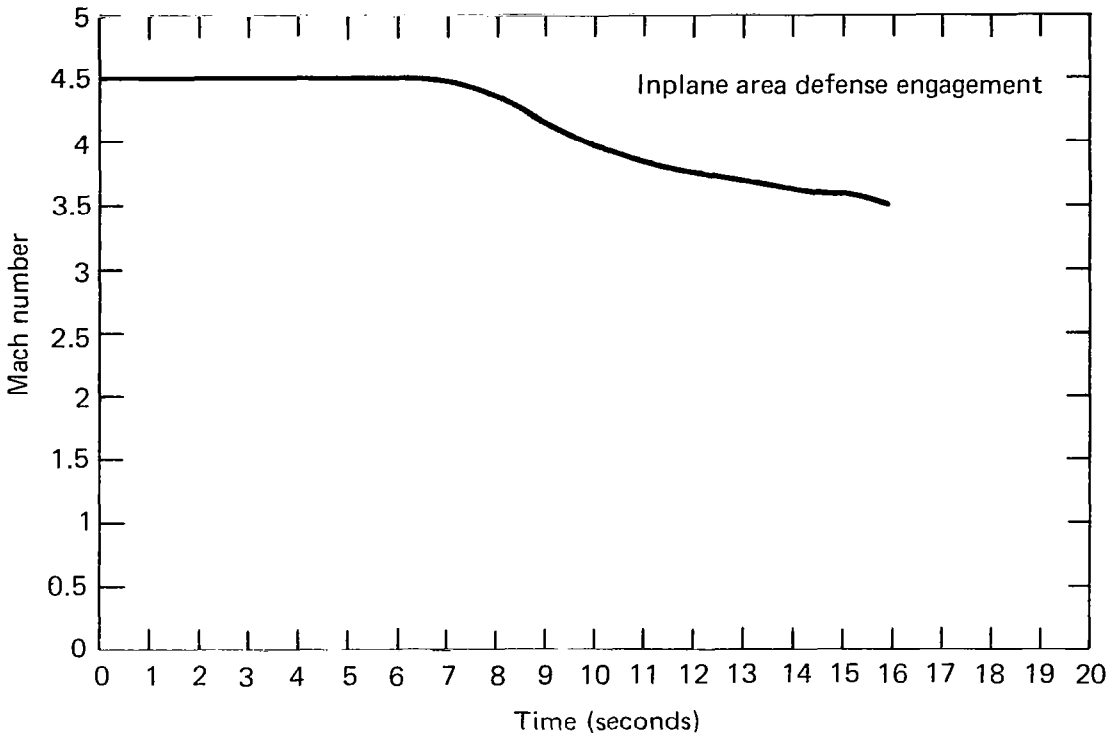

Fig. F.13 Mach number time history.

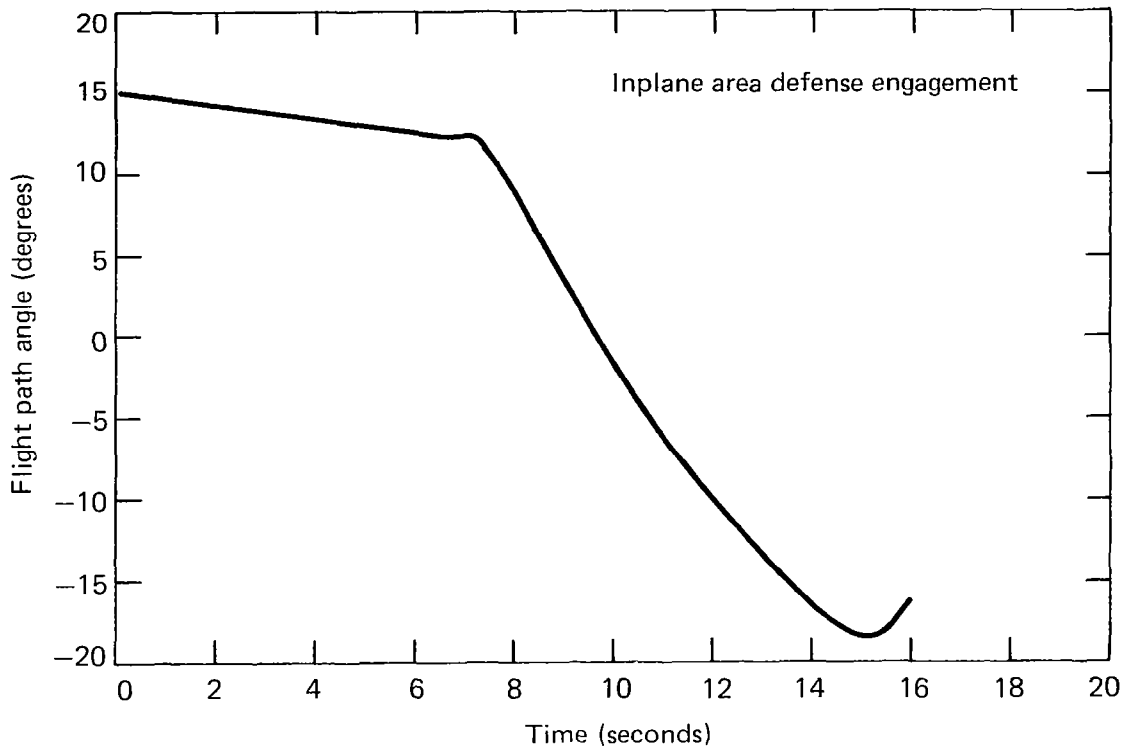

Fig. F.14 Flight path angle time history.

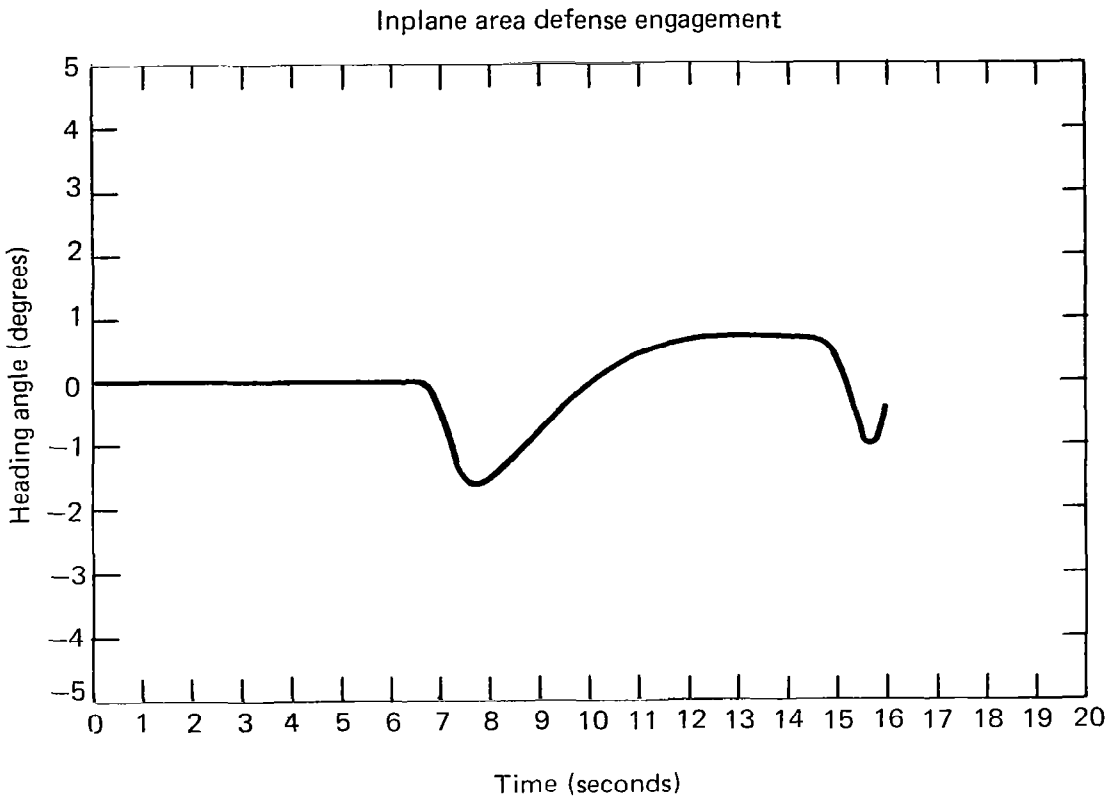

Fig. F.15 Heading angle time history.

REFERENCES

[1] H.H. Hart, "Supersonic Interference Effects in Low-Aspect Ratio Planar Configurations at Large Angles of Attack," Johns Hopkins University/Applied Physics Laboratory, APL/JHU TG-998, July 1968.

[2] B.E. Kuehne and D.J. Yost, "When are Boresight Error Slopes Excessive," Proceedings of the Fourteenth Symposium on Electromagnetic Windows, Georgia Institute of Technology, June 21-23, 1978.

[3] F.W. Riedel, "Bank-to-Turn Control Technology Survey for Homing Missiles," NASA CR-3325, September 1980.

[4] F.W.Riedel, "A Preliminary Investigation Into the Dynamic Effects of Rolling a Missile to Preferred Orientation," Johns Hopkins University/ Applied Physics Laboratory, APL/JHU F1C(1)-76-U-030, September 30, 1976.

[5] S.A. Martaugh and H.E. Criel, "Fundamentals of Proportional Navigation," IEEE Spectrum, December 1966.

[6] F.W. Nesline and P. Zarchan, "A New Look at Classical Versus Modern Homing Missile Guidance," Proceedings of the 1979 AIAA Guidance and Control Conference, August 6-8, 1979, Boulder, Colorado.

[7] R.T. Reichert, "Bank-to-Turn Terminal Homing Performance of a Long Range Surface-to-Air Missile Against a Nonmaneuvering Threat," Johns Hopkins University/Applied Physics Laboratory, JHU/APL F1C(1)-79-U-002, January, 1979.

[8] R.T. Reichert, "Impact of Imperfect Turn Coordination on Bank-to-Turn Performance, "Johns Hopkins University/Applied Physics Laboratory, JHU/APL F1C(1)-80-U-004, January 23, 1980.

[9] R.T. Reichert, "Development of a Six Degree-of-Freedom Terminal Homing Simulation for the Preliminary Assessment of Bank-to-Turn Control Performance Against Air Targets," Johns Hopkins University/Applied Physics Laboratory, JHU/APL F1C(1)-78-U-010, March 20, 1978.

1. Report No.	2. Government Accession No.	3. Recipient's Catalog No.
NASA CR-3420		

4. Title and Subtitle	5. Report Date
HOMING PERFORMANCE COMPARISON OF SELECTED AIRFRAME CONFIGURATIONS USING SKID-TO-TURN AND BANK-TO-TURN STEERING POLICIES	May 1981
	6. Performing Organization Code

7. Author(s)	8. Performing Organization Report No.
R. T. Reichert	
	10. Work Unit No.

9. Performing Organization Name and Address	11. Contract or Grant No.
The Johns Hopkins University Applied Physics Laboratory Johns Hopkins Road Laurel, Maryland 20810	L-75242A
	13. Type of Report and Period Covered Contractor Report 3/1/79 - 4/1/80

12. Sponsoring Agency Name and Address	14. Sponsoring Agency Code
National Aeronautics and Space Administration Washington, DC 20546	505-43-23-02

15. Supplementary Notes

Langley Technical Monitors: Wallace C. Sawyer and Charlie M. Jackson, Jr.
Appendix A by Edward T. Marley
Final Report

16. Abstract

The terminal homing performance of several tactical missile configurations using bank-to-turn steering policies is assessed. The impact of airframe lift capability and of autopilot and guidance filter response times is evaluated. Some comparisons are made with skid-to-turn steering. It is shown that bank-to-turn steering can provide acceptable performance provided sufficient bank rates can be tolerated.

17. Key Words (Suggested by Author(s))	18. Distribution Statement
Skid-to-Turn Bank-to-Turn Steering Policies	Unlimited-Unclassified Subject Category 02

19. Security Classif. (of this report)	20. Security Classif. (of this page)	21. No. of Pages	22. Price
Unclassified	Unclassified	168	A08

For sale by the National Technical Information Service, Springfield, Virginia 22161

NASA-Langley, 1981